

CITATION REPORT

List of articles citing

Physics and Applications of Bismuth Ferrite

DOI: 10.1002/adma.200802849

Advanced Materials, 2009, 21, 2463-2485.

Source: <https://exaly.com/paper-pdf/46035599/citation-report.pdf>

Version: 2024-04-10

This report has been generated based on the citations recorded by exaly.com for the above article. For the latest version of this publication list, visit the link given above.

The third column is the impact factor (IF) of the journal, and the fourth column is the number of citations of the article.

#	Paper	IF	Citations
2265	.		
2264	The Evidence of Giant Surface Flexoelectric Field in (111) Oriented BiFeO ₃ Thin Film.		
2263	Ferroelectric, Optical, and Photovoltaic Properties of Morphotropic Phase Boundary Compositions in the PbTiO ₃ BiFeO ₃ Bi(Ni _{1/2} Ti _{1/2})O ₃ System.		
2262	Inorganic Spintronic Materials. 2004 , 1-15		
2261	Room temperature multiferroic properties of Nd:BiFeO ₃ /Bi ₂ FeMnO ₆ bilayered films. 2009 , 95, 232904		36
2260	The magnetic properties of Bi(Fe _{0.95} Co _{0.05})O ₃ ceramics. 2009 , 95, 112510		106
2259	Misfit Strain Relaxation by Secondary Phase Formation in Multiferroic BiFeO ₃ Epitaxial Thin Films. 2009 , 1199, 86		
2258	High Temperature Phase Transitions in BiFeO ₃ . 2009 , 1199, 164		
2257	ChemInform Abstract: Physics and Applications of Bismuth Ferrite. 2009 , 40, no		1
2256	Magnetoelectric memories--a disruptive technology?. 2009 , 10, 1761-2		8
2255	Indium-Based Perovskites: A New Class of Near-Room-Temperature Multiferroics. 2009 , 121, 6233-6236		14
2254	Indium-based perovskites: a new class of near-room-temperature multiferroics. 2009 , 48, 6117-20		51
2253	Deterministic control of ferroelastic switching in multiferroic materials. 2009 , 4, 868-75		299
2252	Mechanical stress induced polarization reorientation in polycrystalline Bi _{3.25} La _{0.75} Ti ₃ O ₁₂ films. 2009 , 374, 360-365		4
2251	Polarization switching characteristics of BiFeO ₃ thin films epitaxially grown on Pt/MgO at a low temperature. 2009 , 95, 242902		29
2250	Phase transitions and ferroelectrics: revival and the future in the field. 2009 , 82, 633-661		44
2249	Magnetoelectric response of multiferroic BiFeO ₃ and related materials from first-principles calculations. 2009 , 103, 267205		80

2248	B-cation effects in relaxor and ferroelectric tetragonal tungsten bronzes. 2009 , 19, 6485	52
2247	Structure and Properties of Multiferroic Oxygen Hyperstoichiometric $\text{BiFe}_{1-x}\text{Mn}_x\text{O}_{3+\delta}$. 2009 , 21, 5176-5186	86
2246	Effect of chemical substitution on the Néel temperature of multiferroic $\text{Bi}_{1-x}\text{Ca}_x\text{FeO}_3$. 2009 , 79,	100
2245	The morphology of Au@MgO nanopeapods. 2009 , 20, 455603	13
2244	Dielectric spectra of $\text{Bi}_{0.98}\text{Nd}_{0.02}\text{FeO}_{3.00}$ multiferroic thin films in the terahertz frequency range. 2010 , 52, 1842-1849	8
2243	On the room temperature multiferroic BiFeO_3 : magnetic, dielectric and thermal properties. 2010 , 75, 451-460	115
2242	Multiferroic thin-film integration onto semiconductor devices. 2010 , 22, 423201	75
2241	Reorientation of magnetic dipoles at the antiferroelectric-paraelectric phase transition of $\text{Bi}_{1-x}\text{Nd}_x\text{FeO}_3$ (0.15 \leq 0.25). 2010 , 81,	106
2240	Ferroelectric properties of BiFeO_3 thin films deposited on substrates with large lattice mismatch. 2010 , 4, 79-81	21
2239	Optical properties of integrated multiferroic BiFeO_3 thin films for microwave applications. 2010 , 96, 182902	49
2238	Landau theory of domain wall magnetoelectricity. 2010 , 81,	121
2237	Preparation and characterization of $\text{BiFeO}_3/\text{LaNiO}_3$ heterostructure films grown on silicon substrate. 2010 , 312, 617-620	8
2236	Effect of Cr substitution on the multiferroic properties of $\text{BiFe}_{1-x}\text{Cr}_x\text{O}_3$ compounds. 2010 , 374, 4265-4268	41
2235	Intermediate structural phases in rare-earth substituted BiFeO_3 . 2010 , 45, 416-419	28
2234	Effect of Gd substitution on ferroelectric and magnetic properties of $\text{Bi}_4\text{Ti}_3\text{O}_{12}$. 2010 , 64, 1066-1068	21
2233	Effect of Sm substitution on ferroelectric and magnetic properties of BiFeO_3 . 2010 , 62, 238-241	82
2232	Universal Behavior and Electric-Field-Induced Structural Transition in Rare-Earth-Substituted BiFeO_3 . 2010 , 20, 1108-1115	312
2231	The E_0 - Γ Transition in BiFeO_3 : A Powder Neutron Diffraction Study. 2010 , 20, 2116-2123	81

2230	Epitaxial growth and properties of doped transition metal and complex oxide films. <i>Advanced Materials</i> , 2010 , 22, 219-48	24	183
2229	Multiferroics with spiral spin orders. <i>Advanced Materials</i> , 2010 , 22, 1554-65	24	498
2228	Bulk photovoltaic effect at visible wavelength in epitaxial ferroelectric BiFeO ₃ thin films. <i>Advanced Materials</i> , 2010 , 22, 1763-6	24	469
2227	Magnetoelectric coupling effects in multiferroic complex oxide composite structures. <i>Advanced Materials</i> , 2010 , 22, 2900-18	24	687
2226	Uniaxial magnetic anisotropy in La _{0.7} Sr _{0.3} MnO ₃ thin films induced by multiferroic BiFeO ₃ with striped ferroelectric domains. <i>Advanced Materials</i> , 2010 , 22, 4964-8	24	45
2225	Ferroelectricity in Perovskites with s0 A-Site Cations: Toward Near-Room-Temperature Multiferroics. 2010 , 122, 1647-1650		8
2224	Ferroelectricity in perovskites with s0 A-site cations: toward near-room-temperature multiferroics. 2010 , 49, 1603-6		22
2223	Phase transitions, electrical conductivity and chemical stability of BiFeO ₃ at high temperatures. 2010 , 183, 1205-1208		42
2222	Magneto-thermal and dielectric properties of biferroic YCrO ₃ prepared by combustion synthesis. 2010 , 183, 1863-1871		75
2221	The role of Coulomb and exchange interaction on the Dzyaloshinskii-Moriya interaction (DMI) in BiFeO ₃ . 2010 , 322, 1765-1769		24
2220	Magnetism and electronic properties of BiFeO ₃ under lower pressure. 2010 , 322, 3755-3759		26
2219	Change in periodicity of the incommensurate magnetic order towards commensurate order in bismuth ferrite lead titanate. 2010 , 322, L64-L67		36
2218	Advances in the growth and characterization of magnetic, ferroelectric, and multiferroic oxide thin films. 2010 , 68, 89-133		501
2217	Nanoscale polarization relaxation of epitaxial BiFeO ₃ thin film. 2010 , 518, e169-e173		5
2216	Enhanced ferromagnetism at the rhombohedral-tetragonal phase boundary in Pr and Mn co-substituted powders. 2010 , 150, 2081-2084		47
2215	Mode crystallography of distorted structures. 2010 , 66, 558-90		267
2214	Magnetic peculiarity and crystal structure of Pr _{0.5} Sr _{0.5} Co _{1-x} Fe _x O ₃ . 2010 , 247, 411-415		2
2213	Ferroelectric and Impedance Behavior of La- and Ti-Codoped BiFeO ₃ Thin Films. 2010 , 93, 2795-2803		126

2212	The Synthesis of Pure-Phase Bismuth Ferrite in the BiFeO ₃ System Under Hydrothermal Conditions without a Mineralizer. 2010 , 93, 3173-3179	22
2211	Hydrothermal Synthesis and Size-Dependent Properties of Multiferroic Bismuth Ferrite Crystallites. 2010 , 93, 3842-3849	34
2210	Ferroelastic switching for nanoscale non-volatile magnetoelectric devices. 2010 , 9, 309-14	344
2209	Light-induced size changes in BiFeO ₃ crystals. 2010 , 9, 803-5	243
2208	Electric-field control of spin waves at room temperature in multiferroic BiFeO ₃ . 2010 , 9, 975-9	205
2207	Size-dependent structural preferences and magnetization enhancement in 0.5Bi _{0.8} La _{0.2} FeO ₃ 0.5PbTiO ₃ . 2010 , 108, 124108	5
2206	Morphology and orientation of iron oxide precipitates in epitaxial BiFeO ₃ thin films grown under two non-optimized oxygen pressures. 2010 , 90, 4551-4567	6
2205	Hydrothermal synthesis of perovskite bismuth ferrite crystallites with the help of NH ₄ Cl. 2010 ,	
2204	Strain-driven phase transitions and associated dielectric/piezoelectric anomalies in BiFeO ₃ thin films. 2010 , 97, 152901	34
2203	Optical spectroscopy of charge transfer transitions in multiferroic manganites, ferrites, and related insulators. 2010 , 36, 489-510	34
2202	Evidence for a first-order transition from monoclinic β to monoclinic β' phase in BiFeO ₃ thin films. 2010 , 81,	30
2201	Dielectric, magnetic, and magnetoelectric properties of La and Ti codoped BiFeO ₃ . 2010 , 97, 222904	97
2200	Fatigue and ferroelectric behavior of La and Zn comodified BiFeO ₃ thin films. 2010 , 108, 024104	23
2199	Twinning rotation and ferroelectric behavior of epitaxial BiFeO ₃ (001) thin film. 2010 , 96, 012901	33
2198	Nanoscale domains in strained epitaxial BiFeO ₃ thin Films on LaSrAlO ₄ substrate. 2010 , 96, 252903	71
2197	Thickness-dependent structural and magnetic properties of BiFeO ₃ films prepared by metal organic decomposition method. 2010 , 97, 222901	24
2196	Cluster spin glass behavior in Bi(Fe _{0.95} Co _{0.05})O ₃ . 2010 , 107, 093920	32
2195	Finite size and intrinsic field effect on the polar-active properties of ferroelectric-semiconductor heterostructures. 2010 , 81,	55

2194	Tuning the atomic and domain structure of epitaxial films of multiferroic BiFeO ₃ . 2010 , 81,	68
2193	Domain pattern and piezoelectric response across polymorphic phase transition in strained bismuth ferrite films. 2010 , 97, 242906	17
2192	Resistance switching in polycrystalline BiFeO ₃ thin films. 2010 , 97, 042101	129
2191	Thickness-dependent twinning evolution and ferroelectric behavior of epitaxial BiFeO ₃ (001) thin films. 2010 , 82,	28
2190	Effect of Zn Concentration on Multiferroic and Fatigue Behavior of Bi[sub 0.90]La[sub 0.10]Fe[sub 1-x]Zn[sub x]O[sub 3] Thin Films. 2010 , 13, G105	8
2189	Nonstoichiometric BiFe _{0.9} Ti _{0.05} O ₃ multiferroic ceramics with ultrahigh electrical resistivity. 2010 , 108, 094112	36
2188	ZnO as a buffer layer for growth of BiFeO ₃ thin films. 2010 , 108, 034102	39
2187	Advances in lead-free piezoelectric materials for sensors and actuators. 2010 , 10, 1935-54	302
2186	Polarization switching in quasiplanar BiFeO ₃ capacitors. 2010 , 97, 062910	25
2185	Low symmetry monoclinic MC phase in epitaxial BiFeO ₃ thin films on LaSrAlO ₄ substrates. 2010 , 97, 242903	44
2184	Nonvolatile resistive switching in metal/La-doped BiFeO ₃ /Pt sandwiches. 2010 , 21, 425202	94
2183	Effect of Reduced Particle Size on the Magnetic Properties of Chemically Synthesized BiFeO ₃ Nanocrystals. 2010 , 114, 2108-2115	169
2182	Synthesis, Structural Characterization, and Properties of Perovskites Belonging to the xBiMnO ₃ (1-x)PbTiO ₃ System. 2010 , 22, 541-550	13
2181	Microstructure-electromechanical property correlations in rare-earth-substituted BiFeO ₃ epitaxial thin films at morphotropic phase boundaries. 2010 , 97, 212905	69
2180	Temperature-Dependent Raman and Dielectric Spectroscopy of BiFeO ₃ Nanoparticles: Signatures of Spin-Phonon and Magnetoelectric Coupling. 2010 , 114, 12432-12439	53
2179	Enhanced Multiferroic Properties and Valence Effect of Ru-Doped BiFeO ₃ Thin Films. 2010 , 114, 6994-6998	162
2178	Temperature dependence of electronic transitions and optical properties in multiferroic BiFeO ₃ nanocrystalline film determined from transmittance spectra. 2010 , 97, 121102	33
2177	Substrate influence on the optical and structural properties of pulsed laser deposited BiFeO ₃ epitaxial films. 2010 , 107, 123524	57

2176	Variations of ferroelectric off-centering distortion and 3d π orbital mixing in La-doped BiFeO ₃ multiferroics. 2010 , 82,	70
2175	Bridging multiferroic phase transitions by epitaxial strain in BiFeO ₃ . 2010 , 105, 057601	136
2174	Density functional theory plus U study of vacancy formations in bismuth ferrite. 2010 , 96, 232906	62
2173	Coexistence of strong ferromagnetism and polar switching at room temperature in Fe ₃ O ₄ /BiFeO ₃ nanocomposite thin films. 2010 , 97, 153121	25
2172	Crystal and magnetic structures and properties of BiMnO ₃ δ . 2010 , 132, 8137-44	46
2171	Magnetoelectric and magnetoelastic properties of rare-earth ferroborates. 2010 , 36, 511-521	132
2170	. 2010 ,	0
2169	Effect of Ce and Zr codoping on the multiferroic properties of BiFeO ₃ thin films. 2010 , 89, 57004	29
2168	Electronic structure of multiferroic BiFeO ₃ and related compounds: Electron energy loss spectroscopy and density functional study. 2010 , 82,	48
2167	Rhombohedral-to-orthorhombic transition and multiferroic properties of Dy-substituted BiFeO ₃ . 2010 , 108, 074109	80
2166	Ab initio indications for giant magnetoelectric effects driven by structural softness. 2010 , 105, 037208	90
2165	Nonmagnetic Fe-site doping of BiFeO ₃ multiferroic ceramics. 2010 , 96, 102509	105
2164	Study of defect-dipoles in an epitaxial ferroelectric thin film. 2010 , 96, 052903	52
2163	Mesosopic metal-insulator transition at ferroelastic domain walls in VO ₂ . 2010 , 4, 4412-9	63
2162	Improved Ferroelectric and Fatigue Behavior of Bi _{0.95} Gd _{0.05} FeO ₃ /BiFe _{0.95} Mn _{0.05} O ₃ Bilayered Thin Films. 2010 , 114, 19318-19321	16
2161	Competing phases in BiFeO ₃ thin films under compressive epitaxial strain. 2010 , 81,	90
2160	Microwave and THz applications of ferroelectrics and multiferroics. 2010 ,	1
2159	Suppression of octahedral tilts and associated changes in electronic properties at epitaxial oxide heterostructure interfaces. 2010 , 105, 087204	288

2158	Systematic variations in structural and electronic properties of BiFeO ₃ by A-site substitution. 2010 , 96, 012905	57
2157	Multiferroic behavior of BiFeO ₃ /TiO ₃ (Mg, Sr, Ca, Ba, and Pb) thin films. 2010 , 108, 026101	6
2156	Enhancement of ferromagnetic and dielectric properties in lanthanum doped BiFeO ₃ by hydrothermal synthesis. 2010 , 490, 637-641	79
2155	Structural and multiferroic properties of the Ce-doped BiFeO ₃ thin films. 2010 , 493, 544-548	77
2154	The magnetic properties of La doped and codoped BiFeO ₃ . 2010 , 499, 108-112	81
2153	Structural, dielectric and magnetic properties of Pr substituted Bi _{1-x} Pr _x FeO ₃ (0 ≤ x ≤ 0.15) multiferroic compounds. 2010 , 501, L29-L32	73
2152	Preparation and properties of (1-x)BiFeO ₃ -xBaTiO ₃ multiferroic ceramics. 2010 , 506, 862-867	67
2151	Multiferroic behavior and electrical conduction of BiFeO ₃ thin film deposited on quartz substrate. 2010 , 507, L4-L7	16
2150	Effect of Eu substitution on the crystal structure and multiferroic properties of BiFeO ₃ . 2010 , 507, 157-161	159
2149	Phonon spectroscopy near phase transition temperatures in multiferroic BiFeO ₃ epitaxial thin films. 2010 , 81,	31
2148	Optimal multiferroic properties and enhanced magnetoelectric coupling in SmFeO ₃ /BaTiO ₃ solid solutions. 2010 , 107, 084106	23
2147	Engineering functionality in the multiferroic BiFeO ₃ --controlling chemistry to enable advanced applications. 2010 , 39, 10813-26	53
2146	Enhanced multiferroic properties in Ti-doped Bi ₂ Fe ₄ O ₉ ceramics. 2010 , 108, 064110	50
2145	Size effects in multiferroic BiFeO ₃ nanodots: A first-principles-based study. 2010 , 82,	33
2144	Strong ferroelectric domain-wall pinning in BiFeO ₃ ceramics. 2010 , 108, 074107	246
2143	Magnetic properties of La doped Bi ₂ FeMnO ₆ ceramic and film. 2010 , 108, 093903	7
2142	Ferromagnetism in multiferroic BiFeO ₃ films: A first-principles-based study. 2010 , 81,	99
2141	Effect of substrate orientation on lattice relaxation of epitaxial BiFeO ₃ thin films. 2010 , 108, 014104	42

2140	Neutron diffraction study of the BiFeO ₃ spin cycloid at low temperature. 2010 , 22, 256001	32
2139	Superconducting gap induced barrier enhancement in a BiFeO ₃ -based heterostructure. 2010 , 97, 252905	21
2138	Mapping octahedral tilts and polarization across a domain wall in BiFeO ₃ from Z-contrast scanning transmission electron microscopy image atomic column shape analysis. 2010 , 4, 6071-9	135
2137	THz radiation by optically controlled depolarization in BiFeO ₃ . 2010 ,	
2136	Electron spin resonance probed suppressing of the cycloidal spin structure in doped bismuth ferrites. 2010 , 96, 232507	31
2135	The ferromagnetic and ferroelectric properties of (Bi _{0.9} La _{0.1})(Fe _{0.95} Co _{0.05})O ₃ . 2010 ,	
2134	The study of BST buffered BiFeO ₃ thin film. 2010 ,	
2133	Orientational dependence of multiferroic behaviors of La and Mn modified BiFeO ₃ thin films. 2011 ,	1
2132	The enhanced ferromagnetic property of BiFeO ₃ -YMnO ₃ system. 2011 ,	1
2131	Leakage mechanism of cation -modified BiFeO ₃ thin film. 2011 , 1, 022138	60
2130	Comparative study on aging effect in BiFeO ₃ thin films substituted at A- and B-sites. 2011 , 99, 262901	32
2129	Continuously tunable magnetic phase transitions in the DyMn _{1-x} Fe _x O ₃ system. 2011 , 99, 092502	43
2128	Origin and magnitude of the large piezoelectric response in the lead-free (1-x)BiFeO ₃ -xBaTiO ₃ solid solution. 2011 , 26, 9-17	47
2127	Investigations of Low Temperature Phase Transitions in BiFeO ₃ Ceramic by Infrared Spectroscopy. 2011 , 417, 63-69	6
2126	Migration kinetics of oxygen vacancies in Mn-modified BiFeO ₃ thin films. 2011 , 3, 2504-11	58
2125	Isothermal structural transitions, magnetization and large piezoelectric response in Bi _{1-x} LaxFeO ₃ perovskites. 2011 , 83,	117
2124	Effect of crystal and domain orientation on the visible-light photochemical reduction of Ag on BiFeO ₃ . 2011 , 3, 1562-7	56
2123	Acoustic properties of multiferroics PbFe _{1/2} Ta _{1/2} O ₃ and BiFeO ₃ at Néel temperature. 2011 ,	

2122	High temperature dielectric properties of YMnO ₃ ceramics. 2011 , 110, 064116	30
2121	Perovskite, LiNbO ₃ , corundum, and hexagonal polymorphs of (In _{1-x} M _x)MO ₃ . 2011 , 133, 9405-12	37
2120	Influence of La and Ru Dopants on Multiferroic Properties of Polycrystalline BiFeO ₃ Thin Films. 2011 , 4, 111502	12
2119	A large polarization in Ce-modified bismuth ferrite thin films. 2011 , 109, 124105	13
2118	Epitaxial strain and electric boundary condition effects on the structural and ferroelectric properties of BiFeO ₃ films. 2011 , 84,	53
2117	Polarization fatigue of Pr and Mn co-substituted BiFeO ₃ thin films. 2011 , 99, 012903	32
2116	Dielectric, magnetic and magnetoelectric properties of La and Nb codoped bismuth ferrite. 2011 , 23, 385901	34
2115	BiFeO ₃ : A Review on Synthesis, Doping and Crystal Structure. 2011 , 126, 47-59	186
2114	Local weak ferromagnetism in single-crystalline ferroelectric BiFeO ₃ . 2011 , 107, 207206	101
2113	Dynamic conductivity of ferroelectric domain walls in BiFeO ₃ . 2011 , 11, 1906-12	204
2112	A phase transition close to room temperature in BiFeO ₃ thin films. 2011 , 23, 342202	46
2111	Growth of Highly Insulating Bulk Single Crystals of Multiferroic BiFeO ₃ and Their Inherent Internal Strains in the Domain-Switching Process. 2011 , 11, 5139-5143	43
2110	Evidence of bulk photovoltaic effect and large tensor coefficient in ferroelectric BiFeO ₃ thin films. 2011 , 84,	96
2109	Strain Effects of the Structural Characteristics of Ferroelectric Transition in Single-Domain Epitaxial BiFeO ₃ Films. 2011 , 28, 067702	4
2108	Magnetoelectricity in BiFeO ₃ films: First-principles-based computations and phenomenology. 2011 , 83,	40
2107	Displacement-type ferroelectricity with off-center magnetic ions in perovskite Sr _{1-x} Ba _x MnO ₃ . 2011 , 107, 137601	118
2106	Magnetoelectric coupling and phase transition in BiFeO ₃ and (BiFeO ₃) _{0.95} (BaTiO ₃) _{0.05} ceramics. 2011 , 109, 044101-044101-4	48
2105	Effect of bottom electrodes on nanoscale switching characteristics and piezoelectric response in polycrystalline BiFeO ₃ thin films. 2011 , 110, 084102	31

2104	Hydrothermal synthesis and magnetic properties of single-crystalline BiFeO ₃ nanowires. 2011 , 47, 8166-8	98
2103	Structure, Magnetic, and Ferroelectric Properties of Bi _{1-x} GdxFeO ₃ Nanoparticles. 2011 , 115, 8869-8875	60
2102	Energetic stability, structural transition, and thermodynamic properties of ZnSnO ₃ . 2011 , 98, 091914	29
2101	Introduction to magnetoelectric coupling and multiferroic films. 2011 , 44, 243001	240
2100	Multiple high-pressure phase transitions in BiFeO ₃ . 2011 , 84,	80
2099	Multiferroic coupling in nanoscale BiFeO ₃ . 2011 , 99, 073106	49
2098	Neutron diffraction study of the coupling between spin, lattice, and structural degrees of freedom in 0.8BiFeO ₃ -0.2PbTiO ₃ . 2011 , 109, 063522	19
2097	Phase transitions in epitaxial (-110) BiFeO ₃ films from first principles. 2011 , 107, 117602	31
2096	Ferroelectric behavior in bismuth ferrite thin films of different thickness. 2011 , 3, 3261-3	44
2095	Low-temperature evolution of the modulated magnetic structure in the ferroelectric antiferromagnet BiFeO ₃ . 2011 , 84,	48
2094	Spin-glass behavior of nanocrystalline multiferroic bismuth ferrite lead titanate. 2011 , 21, 781-788	13
2093	Visible Light Responsive Perovskite BiFeO ₃ Pills and Rods with Dominant {111} _c Facets. 2011 , 11, 1049-1053	106
2092	Magnetic symmetry of low-dimensional multiferroics and ferroelastics. 2011 , 84, 421-437	10
2091	High-pressure phase transitions in BiFeO ₃ : hydrostatic versus non-hydrostatic conditions. 2011 , 84, 474-482	23
2090	Tip-enhanced photovoltaic effects in bismuth ferrite. 2011 , 2,	325
2089	Multiferroic phase transition near room temperature in BiFeO ₃ films. 2011 , 107, 237601	80
2088	Preparation and Characterization of BiFeO ₃ Film via Sol-Gel Spin-Coating Process. 2011 , 492, 202-205	2
2087	Role of Pb(Zr _{0.52} Ti _{0.48})O ₃ substitution in multiferroic properties of polycrystalline BiFeO ₃ thin films. 2011 , 110, 114116	16

2086	Particle size dependence of magnetization and noncentrosymmetry in nanoscale BiFeO ₃ . 2011 , 109, 07D737	52
2085	BiFeO ₃ /Zn _{1-x} MnxO bilayered thin films. 2011 , 258, 1390-1394	10
2084	Ab initio study of proper topological ferroelectricity in layered perovskite La ₂ Ti ₂ O ₇ . 2011 , 84,	42
2083	Mechanosynthesis of the whole xBiFeO ₃ (1-x)PbTiO ₃ multiferroic system: structural characterization and study of phase transitions. 2011 , 21, 3125	48
2082	Linear-quadratic order parameter coupling and multiferroic phase transitions. 2011 , 23, 462202	22
2081	Structural, electronic and optical properties of BiFeO ₃ studied by first-principles. 2011 , 509, 1901-1905	79
2080	Effect of bottom electrode and resistive layer on the dielectric and ferroelectric properties of sol-gel derived BiFeO ₃ thin films. 2011 , 509, 2054-2059	34
2079	Effects of Mn substitution on ferro- and piezoelectric properties of Bi _{0.86} Sm _{0.14} FeO ₃ thin films. 2011 , 509, 3766-3770	11
2078	Optimization of the mechanochemical conditions for the synthesis of the xBiFeO ₃ (1-x)PbTiO ₃ multiferroic system. 2011 , 509, 5483-5487	2
2077	Multiferroic and magnetoelectric properties of single-phase Bi _{0.85} La _{0.1} Ho _{0.05} FeO ₃ ceramics. 2011 , 509, 5908-5912	34
2076	Processing and characterization of Sr doped BiFeO ₃ multiferroic materials by high energetic milling. 2011 , 509, 7042-7046	22
2075	Structure and magnetic properties of Cd doped copper ferrite. 2011 , 509, 7585-7590	11
2074	Ferroelectric and magnetic properties in high-pressure synthesized BiFeO ₃ compound. 2011 , 509, 7591-7594	8
2073	Sintering and microstructural characterization of W ⁶⁺ , Nb ⁵⁺ and Ti ⁴⁺ iron-substituted BiFeO ₃ . 2011 , 509, 7290-7296	31
2072	Bismuth ferrite bilayered thin films of different constituent layer thicknesses. 2011 , 509, 7742-7748	
2071	Compositionally graded bismuth ferrite thin films. 2011 , 509, L319-L323	4
2070	Effect of A site and B site doping on structural, thermal, and dielectric properties of BiFeO ₃ ceramics. 2011 , 509, 8421-8426	126
2069	A giant polarization value in bismuth ferrite thin films. 2011 , 509, L362-L364	12

2068	Spiral ground state against ferroelectricity in the frustrated magnet BiMnFe ₂ O ₆ . 2011 , 83,	11
2067	Orthorhombic polar Nd-doped BiFeO ₃ thin film on MgO substrate. 2011 , 23, 332201	6
2066	Combinatorial and high-throughput screening of materials libraries: review of state of the art. 2011 , 13, 579-633	348
2065	Crystal structure of Bi(0.9)Sm(0.1)Fe(1-x)Mn(x)O ₃ multiferroics. 2011 , 40, 3462-5	16
2064	Structure and Magnetic Properties of BiFe _{0.75} Mn _{0.25} O ₃ Perovskite Prepared at Ambient and High Pressure. 2011 , 23, 4505-4514	66
2063	Effects of Doping and Oxygen Nonstoichiometry on the Thermodynamic Properties of Some Multiferroic Ceramics. 2011 ,	1
2062	Low temperature magnetic behaviour of PZT-PFW bulk multiferroic ceramics. 2011 , 303, 012065	6
2061	Enhancement of Multiferroic Properties in BiFeO ₃ Ba(Cu _{1/3} Nb _{2/3})O ₃ : Film Fabricated by Aerosol Deposition. 2011 , 94, 355-358	16
2060	Microwave Hydrothermal Synthesis, Structural Characterization, and Visible-Light Photocatalytic Activities of Single-Crystalline Bismuth Ferric Nanocrystals. 2011 , 94, 2688-2693	63
2059	Effect of (Bi,Gd)FeO ₃ Layer Thickness on the Microstructure and Electrical Properties of BiFeO ₃ Thin Films. 2011 , 94, 4291-4298	9
2058	Effects of Dy and Mn Codoping on Ferroelectric Properties of BiFeO ₃ Thin Films. 2011 , 94, 2792-2795	32
2057	Probing Ferroelectrics Using Optical Second Harmonic Generation. 2011 , 94, 2699-2727	198
2056	Phase Transitions, Magnetic and Piezoelectric Properties of Rare-Earth-Substituted BiFeO ₃ Ceramics. 2011 , 94, 4502-4506	93
2055	Large Electric-Field Induced Strain in BiFeO ₃ Ceramics. 2011 , 94, 4108-4111	65
2054	Conditions favoring the polar weak ferromagnetic state in BiFeO ₃ -type multiferroics. 2011 , 93, 512-516	6
2053	Crystallographic, magnetic and dielectric studies of the potential multiferroic cryolite (NH ₄) ₃ FeF ₆ . 2011 , 13, 953-958	4
2052	Structural stability and magnetic properties of Bi _{1-x} La(Pr) _x FeO ₃ solid solutions. 2011 , 151, 1686-1689	28
2051	Investigation of BiFe _{0.95} Mn _{0.03} Zn _{0.02} O ₃ /Bi _{3.15} Nd _{0.85} Ti _{2.9} Zr _{0.1} O ₁₂ heterostructure thin film fabricated by a chemical solution deposition technique. 2011 , 14, 253-256	2

2050	Reaction pathways in the solid state synthesis of multiferroic BiFeO ₃ . 2011 , 31, 3047-3053	124
2049	Investigation of nanodomain pattern and piezoelectric behavior of mixed phases in epitaxial BiFeO ₃ films. 2011 , 31, 3063-3071	9
2048	Large-scale growth and shape evolution of bismuth ferrite particles with a hydrothermal method. 2011 , 126, 560-567	59
2047	Self-controlled growth of Fe ₃ BO ₆ crystallites in shape of nanorods from iron-borate glass of small templates. 2011 , 129, 1020-1026	17
2046	The magnetic properties of Bi _{0.9} Ba _{0.1} Fe _{0.81} M _{0.09} Ti _{0.1} O ₃ solid solutions (M=Co, Mn, Sc, Al). 2011 , 46, 1848-1852	3
2045	Structural phase evolution in Bi _{7/8} Ln _{1/8} FeO ₃ (Ln = LaDy) series. 2011 , 65, 1970-1972	27
2044	Investigation of dark and light conductivities in calcium doped bismuth ferrite thin films. 2011 , 65, 3086-3088	14
2043	Synthesis and Magnetic Properties of BiFeO_3 , $\text{Bi}_{0.95}\text{Ba}_{0.05}\text{FeTi}_{0.95}\text{O}_3$, and $\text{Bi}_{0.95}\text{Ba}_{0.05}\text{Fe}_{0.95}\text{Ti}_{0.05}\text{O}_3$ Ceramics. 2011 , 47, 706-709	3
2042	Multiferroic Properties and Leakage Current Mechanisms of $\text{Bi}_{0.9}\text{Eu}_{0.1}\text{FeO}_3$ Thin Films. 2011 , 47, 2784-2787	1
2041	Sm ³⁺ co-substituted BiFeO ₃ thin films prepared by sol-gel technique. 2011 , 11, S255-S259	31
2040	Prediction of transparency and non-linear optical susceptibility of acentric bismuthate crystals. 2011 ,	0
2039	Antiferroelectric (Pb,Bi) _{1-x} Fe _{1+x} O ₃ Perovskites Modulated by Crystallographic Shear Planes. 2011 , 23, 255-265	30
2038	Interface-induced room-temperature multiferroicity in BaTiO ₃ . 2011 , 10, 753-8	310
2037	Local distortions in multiferroic BiMnO as a function of doping. 2011 , 12, 044610	8
2036	Coexistence of ferroelectric triclinic phases in highly strained BiFeO ₃ films. 2011 , 84,	92
2035	Skin layer of BiFeO ₃ single crystals. 2011 , 106, 236101	72
2034	First-principles investigation of morphotropic transitions and phase-change functional responses in BiFeO ₃ -BiCoO ₃ multiferroic solid solutions. 2011 , 107, 057601	73
2033	Temperature-dependent properties of the magnetic order in single-crystal BiFeO ₃ . 2011 , 83,	81

2032	First-principles predictions of low-energy phases of multiferroic BiFeO ₃ . 2011 , 83,	191
2031	Electric control of magnon frequencies and magnetic moment of bismuth ferrite thin films at room temperature. 2011 , 99, 62504-625043	34
2030	Optical anisotropy and charge-transfer transition energies in BiFeO ₃ from 1.0 to 5.5 eV. 2011 , 83,	27
2029	Angular dispersion of oblique phonon modes in BiFeO ₃ from micro-Raman scattering. 2011 , 83,	100
2028	Morphotropic phase boundary, weak ferromagnetism, and strong piezoelectric effect in Bi _{1-x} Ca _x FeO ₃ $\frac{1}{2}$ compounds. 2011 , 113, 1025-1031	18
2027	Spatially modulated antiferromagnetic structures in an easy-plane multiferroic. 2011 , 53, 970-977	18
2026	Acoustic properties of multiferroic BiFeO ₃ over the temperature range 4.2-30 K. 2011 , 83, 39-45	29
2025	Displacive Phase Transitions and Magnetic Structures in Nd-Substituted BiFeO ₃ . 2011 , 23, 2166-2175	104
2024	Antipolar phase in multiferroic BiFeO ₃ at high pressure. 2011 , 84,	46
2023	Structural Evolution of the BiFeO ₃ /LaFeO ₃ System. 2011 , 23, 285-292	148
2022	High-Temperature and High-Pressure Aqueous Solution Formation, Growth, Crystal Structure, and Magnetic Properties of BiFeO ₃ Nanocrystals. 2011 , 23, 1158-1165	44
2021	Dynamic properties of spin cluster glass and the exchange bias effect in BiFeO ₃ nanocrystals. 2011 , 22, 385701	52
2020	Effect of oxygen content during sputtering on the electrical properties of bismuth ferrite thin films. 2011 , 5, 190-192	7
2019	Dielectric properties of BiFeO ₃ ceramics obtained from mechanochemically synthesized nanopowders. 2011 , 27, 154-161	40
2018	Influence of Dy-doping on ferroelectric and dielectric properties in Bi _{1.05} Dy _x FeO ₃ ceramics. 2011 , 22, 323-327	26
2017	The Multiferroic Properties of (Bi _{0.9} Ba _{0.1})(Fe _{0.95} Mn _{0.05})O ₃ Films. 2011 , 24, 1497-1500	5
2016	Room Temperature Multiferroicity in Zn _{0.98} Cu _{0.02} O Film Prepared in N Plasma. 2011 , 24, 2119-2122	
2015	Nanomagnetism in nanocrystalline multiferroic bismuth ferrite lead titanate films. 2011 , 13, 5603-5613	5

2014	Effects of ion-doping at different sites on multiferroic properties of BiFeO ₃ thin films. 2011 , 102, 713-717	23
2013	Crystal structure of Bi _{1-x} TbxFeO ₃ from high-resolution neutron diffraction. 2011 , 184, 1576-1579	12
2012	Block copolymer-templated BiFeO ₃ nanoarchitectures composed of phase-pure crystallites intermingled with a continuous mesoporosity: Effective visible-light photocatalysts?. 2011 , 4, 414-424	37
2011	Microstructure and frequency sensitive electrical conductivity in Fe ₃ BO ₆ :B ₂ O ₃ of a hybrid vitroceramic nanocomposite. 2011 , 208, 2130-2139	3
2010	Low-Symmetry Monoclinic Phases and Polarization Rotation Path Mediated by Epitaxial Strain in Multiferroic BiFeO ₃ Thin Films. 2011 , 21, 133-138	216
2009	E-Field Control of Exchange Bias and Deterministic Magnetization Switching in AFM/FM/FE Multiferroic Heterostructures. 2011 , 21, 2593-2598	132
2008	Reduced coercive field in BiFeO ₃ thin films through domain engineering. <i>Advanced Materials</i> , 2011 , 23, 669-72	24 68
2007	The nature of polarization fatigue in BiFeO ₃ . <i>Advanced Materials</i> , 2011 , 23, 1621-5	24 117
2006	Recent progress in multiferroic magnetoelectric composites: from bulk to thin films. <i>Advanced Materials</i> , 2011 , 23, 1062-87	24 1447
2005	Atomic-scale evolution of local electronic structure across multiferroic domain walls. <i>Advanced Materials</i> , 2011 , 23, 1530-4	24 82
2004	Atomically resolved mapping of polarization and electric fields across ferroelectric/oxide interfaces by Z-contrast imaging. <i>Advanced Materials</i> , 2011 , 23, 2474-9	24 72
2003	One-dimensional nanostructures of ferroelectric perovskites. <i>Advanced Materials</i> , 2011 , 23, 4007-34	24 231
2002	Conduction at domain walls in insulating Pb(Zr _{0.2} Ti _{0.8})O ₃ thin films. <i>Advanced Materials</i> , 2011 , 23, 5377-82	24 296
2001	Structural, ferroelectric and magnetic properties of Bi _{0.85} Sm _{0.15} FeO ₃ perovskite. 2011 , 46, 238-242	39
2000	First-principles lattice dynamics and heat capacity of BiFeO ₃ . 2011 , 59, 4229-4234	46
1999	Multiferroic properties of (Bi _{1-x} Pr _x)(Fe _{0.95} Mn _{0.05})O ₃ thin films. 2011 , 176, 990-995	29
1998	Mn ⁴⁺ :BiFeO ₃ /Zn ²⁺ :BiFeO ₃ bilayered thin films of (1 1 1) orientation. 2011 , 257, 7226-7230	18
1997	Novel carbonyl iron-Bismuth clusters [Synthesis, structure, CO ₂ insertion and potential as molecular precursors for BiFeO ₃ . 2011 , 696, 1647-1651	16

1996	Structure and magnetic order in the series $\text{Bi}_x\text{RE}_{1-x}\text{Fe}_{0.5}\text{Mn}_{0.5}\text{O}_3$ (RE=La,Nd). 2011 , 184, 830-842	14
1995	$\text{BiFeO}_3\text{-PbZrO}_3\text{-PbTiO}_3$ ternary system for high Curie temperature piezoceramics. 2011 , 31, 801-807	26
1994	Epitaxial $\text{SrRuO}_3/\text{BiFeO}_3/\text{SrRuO}_3$ heterostructure sputtered at low temperature. 2011 , 316, 71-74	11
1993	Magnetic characterization of $\text{Bi}(\text{Fe}_{1-x}\text{Mn}_x)\text{O}_3$. 2011 , 375, 1209-1212	8
1992	Enhanced ferroelectric, magnetic and magnetoelectric properties of $\text{Bi}_{1-x}\text{Ca}_x\text{Fe}_{1-x}\text{Ti}_x\text{O}_3$ solid solutions. 2011 , 151, 536-540	36
1991	Enhanced room temperature ferromagnetism in porous BiFeO_3 prepared using cotton templates. 2011 , 151, 624-627	18
1990	Low temperature properties of multiferroic $\text{BiFe}_{0.9}\text{Cr}_{0.1}\text{O}_3$ compound. 2011 , 151, 712-715	16
1989	A study of the optical properties of $\text{Bi}_{0.7}\text{Ba}_{0.15}\text{La}_{0.15}\text{FeO}_3$ thin film. 2011 , 519, 3632-3635	6
1988	The study of the electric and magnetic properties of $\text{PbZr}_{0.2}\text{Ti}_{0.8}\text{O}_3\text{-BiFeO}_3$ multilayers. 2011 , 519, 6269-6277	15
1987	Raman spectra and dielectric function of BiCrO_3 : Experimental and first-principles studies. 2011 , 110, 073501	18
1986	Anisotropic mechanism on distinct transition modes of tip-activated multipolarization switching in epitaxial BiFeO_3 films. 2011 , 109, 024102	2
1985	BiFeO_3 Heterostructures for Electro-Optic Modulators. 2011 ,	
1984	Ferroic phase transition sequence in epitaxial BiFeO_3 thin films. 2011 , 84, 453-473	2
1983	Origin and stability of the dipolar response in a family of tetragonal tungsten bronze relaxors. 2011 , 83,	36
1982	Giant effect of uniaxial pressure on magnetic domain populations in multiferroic bismuth ferrite. 2011 , 107, 067203	28
1981	Epitaxial BiFeO_3 nanostructures fabricated by differential etching of BiFeO_3 films. 2011 , 99, 082904	15
1980	Magneto-elastic tuning of ferroelectricity within a magnetoelectric nanowire. 2011 , 99, 182901	9
1979	EuMnO_3 effects on structure and electrical properties of chemical solution deposited BiFeO_3 thin films. 2011 ,	

1978	Variation of leakage mechanism and potential barrier in La and Ru co-doped BiFeO ₃ thin films. 2011 , 44, 435302	10
1977	Rietveld analysis, dielectric and magnetic properties of Sr and Ti codoped BiFeO ₃ multiferroic. 2011 , 110, 073909	112
1976	Combined effects of bilayer structure and ion substitutions on bismuth ferrite thin films. 2011 , 109, 074101	11
1975	Highly textured Sr, Nb co-doped BiFeO ₃ thin films grown on SrRuO ₃ /Si substrates by rf- sputtering. 2011 , 110, 024114	28
1974	Terahertz and infrared studies of antiferroelectric phase transition in multiferroic Bi _{0.85} Nd _{0.15} FeO ₃ . 2011 , 110, 074112	13
1973	Valence-driven electrical behavior of manganese-modified bismuth ferrite thin films. 2011 , 109, 124118	24
1972	Impedance spectroscopy of bilayered bismuth ferrite thin films. 2011 , 110, 064104	34
1971	Effect of nonmagnetic alkaline-earth dopants on magnetic properties of BiFeO ₃ thin films. 2011 , 110, 033922	26
1970	Ferroelectric and electrical characterization of multiferroic BiFeO ₃ at the single nanoparticle level. 2011 , 99, 252905	9
1969	First-principles prediction of a two dimensional electron gas at the BiFeO ₃ /SrTiO ₃ interface. 2011 , 99, 062902	26
1968	Control of Rectifying and Resistive Switching Behavior in BiFeO ₃ Thin Films. 2011 , 4, 095802	20
1967	The role of SrRuO ₃ bottom layer in strain relaxation of BiFeO ₃ thin films deposited on lattice mismatched substrates. 2011 , 109, 07D914	19
1966	Local leakage current behaviours of BiFeO ₃ films. 2011 , 20, 117701	9
1965	Enhanced Piezoelectric Constant of (1-x)BiFeO ₃ -xBiCoO ₃ Thin Films Grown on LaAlO ₃ Substrate. 2011 , 50, 031505	21
1964	PHASE STRUCTURE, PIEZOELECTRIC AND MULTIFERRIOIC BEHAVIOR OF (K _{0.48} Na _{0.52})NbO ₃ -Co ₂ O ₃ PIEZOELECTRIC CERAMICS. 2011 , 04, 225-229	6
1963	FERROELECTRIC SWITCHING PATH IN MONODOMAIN RHOMBOHEDRAL BiFeO ₃ CRYSTAL: A FIRST-PRINCIPLES STUDY. 2011 , 01, 179-184	1
1962	Broken Symmetry, Ferroic Phase Transitions and Multifunctional Materials. 2011 , 131, 3-24	9
1961	Enhanced piezoelectric and magnetic properties of Bi _{1-x} CaxFe _{1-x/2} Nbx/2O ₃ solid solutions. 2011 , 109, 114102	9

1960	Multiferroism in orientational engineered (La, Mn) co-substituted BiFeO ₃ thin films. 2011 , 109, 114105	31
1959	Composition and temperature-induced structural evolution in La, Sm, and Dy substituted BiFeO ₃ epitaxial thin films at morphotropic phase boundaries. 2011 , 110, 014106	45
1958	Magnetoelectric Feedback among Magnetic Order, Polarization, and Lattice in Multiferroic BiFeO ₃ . 2011 , 80, 114714	35
1957	MAGNETOELECTRIC RESPONSES IN MULTIFERROIC COMPOSITE THIN FILMS. 2011 , 01, 1-16	10
1956	Ferroelectric and Magnetic Properties of Hot-Pressed BiFeO ₃ -PVDF Composite Films. 2011 , 2011, 1-5	14
1955	Nanoscale polarization switching mechanisms in multiferroic BiFeO ₃ thin films. 2011 , 23, 142201	21
1954	High Field Neutron Diffraction Studies on Metamagnetic Transition of Multiferroic BiFeO ₃ . 2011 , 80, 125001	28
1953	Growth rate induced monoclinic to tetragonal phase transition in epitaxial BiFeO ₃ (001) thin films. 2011 , 98, 102902	37
1952	The Structure and Ferromagnetic Properties of the Single Phase Bi _{0.95} Eu _{0.05} Fe _{0.95} Co _{0.05} O ₃ Nanoparticles Prepared by Sol-Gel. 2012 , 512-515, 1434-1437	
1951	Exchange bias in sputtered FM/BiFeO ₃ thin films (FM = Fe and Co). 2012 , 111, 07B105	19
1950	Optical Properties of 0.95BiFeO ₃ -RTiO ₃ (R = Mg, Pb, Ba, Ca and Sr) Thin Films. 2012 , 139, 1-6	
1949	Spectroscopic imaging in piezoresponse force microscopy: New opportunities for studying polarization dynamics in ferroelectrics and multiferroics. 2012 , 2, 61-73	34
1948	Low-Temperature Synthesis and Characterization of Single-Phase BiFeO ₃ Nano-Crystallites. 2012 , 164, 115-119	
1947	Effect of the Type of Solvent and Bi-Stoichiometric Excess on the Purity of Nanocrystalline Bismuth Ferrite Single Phase. 2012 , 1454, 45-50	1
1946	Piezoresponse Force Microscopy Studies on (100), (110) and (111) Epitaxially Growth BiFeO ₃ Thin Films. 2012 , 1477, 7	1
1945	Structural and Magnetic Properties of Bi(Fe _{1-x} Mnx)O ₃ . 2012 , 25, 204-208	2
1944	Origin of magnetic anisotropy and spiral spin order in multiferroic BiFeO ₃ . 2012 , 100, 242413	21
1943	Effects of local structural distortion on magnetization in BiFeO ₃ with Pr, Ba co-doping. 2012 , 111, 07C707	39

1942	Synthesis and study of Bi _{0.9} Tb _{0.1} Fe _{0.9} Mn _{0.1} O ₃ ceramics. 2012 ,	1
1941	Effect of (Bi, La)(Fe, Zn)O ₃ thickness on the microstructure and multiferroic properties of BiFeO ₃ thin films. 2012 , 112, 094109	5
1940	Aging and rejuvenation effects in bismuth ferrite micro-cubes. 2012 ,	
1939	Room temperature ferroelectric and magnetic investigations and detailed phase analysis of Aurivillius phase Bi ₅ Ti ₃ Fe _{0.7} Co _{0.3} O ₁₅ thin films. 2012 , 112, 052010	37
1938	Multiferroic properties of Aurivillius phase Bi ₆ Fe ₂ Co _x Ti ₃ O ₁₈ thin films prepared by a chemical solution deposition route. 2012 , 101, 122402	70
1937	Structural transitions and unusual magnetic behavior in Mn-doped Bi _{1-x} La _x FeO ₃ perovskites. 2012 , 112, 084102	21
1936	Effects of Ambient Pressure on the Structural and Magnetic Properties of Bismuth Ferrite Nanoparticles Prepared by Pulsed Laser Deposition (PLD). 2012 , 722, 53-60	
1935	The magnetic structure of an epitaxial BiMn _{0.5} Fe _{0.5} O ₃ thin film on SrTiO ₃ (001) studied with neutron diffraction. 2012 , 101, 172404	14
1934	Domain switching in spray pyrolysis-deposited nano-crystalline BiFeO ₃ films. 2012 , 86, 065701	3
1933	Structural and insulator-to-metal phase transition at 50 GPa in GdMnO ₃ . 2012 , 85,	23
1932	Piezoresponse force microscopy and vibrating sample magnetometer study of single phased Mn induced multiferroic BiFeO ₃ thin film. 2012 , 111, 064110	23
1931	Orientation-dependent surface potential behavior in Nb-doped BiFeO ₃ . 2012 , 100, 172901	12
1930	Mapping of the epitaxial stabilization of quasi-tetragonal BiFeO ₃ with deposition temperature. 2012 , 100, 122905	12
1929	Anisotropic conductivity of uncharged domain walls in BiFeO ₃ . 2012 , 86,	53
1928	Investigation of the improved performance in a graphene/polycrystalline BiFeO ₃ /Pt photovoltaic heterojunction: Experiment, modeling, and application. 2012 , 112, 054103	20
1927	Influence of La and Mn dopants on the current-voltage characteristics of BiFeO ₃ /ZnO heterojunction. 2012 , 111, 074101	34
1926	Origin of ferromagnetism and oxygen-vacancy ordering induced cross-controlled magnetoelectric effects at room temperature. 2012 , 111, 073904	33
1925	Wavelength dependence of photoinduced deformation in BiFeO ₃ . 2012 , 85,	43

1924	Effects of Structural Collapse and Magnetic Moment on Magnetization in $\text{Bi}_{0.8-x}\text{Pr}_x\text{Ba}_{0.2}\text{FeO}_3$ ($x \leq 0.1$) Multiferroics. 2012 , 48, 4022-4025	1
1923	Effects of Annealing Atmosphere on Structure and Electrical Properties of $(\text{Bi}_{0.9}\text{Eu}_{0.1})(\text{Fe}_{0.9}\text{Mn}_{0.1})\text{O}_3$ Thin Films. 2012 , 132, 39-44	2
1922	Reliable polarization switching of BiFeO_3 . 2012 , 370, 4872-89	29
1921	Origin of the enhanced polarization in La and Mg co-substituted BiFeO_3 thin film during the fatigue process. 2012 , 100, 042902	33
1920	Exchange Bias in Polycrystalline $\text{BiFe}_{1-x}\text{Mn}_x\text{O}_3/\text{Ni}_{81}\text{Fe}_{19}$ Bilayers. 2012 , 29, 097701	6
1919	Dielectric and Magnetic Behaviors of a Composite of BiFeO_3/Ba Ferrite Synthesized by a Process. 2012 , 1, N49-N52	
1918	Sputter-prepared $\text{BiFeO}_3(001)$ films on $\text{La}_{10}\text{FePt}(001)/\text{glass}$ substrates. 2012 , 111, 07D918	17
1917	Structural transformation and improved dielectric and magnetic properties in Ti-substituted $\text{Bi}_{0.8}\text{La}_{0.2}\text{FeO}_3$ multiferroics. 2012 , 45, 165001	46
1916	Study on the Structural, Electrical, and Magnetic Properties of Pure and $(\text{Pr}^{3+}, \text{Co}^{2+})$ -Doped BiFeO_3 Powders and Thin Films. 2012 , 51, 11PG06	
1915	Effect of Praseodymium Species on the Structural and Functional Properties of Nanocrystalline BiFeO_3 Powders and Thin Films. 2012 , 1454, 39-44	0
1914	Preparation and Properties of Multiferroic La-Doped BiFeO_3 Thin Film. 2012 , 486, 417-421	2
1913	Magnetoelectricity in multiferroic particulate composites with arbitrary crystallographic orientation. 2012 , 21, 105038	4
1912	Active control of ferroelectric switching using defect-dipole engineering. <i>Advanced Materials</i> , 2012 , 24, 6490-5	24 62
1911	Elimination of domain backswitching in $\text{BiFe}_{0.95}\text{Mn}_{0.05}\text{O}_3$ thin films by lowering the layer thickness. 2012 , 111, 066107	7
1910	Ferroic states and phase coexistence in $\text{BiFeO}_3\text{-BaTiO}_3$ solid solutions. 2012 , 112, 104112	54
1909	Phase Transition and Electrical Properties of $\text{Ba}_{0.7}\text{Ca}_{0.3}\text{TiO}_3\text{BiFeO}_3$ Ceramics. 2012 , 95, 3901-3905	9
1908	Low Temperature Synthesis, Structural, Optical and Magnetic Properties of Bismuth Ferrite Nanoparticles. 2012 , 95, 3678-3682	51
1907	Hydrothermal Synthesis and Magnetic Properties of Bismuth Ferrites Nanocrystals with Various Morphology. 2012 , 95, 3922-3927	33

1906	Advanced synthesis techniques and routes to new single-phase multiferroics. 2012 , 16, 199-215	84
1905	Magnetically Driven Dielectric and Structural Behavior in Bi _{0.5} La _{0.5} FeO ₃ . 2012 , 24, 4563-4571	20
1904	Magnetoelastic coupling and multiferroic ferroelastic/magnetic phase transitions in the perovskite KMnF ₃ . 2012 , 85,	48
1903	Integration of first-principles methods and crystallographic database searches for new ferroelectrics: Strategies and explorations. 2012 , 195, 21-31	38
1902	Non-linear thermal evolution of the crystal structure and phase transitions of LaFeO ₃ investigated by high temperature X-ray diffraction. 2012 , 196, 249-254	61
1901	Electric-field control of magnetic ordering in the tetragonal-like BiFeO ₃ . 2012 , 97, 57007	21
1900	Magnetoelectric and multiferroic media. 2012 , 55, 557-581	404
1899	Suppression of mixed-phase areas in highly elongated BiFeO ₃ thin films on NdAlO ₃ substrates. 2012 , 86,	31
1898	Rhombohedral↔orthorhombic morphotropic phase boundary in BiFeO ₃ -based multiferroics: first-principles prediction. 2012 , 22, 1667-1672	45
1897	Polar and nonpolar phases of BiMO ₃ : A review. 2012 , 195, 32-40	118
1896	Evidence of sharp and diffuse domain walls in BiFeO ₃ by means of unit-cell-wise strain and polarization maps obtained with high resolution scanning transmission electron microscopy. 2012 , 109, 047601	50
1895	Potential barrier increase due to Gd doping of BiFeO ₃ layers in Nb:SrTiO ₃ -BiFeO ₃ -Pt structures displaying diode-like behavior. 2012 , 100, 252903	19
1894	Structural and magnetic properties of isovalently substituted multiferroic BiFeO ₃ : Insights from Raman spectroscopy. 2012 , 86,	140
1893	Domain structure and piezoelectric response in lanthanide rare earth-substituted multiferroic BiFeO ₃ thin films. 2012 , 45, 325001	14
1892	Perovskite B-Site Compositional Control of [110] Polar Displacement Coupling in an Ambient-Pressure-Stable Bismuth-based Ferroelectric. 2012 , 124, 10928-10933	4
1891	Perovskite B-site compositional control of [110] _p polar displacement coupling in an ambient-pressure-stable bismuth-based ferroelectric. 2012 , 51, 10770-5	11
1890	Effect of bilayer structure and a SrRuO ₃ buffer layer on ferroelectric properties of BiFeO ₃ thin films. 2012 , 109, 57-61	9
1889	Effect of particle morphology on the photocatalytic activity of BiFeO ₃ microcrystallites. 2012 , 23, 1869-1874	24

1888	Structure evolution and photocatalytic activity of BiFeO ₃ powders synthesized by hydrothermal decomposition of metal-EDTA complexes. 2012 , 23, 2145-2151	3
1887	Tunable morphology and optical absorption of bismuth ferrite synthesized by sol-gel/hydrothermal method. 2012 , 23, 2276-2281	9
1886	Synthesis of BiFeO ₃ nanoparticles with small size. 2012 , 64, 104-109	5
1885	Particle size dependent magnetic properties and phase transitions in multiferroic BiFeO ₃ nano-particles. 2012 , 543, 206-212	96
1884	Lattice dynamics and dielectric functions of multiferroic BiFeO ₃ /c-sapphire films determined by infrared reflectance spectra and temperature-dependent Raman scattering. 2012 , 525, 188-194	8
1883	Magnon Raman spectroscopy and in-plane dielectric response in BiFeO ₃ : Relation to the Polomska transition. 2012 , 85,	28
1882	Photoluminescence Investigation of Defects and Optical Band Gap in Multiferroic BiFeO ₃ Single Crystals. 2012 , 5, 035802	40
1881	Emergent phenomena at multiferroic heterointerfaces. 2012 , 370, 4856-71	38
1880	The structural and multiferroic properties of (Bi _{1-x} La _x)(Fe _{0.95} Co _{0.05})O ₃ ceramics. 2012 , 407, 4793-4796	10
1879	Slow magnetic dynamics in the K ₃ M ₃ IM ₂ IF ₁₅ multiferroic system. 2012 , 112, 073908	4
1878	Weak ferromagnetism in La-doped BiFeO ₃ multiferroic thin films. 2012 , 111, 123916	38
1877	Effect of Barium Titanate buffer layer on dielectric properties of Sodium Bismuth Titanate thin films grown using Pulsed Laser Deposition. 2012 ,	
1876	Study of strain effect on in-plane polarization in epitaxial BiFeO ₃ thin films using planar electrodes. 2012 , 86,	43
1875	Combinatorial search of structural transitions: Systematic investigation of morphotropic phase boundaries in chemically substituted BiFeO ₃ . 2012 , 27, 2691-2704	38
1874	Electrical Properties of (Bi _{0.9} Ho _{0.1})(Fe _{0.975} Cr _{0.025})O ₃ Thin Films Prepared by Using a Chemical Solution Deposition. 2012 , 140, 49-55	
1873	A method to improve electrical properties of BiFeO ₃ thin films. 2012 , 4, 1182-5	45
1872	A simple law governing coupled magnetic orders in perovskites. 2012 , 24, 312201	46
1871	Core/Shell Magnetite/Bismuth Oxide Nanocrystals with Tunable Size, Colloidal, and Magnetic Properties. 2012 , 24, 319-324	22

1870	Discovery and Design of Functional Materials: Integration of Database Searching and First Principles Calculations. 2012 , 34, 14-23	22
1869	Resistive switching in ceramic multiferroic Bi _{0.9} Ca _{0.1} FeO ₃ . 2012 , 407, 3144-3146	15
1868	Physics, chemistry and synthesis methods of nanostructured bismuth ferrite (BiFeO ₃) as a ferroelectro-magnetic material. 2012 , 40, 6-15	106
1867	Enhanced magnetic parameters in the morphotropic phase boundary region of nanocrystalline multiferroic Bi _{1-x} La _x FeO ₃ . 2012 , 152, 1609-1612	16
1866	Strain dependence of polarization and piezoelectric response in epitaxial BiFeO ₃ thin films. 2012 , 24, 162202	53
1865	Regular nanodomain vertex arrays in BiFeO ₃ single crystals. 2012 , 85,	7
1864	First-principles investigation of the structural phases and enhanced response properties of the BiFeO ₃ -LaFeO ₃ multiferroic solid solution. 2012 , 85,	50
1863	On the Link Between Octahedral Rotations and Conductivity in the Domain Walls of BiFeO ₃ . 2012 , 433, 65-73	15
1862	Sillen-Laurivillius Intergrowth Phases as Templates for Naturally Layered Multiferroics. 2012 , 24, 3932-3942	23
1861	Piezoelectric nonlinearity and frequency dispersion of the direct piezoelectric response of BiFeO ₃ ceramics. 2012 , 112, 064114	33
1860	Magnetoelectric properties of PbZr _{0.53} Ti _{0.47} O ₃ /Ni _{0.65} Zn _{0.35} Fe ₂ O ₄ multiferroic nanocomposites. 2012 , 2, 261-273	69
1859	Spintronic oxides grown by laser-MBE. 2012 , 45, 033001	97
1858	Nanostructured BiMnO ₃ +Fe obtained at ambient pressure: analysis of its multiferroicity. 2012 , 22, 9928	23
1857	Enhanced magnetic properties of chemical solution deposited BiFeO ₃ thin film with ZnO buffer layer. 2012 , 177, 908-912	6
1856	Dielectric and optical properties of BiFeO ₃ /(Na _{0.5} Bi _{0.5})TiO ₃ thin films deposited on Si substrate using LaNiO ₃ as buffer layer for photovoltaic devices. 2012 , 513, 154-158	16
1855	Multiferroic properties of Y-doped BiFeO ₃ . 2012 , 540, 36-38	38
1854	High optical performance and practicality of active plasmonic devices based on rhombohedral BiFeO ₃ . 2012 , 6, 684-689	15
1853	Magnetic and electrical properties of multiferroic BiFeO ₃ , its synthesis and applications. 2012 , 48, 1210-1225	7

1852	Sputter-prepared (001) BiFeO ₃ thin films with ferromagnetic L10-FePt(001) electrode on glass substrates. 2012 , 7, 435	17
1851	Structural and Multiferroic Properties of Chemical-Solution-Deposited (Bi _{0.95} La _{0.05})(Fe _{0.97} Cr _{0.03})O ₃ /NiFe ₂ O ₄ Double-Layered Thin Film. 2012 , 51, 09MD06	1
1850	Multiferroic properties of Ba ²⁺ and Gd ³⁺ -co-doped bismuth ferrite: magnetic, ferroelectric and impedance spectroscopic analysis. 2012 , 45, 455002	91
1849	Multiferroic and fatigue behavior of BiFe(0.95)Mn(0.05)O ₃ /Bi(0.90)La(0.10)Fe(0.85)Zn(0.15)O ₃ bilayered thin films. 2012 , 59, 14-20	3
1848	Prominent electrochromism through vacancy-order melting in a complex oxide. 2012 , 3, 799	69
1847	Anisotropic bimodal distribution of blocking temperature with multiferroic BiFeO ₃ epitaxial thin films. 2012 , 100, 072402	19
1846	Nanoscale characterization of emergent phenomena in multiferroics. 2012 , 16, 216-226	14
1845	On the problem of coexistence of the weak ferromagnetism and the spin flexoelectricity in multiferroic bismuth ferrite. 2012 , 99, 57003	39
1844	Electrical properties in lanthanides substituted (Bi _{0.9} A _{0.1})(Fe _{0.975} Co _{0.025})O ₃ [A = La, Eu, Gd] thin films. 2012 , 61, 1409-1412	3
1843	Effect of sintering temperature on the piezoelectric properties in BiFeO ₃ -BaTiO ₃ ceramics. 2012 , 61, 947-950	34
1842	Crystal structure and piezoelectric properties of KNbO ₃ -BiFeO ₃ ceramics. 2012 , 61, 956-960	3
1841	Thermal evolution of the full three-dimensional magnetic excitations in the multiferroic BiFeO ₃ . 2012 , 86,	17
1840	Magnetic cycloid of BiFeO ₃ from atomistic simulations. 2012 , 109, 037207	67
1839	Enhanced Magnetization and Ferroelectric Switching in Multiferroic BST/BNFO Superstructures. 2012 , 433, 158-163	10
1838	Observation of Enhanced Dielectric Coupling and Room-Temperature Ferromagnetism in Chemically Synthesized BiFeO ₃ @SiO ₂ Core-Shell Particles. 2012 , 116, 19503-19511	38
1837	Structural, Magnetic, and Electrical Properties of Bi _{1-x} La _x MnO ₃ (x = 0.0, 0.1, and 0.2) Solid Solutions. 2012 , 24, 199-208	15
1836	magnetic dispersion and anisotropy in multiferroic BiFeO ₃ . 2012 , 109, 067205	79
1835	Ferroelectric and magnetic properties of Fe-doped BaTiO ₃ thin films grown by the pulsed laser deposition. 2012 ,	

1834	High-temperature phonon spectra of multiferroic BiFeO ₃ from inelastic neutron spectroscopy. 2012 , 100, 142901	7
1833	Development of NMR: Solid-State NMR and Materials Science, Post 1995. 2012 ,	3
1832	The Structure-Property Investigation of Bi _{1-x} CexFeO ₃ (x = 0, 0.05) Li Battery: In Situ XRD and XANES Studies. 2012 , 116, 20230-20238	16
1831	Oxide interfaces: pathways to novel phenomena. 2012 , 15, 320-327	114
1830	BiFeO ₃ /Na _{0.5} Bi _{0.5} TiO ₃ butterfly wing scales: Synthesis, visible-light photocatalytic and magnetic properties. 2012 , 32, 4335-4340	24
1829	Study of structural, magnetic and electrical properties on Ho-substituted BiFeO ₃ . 2012 , 152, 2071-2077	45
1828	Strain-induced phase transitions in multiferroic BiFeO ₃ . 2012 , 376, 3368-3371	5
1827	Structure and phase transition of BiFeO ₃ cubic micro-particles prepared by hydrothermal method. 2012 , 47, 3630-3636	28
1826	Low-temperature hydrothermal synthesis of BiFeO ₃ microcrystals and their visible-light photocatalytic activity. 2012 , 47, 3513-3517	44
1825	Preparation, structural, dielectric and magnetic properties of LaFeO ₃ /PbTiO ₃ solid solutions. 2012 , 47, 3253-3268	27
1824	Nanoscale piezoresponse and magnetic studies of multiferroic Co and Pr co-substituted BFO thin films. 2012 , 47, 4240-4245	35
1823	Microwave Response of BiFeO ₃ Films in Parallel-Plate Capacitors. 2012 , 134, 111-117	2
1822	Doping BiFeO ₃ : approaches and enhanced functionality. 2012 , 14, 15953-62	286
1821	Electronic structure of YMn ₂ O ₅ studied by EELS and first-principles calculations. 2012 , 7, 429-434	3
1820	Electric field driven phase transition and possible twinning quasi-tetragonal phase in compressively strained BiFeO ₃ thin films. 2012 , 7, 424-428	3
1819	Microstructure of BaTiO ₃ /Bi(Mg _{1/2} Ti _{1/2})O ₃ /BiFeO ₃ Piezoelectric Ceramics. 2012 , 51, 09LD04	18
1818	Multiferroic complex metal oxides: Main features of preparation, structure, and properties. 2012 , 163-238	12
1817	Dielectric and Magnetic Properties of Magnetoelectric Delafossites. 2012 , 438, 101-106	4

1816	Microstructure of the potentially multiferroic Fe/BaTiO ₃ epitaxial interface. 2012 , 92, 1733-1747	1
1815	Lead-Free Relaxor-Like 0.75Bi _{0.5} K _{0.5} TiO ₃ -0.25BiFeO ₃ Ceramics with Large Electric Field-Induced Strain. 2012 , 439, 88-94	25
1814	Mn doping-induced structural and magnetic transformations in the antiferroelectric phase of the Bi _{1-x} NdxFeO ₃ perovskites. 2012 , 112, 064105	12
1813	Controlling magnetoelectric coupling by nanoscale phase transformation in strain engineered bismuth ferrite. 2012 , 4, 3175-83	34
1812	Photo-to-current response of Bi ₂ Fe ₄ O ₉ nanocrystals synthesized through a chemical co-precipitation process. 2012 , 36, 1297	35
1811	Enhanced electric conductivity at ferroelectric vortex cores in BiFeO ₃ . 2012 , 8, 81-88	271
1810	Mechanical milling assisted synthesis of Ba _{1-x} Mn _x co-substituted BiFeO ₃ ceramics and their properties. 2012 , 45, 415302	27
1809	Electric field control of magnetism in multiferroic heterostructures. 2012 , 24, 333201	289
1808	Effect of Mn substitution on crystal structure and magnetic properties of Bi _{1-x} Pr _x FeO ₃ multiferroics. 2012 , 45, 045302	28
1807	Photoluminescence from Bi ₅ (GaCl ₄) ₃ molecular crystal. 2012 , 41, 11055-61	24
1806	Soft phonon mode coupled with antiferromagnetic order in incipient-ferroelectric Mott insulators Sr _{1-x} BaxMnO ₃ . 2012 , 86,	30
1805	Heliconical magnetic order and field-induced multiferroicity of the Co ₂ Y-type hexaferrite Ba _{0.3} Sr _{1.7} Co ₂ Fe ₁₂ O ₂₂ . 2012 , 86,	41
1804	Pressure-induced phase transitions and structure of chemically ordered nanoregions in the lead-free relaxor ferroelectric Na _{1/2} Bi _{1/2} TiO ₃ . 2012 , 86,	28
1803	Antiferromagnetic transitions in tetragonal-like BiFeO ₃ . 2012 , 85,	53
1802	A polar corundum oxide displaying weak ferromagnetism at room temperature. 2012 , 134, 3737-47	59
1801	Polarization and strain response in Bi _{0.5} K _{0.5} TiO ₃ -BiFeO ₃ ceramics. 2012 , 101, 252904	44
1800	Anharmonic phonons and magnons in BiFeO ₃ . 2012 , 85,	28
1799	High-temperature ferroic phase transitions and paraelectric cubic phase in multiferroic Bi _{0.95} Hf _{0.05} Zr _{0.1} O ₃ . 2012 , 111, 114106	5

1798	Structural, morphological and piezoresponse studies of Pr and Sc co-substituted BiFeO ₃ ceramics. 2012 , 45, 055302	63
1797	Negative capacitance induced by redistribution of oxygen vacancies in the fatigued BiFeO ₃ -based thin film. 2012 , 101, 022904	8
1796	Multiferroic Memories. 2012 , 2012, 1-12	73
1795	Electronic Band Structures and Phase Transitions of Ferroelectric and Multiferroic Oxides. 2012 ,	
1794	In-plane dielectric and magnetoelectric studies of BiFeO ₃ . 2012 , 209, 1207-1212	24
1793	Grain and grain boundary effects in Ca ²⁺ doped BiFeO ₃ multiferroic ceramics. 2012 , 249, 1639-1645	26
1792	Direct imaging of both ferroelectric and antiferromagnetic domains in multiferroic BiFeO ₃ single crystal using x-ray photoemission electron microscopy. 2012 , 100, 042406	13
1791	A separation mechanism of photogenerated charges and magnetic properties for BiFeO ₃ microspheres synthesized by a facile hydrothermal method. 2012 , 14, 8376-81	18
1790	Advanced nanoarchitectures for solar photocatalytic applications. 2012 , 112, 1555-614	1888
1789	BiGaO ₃ -Based Perovskites: A Large Family of Polar Materials. 2012 , 24, 3056-3064	45
1788	Observation of room temperature saturated ferroelectric polarization in Dy substituted BiFeO ₃ ceramics. 2012 , 111, 074105	65
1787	Relaxor ferroelectric behavior of BaMnO ₃ (2H) at room temperature. 2012 , 100, 042904	16
1786	Magnetic enhancement across a ferroelectric-antiferroelectric phase boundary in Bi _{1-x} NdxFeO ₃ . 2012 , 111, 053927	61
1785	Structure and magnetic properties of Y _{1-x} LuxFeO ₃ (0 ≤ x ≤ 1) ceramics. 2012 , 111, 053911	39
1784	Magnetocapacitance effect in nonmultiferroic YFeO ₃ single crystal. 2012 , 111, 034103	46
1783	Dielectric relaxation in the DyMn _{1-x} FexO ₃ system. 2012 , 111, 034104	21
1782	Ferroelectric properties of BiFeO ₃ ceramics sintered under low oxygen partial pressure. 2012 , 60, 83-87	11
1781	Local mapping of generation and recombination lifetime in BiFeO ₃ single crystals by scanning probe photoinduced transient spectroscopy. 2012 , 12, 2193-8	60

1780	Surface phase transitions in BiFeO ₃ below room temperature. 2012 , 85,	59
1779	Local Oxygen-Vacancy Ordering and Twinned Octahedral Tilting Pattern in the Bi _{0.81} Pb _{0.19} FeO _{2.905} Cubic Perovskite. 2012 , 24, 1378-1385	31
1778	Temperature Dependent Magnetic, Dielectric Studies of Sm-Substituted Bulk BiFeO ₃ . 2012 , 25, 1109-1114	10
1777	Raman study of the phonon symmetries in BiFeO ₃ single crystals. 2012 , 86,	44
1776	Ultrathin limit and dead-layer effects in local polarization switching of BiFeO ₃ . 2012 , 85,	60
1775	Effect of pressure on the band gap and the local FeO ₆ environment in BiFeO ₃ . 2012 , 85,	43
1774	Studies on multiferroic materials in high magnetic fields. 2012 , 7, 386-398	20
1773	High temperature extended x-ray absorption fine structure study of multiferroic BiFeO ₃ . 2012 , 24, 336005	3
1772	Epitaxial Magnetic Oxide Nanocrystals Via Phase Decomposition of Bismuth Perovskite Precursors. 2012 , 22, 5224-5230	24
1771	Electrical control of multiferroic orderings in mixed-phase BiFeO ₃ films. <i>Advanced Materials</i> , 2012 , 24, 3070-5	24 49
1770	Multiferroics by Rational Design: Implementing Ferroelectricity in Molecule-Based Magnets. 2012 , 124, 8481-8485	34
1769	Multiferroics by rational design: implementing ferroelectricity in molecule-based magnets. 2012 , 51, 8356-60	147
1768	Study of nanocrystalline BiMnO ₃ -PbTiO ₃ : synthesis, structural elucidation, and magnetic characterization of the whole solid solution. 2012 , 18, 9075-82	13
1767	Structural, spectroscopic, magnetic and electrical characterization of Ca-doped polycrystalline bismuth ferrite, Bi(1-x)Ca(x)FeO(3-x/2) (x 0.1). 2012 , 24, 045905	29
1766	Domain wall nanoelectronics. 2012 , 84, 119-156	848
1765	Magnetoelectric and multiferroic media. 2012 , 182, 593	63
1764	Photoexcitation of gigahertz longitudinal and shear acoustic waves in BiFeO ₃ multiferroic single crystal. 2012 , 100, 212906	48
1763	Atomic-scale evolution of modulated phases at the ferroelectric-antiferroelectric morphotropic phase boundary controlled by flexoelectric interaction. 2012 , 3, 775	135

1762	Synthesis and dielectric properties of BiFeO ₃ derived from molten salt method. 2012 , 23, 990-994	39
1761	Decomposition behavior and dielectric properties of Ti-doped BiFeO ₃ ceramics derived from molten salt method. 2012 , 23, 1533-1537	14
1760	High temperature piezoelectric BiScO ₃ /PbTiO ₃ synthesized by mechanochemical methods. 2012 , 60, 1174-1183	41
1759	Multiferroic and magnetoelectric heterostructures. 2012 , 60, 2449-2470	158
1758	(Ba, Ca)(Ti, Zr)O ₃ -BiFeO ₃ lead-free piezoelectric ceramics. 2012 , 12, 534-538	49
1757	Dielectric properties and related ferroelectric domain configurations in multiferroic BiFeO ₃ /BaTiO ₃ solid solutions. 2012 , 38, S411-S414	52
1756	Effect of BNBTKNN on the electrical properties of bismuth ferrite thin films. 2012 , 38, 707-711	1
1755	Multiferroic and piezoelectric properties of 0.65BiFeO ₃ /0.35BaTiO ₃ ceramic with pseudo-cubic symmetry. 2012 , 38, 3499-3502	62
1754	Crystal structure refinement of Bi _{1-x} NdxFeO ₃ multiferroic by the Rietveld method. 2012 , 38, 3935-3942	107
1753	Photo-induced properties in BiFeO ₃ film. 2012 , 132, 364-367	7
1752	Mechanism of small-polaron formation in the biferroic YCrO ₃ doped with calcium. 2012 , 133, 1011-1017	35
1751	Enhancing the magnetic characteristics of BiFeO ₃ nanoparticles by Ca, Ba co-doping. 2012 , 135, 144-149	38
1750	Conductor/insulator transition and electronic structure of Ca-doped BiFeO ₃ films. 2012 , 83, 124-126	25
1749	Effect of Ba(Cu _{1/3} Nb _{2/3})O ₃ content on multiferroic properties in BiFeO ₃ ceramics. 2012 , 177, 451-455	8
1748	Magnetism and electrode dependant resistive switching in Ca-doped ceramic bismuth ferrite. 2012 , 177, 471-475	20
1747	Modulations in structural and ferroelectric properties due to tensile strain in BiFeO ₃ films on MgAl ₂ O ₄ substrates induced by thermal-expansion. 2012 , 177, 685-688	2
1746	Bi _{0.75} Sr _{0.25} FeO ₃ Revealing order/disorder phenomena by combining diffraction techniques. 2012 , 152, 331-336	5
1745	Multiferroic, magnetoelectric and optical properties of Mn doped BiFeO ₃ nanoparticles. 2012 , 152, 525-529	125

1744	Raman spectroscopic and X-ray diffraction investigations of epitaxial BiCrO ₃ thin films. 2012 , 520, 4590-4594	2
1743	Growth temperature dependent dielectric properties of BiFeO ₃ thin films deposited on silica glass substrates. 2012 , 520, 4470-4474	23
1742	Study on dielectric and magnetic properties of Ho ₃ Fe ₅ O ₁₂ ceramics. 2012 , 407, 485-488	15
1741	Magnetic properties of Ni-substituted BiFeO ₃ . 2012 , 407, 560-563	17
1740	Enhanced magnetization and suppressed current leakage in BiFeO ₃ ceramics prepared by spark plasma sintering of sol-gel derived nanoparticles. 2012 , 407, 1196-1202	23
1739	Nonmonotonic variation of magnetization in Bi _{0.8} La _{0.2} PbxFeO ₃ (0 ≤ x ≤ 0.2) multiferroics. 2012 , 324, 200-204	16
1738	Wide Range Magnetoresistance in Rare Earth Manganite Through Substitution of Magnetic Impurity. 2012 , 48, 1155-1158	2
1737	Domain walls, magnetization, and magnetoelectric effect in bismuth ferrite films. 2012 , 54, 1070-1078	5
1736	Effect of BiFeO ₃ ceramics morphology on electrodynamic properties in the terahertz frequency range. 2012 , 54, 1191-1198	6
1735	Origin of a Tetragonal BiFeO ₃ Phase with a Giant c/a Ratio on SrTiO ₃ Substrates. 2012 , 22, 937-942	57
1734	Spatially resolved photodetection in leaky ferroelectric BiFeO ₃ . <i>Advanced Materials</i> , 2012 , 24, OP49-53	25
1733	Structural and magnetic phase transitions in Bi _{1-x} Pr _x FeO ₃ perovskites. 2012 , 47, 1578-1581	55
1732	Temperature dependence of optical and structural properties of ferroelectric Bi _{3.15} Nd _{0.85} Ti ₃ O ₁₂ thin film derived by sol-gel process. 2012 , 61, 236-242	5
1731	Multiferroic behavior in elemental selenium below 40 K: effect of electronic topology. 2013 , 3, 2051	8
1730	The Multiferroic Properties of Zn Doped BiFeO ₃ Thin Films. 2013 , 26, 2785-2789	13
1729	Magnetic Field-Induced Ferroelectric Switching in Multiferroic Aurivillius Phase Thin Films at Room Temperature. 2013 , 96, 2339-2357	137
1728	Effect of particle size on ferroelectric and magnetic properties of BiFeO ₃ nanopowders. 2013 , 24, 355701	54
1727	Dielectric, Ferroelectric, and Piezoelectric Properties of BiFeO ₃ /BaTiO ₃ Ceramics. 2013 , 96, 3163-3168	118

1726	Tunable bandgap in BiFeO ₃ nanoparticles: The role of microstrain and oxygen defects. 2013 , 103, 022910	184
1725	Pressure effect on structural and vibrational properties of Y-substituted BiFeO ₃ . 2013 , 25, 365401	5
1724	Structural and improved electrical properties of rare earth (Sm, Tb and Ho) doped BiFe _{0.975} Mn _{0.025} O ₃ thin films. 2013 , 31, 275-279	6
1723	Weak ferromagnetic polar phase in the BiFe _{1-x} Ti _x O ₃ multiferroics. 2013 , 48, 3852-3856	12
1722	Lattice distortion and room-temperature ferroelectric properties of (Sm, Cr) co-doped BiFeO ₃ thin films. 2013 , 24, 4296-4301	6
1721	Raman and electrical studies of multiferroic BiFeO ₃ . 2013 , 24, 3581-3586	11
1720	Effect of Gd-substitution on phase transition and conduction mechanism of BiFeO ₃ . 2013 , 24, 2767-2771	39
1719	Synthesis of single phase bismuth ferrite compound by reliable one-step method. 2013 , 24, 2950-2955	30
1718	Structural, dielectric and magnetic characterization of large scale template synthesized Gd doped BiFeO ₃ nanowires. 2013 , 24, 2112-2115	11
1717	Effect of simultaneous chemical substitution of A and B sites on the electronic structure of BiFeO ₃ films grown on BaTiO ₃ /SiO ₂ /Si substrate. 2013 , 24, 2128-2134	23
1716	Effect of rare earth dopants on the morphologies and photocatalytic activities of BiFeO ₃ microcrystallites. 2013 , 24, 1530-1535	20
1715	Multiferroic and optical properties of Pr-substituted bismuth ferrite ceramics. 2013 , 210, 1442-1447	19
1714	Electrophoretic deposition of multiferroic BiFeO ₃ sub-micrometric particles from stabilized suspensions. 2013 , 33, 1325-1333	29
1713	Enhancement of magnetization in Er doped BiFeO ₃ thin Film. 2013 , 67, 1-7	14
1712	Influence of lone pair doping on the multiferroic property of orthorhombic HoMnO ₃ : ab initio prediction. 2013 , 25, 385901	2
1711	Electromagnon excitations in canted-spin multiferroics. 2013 , 102, 252906	6
1710	Surface distortions in a weak ferromagnet. 2013 , 55, 986-989	2
1709	Ferroelectric and magnetic properties of Fe-doped BaTiO ₃ thin films grown by the pulsed laser deposition. 2013 , 113, 187219	37

1708	Effect of lone-electron-pair cations on the orientation of crystallographic shear planes in anion-deficient perovskites. 2013 , 52, 10009-20	14
1707	Multiferroic and resistive switching behaviors in BiFe _{0.95} Cr _{0.05} O ₃ thin films deposited on Pt/Ti/SiO ₂ /Si substrates. 2013 , 113, 779-785	
1706	Bismuth ferrite composite thin films. 2013 , 111, 1017-1020	4
1705	Electromagnon in multiferroic materials with Dzyaloshinsky-Moriya-interaction-induced helical spin structures. 2013 , 62, 1763-1768	3
1704	Structural phase relations in perovskite-structured BiFeO ₃ -based multiferroic compounds. 2013 , 2, 103-111	18
1703	Thermal diffusion and heat conductivity of BiFeO ₃ and Bi _{0.95} La _{0.05} FeO ₃ multiferroics at high temperatures. 2013 , 97, 470-472	10
1702	Artificial multiferroic heterostructures. 2013 , 1, 6731	66
1701	Transition-Metal Perovskites. 2013 , 1-40	1
1700	Dielectric and magnetic properties of multiferroic BiFeO ₃ ceramics sintered with the powders prepared by hydrothermal method. 2013 , 19, 117-121	26
1699	Evolution of crystal structure and ferroic properties of La-doped BiFeO ₃ ceramics near the rhombohedral-orthorhombic phase boundary. 2013 , 555, 101-107	50
1698	Nucleation-induced self-assembly of multiferroic BiFeO ₃ -CoFe ₂ O ₄ nanocomposites. 2013 , 13, 3884-9	60
1697	Thermally activated magnetization reversal in bulk BiFe _{0.5} Mn _{0.5} O ₃ . 2013 , 88,	21
1696	Structure-Property Correlations in Rare-Earth-Substituted BiFeO ₃ Epitaxial Thin Films at the Morphotropic Phase Boundary. 2013 , 195-219	2
1695	Structural and nanomechanical properties of BiFeO ₃ thin films deposited by radio frequency magnetron sputtering. 2013 , 8, 297	31
1694	Solution Synthesis of BiFeO ₃ Thin Films onto Silicon Substrates with Ferroelectric, Magnetic, and Optical Functionalities. 2013 , 96, 3061-3069	22
1693	Insights into the phase diagram of bismuth ferrite from quasi-harmonic free-energy calculations. 2013 , 88,	46
1692	Exchange bias and magneto-resistance in an all-oxide spin valve with multi-ferroic BiFeO ₃ as the pinning layer. 2013 , 61, 7444-7453	7
1691	Structural phase transition and multiferroic properties of single-phase Bi _{1-x} Er _x Fe _{0.95} Co _{0.05} O ₃ . 2013 , 97, 56-58	25

1690	Magnetic enhancement across a ferroelectric/paraelectric phase boundary in $\text{Bi}_{1-x}\text{Sm}_x\text{FeO}_3$. 2013 , 411, 106-109	27
1689	Oxygen-vacancy ordering in multiferroic $\text{Bi}_{1-x}\text{Ca}_x\text{FeO}_{3-x/2}$ (0.1 $\leq x \leq$ 0.5). 2013 , 102, 27002	3
1688	Crystal structure and properties of high-pressure-synthesized BiRhO_3 , LuRhO_3 , and NdRhO_3 . 2013 , 200, 271-278	12
1687	Effects of microwave sintering power on microstructure, dielectric, ferroelectric and magnetic properties of bismuth ferrite ceramics. 2013 , 554, 64-71	48
1686	Orientation dependence of resistive hysteresis in bismuth ferrite thin films. 2013 , 569, 126-129	10
1685	Application of bismuth ferrite protonic conductor for ammonia gas detection. 2013 , 188, 957-964	38
1684	Effects of annealing temperature on the microstructure, optical, ferroelectric and photovoltaic properties of BiFeO_3 thin films prepared by sol-gel method. 2013 , 39, 8729-8736	58
1683	Optimization of BFO microwave-hydrothermal synthesis: Influence of process parameters. 2013 , 558, 150-159	29
1682	Preparation and functional characterization of BiFeO_3 ceramics: A comparative study of the dielectric properties. 2013 , 23, 79-87	18
1681	Enhanced magnetoelectric coupling in transition-metal-doped BiFeO_3 thin films. 2013 , 171, 40-45	27
1680	Controllable preparation of BiFeO_3 @carbon core/shell nanofibers with enhanced visible photocatalytic activity. 2013 , 376, 1-6	34
1679	Structural, microstructural and magneto-electric properties of single-phase BiFeO_3 nanoceramics prepared by auto-combustion method. 2013 , 141, 423-431	40
1678	Field induced changes in cycloidal spin ordering and coincidence between magnetic and electric anomalies in BiFeO_3 multiferroic. 2013 , 342, 17-26	18
1677	Correlation of microstructural and physical properties in bulk BiFeO_3 prepared by rapid liquid-phase sintering. 2013 , 18, 1-9	32
1676	Hydrothermal epitaxial multiferroic BiFeO_3 thick film by addition of the PVA. 2013 , 577, 44-48	21
1675	Self-limited grain growth, dielectric, leakage and ferroelectric properties of nanocrystalline BiFeO_3 thin films by chemical solution deposition. 2013 , 61, 1739-1747	34
1674	Mechanochemically assisted synthesis of nanocrystalline BiFeO_3 . 2013 , 139, 931-935	18
1673	Easy synthesis of high-purity BiFeO_3 nanoparticles: new insights derived from the structural, optical, and magnetic characterization. 2013 , 52, 10306-17	83

1672	Tunable magnetization and spin transfer induced by electric field in magnetic ultrathin BiFeO ₃ layer. 2013 , 114, 123916	10
1671	Observation of bi-relaxor characteristic in multiferroic 0.70Bi0.90Ca0.10FeO ₃ 0.30PbTiO ₃ ceramics. 2013 , 46, 375304	9
1670	Large nonlinear optical coefficients in pseudo-tetragonal BiFeO ₃ thin films. 2013 , 103, 031906	26
1669	Synthesis and visible-light photocatalysis capability of BiFeO ₃ (Na0.5Bi0.5)TiO ₃ nanopowders by a sol-gel method. 2013 , 19, 69-72	17
1668	Phase transition and magneto-electric coupling of BiFeO ₃ 0.3MnO ₃ multiferroic nanoceramics. 2013 , 114, 144104	24
1667	Structural, raman, dielectric, magnetic and magnetoelectric properties of Ba and Mn doped BiFeO ₃ nanoparticles. 2013 ,	2
1666	Structure and magnetic properties of BiFe(1-x)Co(x)O ₃ and Bi0.9Sm0.1Fe(1-x)Co(x)O ₃ . 2013 , 52, 10698-704	19
1665	Nanoscale studies of ferroelectric domain walls as pinned elastic interfaces. 2013 , 14, 667-684	40
1664	Universal emergence of spatially modulated structures induced by flexoantiferrodistortive coupling in multiferroics. 2013 , 88,	32
1663	Evidence for oxygen vacancy or ferroelectric polarization induced switchable diode and photovoltaic effects in BiFeO ₃ based thin films. 2013 , 24, 275201	93
1662	Origin of the uniaxial magnetic anisotropy in La0.7Sr0.3MnO ₃ on stripe-domain BiFeO ₃ . 2013 , 88,	32
1661	Bismuth-Containing Compounds. 2013 ,	15
1660	Atomic Layer Deposition of BiFeO ₃ Thin Films Using ̢-Diketonates and H ₂ O. 2013 , 117, 24579-24585	28
1659	Ca-Doping of BiFeO ₃ : The Role of Strain in Determining Coupling between Ferroelectric Displacements, Magnetic Moments, Octahedral Tilting, and Oxygen-Vacancy Ordering. 2013 , 25, 4436-4446	37
1658	Oxygen-Vacancy-Related Dielectric Relaxation in BiFeO ₃ Ceramics. 2013 , 450, 42-48	16
1657	Study of A-site and B-site Doping on Multiferroic Properties of BFO Thin Films. 2013 , 454, 41-46	18
1656	Coherent magnon and acoustic phonon dynamics in tetragonal and rare-earth-doped BiFeO ₃ multiferroic thin films. 2013 , 88,	17
1655	Improved dielectric and magnetic properties of Ti modified BiCaFeO ₃ multiferroic ceramics. 2013 , 113, 023908	42

1654	Room temperature Multiferroic properties of Nd doped Ba _{0.9} FeTi ₃ O ₁₂ nanoparticles. 2013 , 564, 162-165	2
1653	Magnetoelectric coupling in multiferroic Tb-doped BiFeO ₃ nanoparticles. 2013 , 111, 55-58	25
1652	Electromechanical and magnetic properties of BiFeO ₃ -LaFeO ₃ -CaTiO ₃ ceramics near the rhombohedral-orthorhombic phase boundary. 2013 , 113, 1872-18	28
1651	Room temperature structure and multiferroic properties in Bi _{0.7} La _{0.3} FeO ₃ ceramics. 2013 , 554, 97-103	27
1650	Raman and X-ray diffraction study of (Ba,Sr)TiO ₃ /(Bi,Nd)FeO ₃ multilayer heterostructures. 2013 , 545, 267-271	2
1649	First-principles study on the magnetic properties in Mg doped BiFeO ₃ with and without oxygen vacancies. 2013 , 114, 2339-12	23
1648	Magnetic properties of ferrites-cobaltites Bi _{1-x} La _x Fe _{1-x} Co _x O ₃ (1.0 ≤ x ≤ 0.7) with a perovskite structure. 2013 , 39, 589-596	5
1647	Structural and electrical properties of chemical solution deposited (Bi _{0.9} Tb _{0.1})(Fe _{0.975} TM _{0.025})O ₃ (TM = Ni, Mn and Ti) thin films. 2013 , 66, 168-174	1
1646	Structure transition and enhanced ferroelectric properties of (Mn, Cr) co-doped BiFeO ₃ thin films. 2013 , 24, 4827-4832	8
1645	Growth of pseudocubic perovskite-type SrRuO ₃ thin films on quartz substrate using pulsed laser deposition method. 2013 , 24, 4698-4703	2
1644	Magnetic structure of the compensated ferromagnet-multiferroic interface. 2013 , 55, 2246-2251	10
1643	Structure, ferromagnetism and microwave absorption properties of La substituted BiFeO ₃ nanoparticles. 2013 , 111, 130-133	42
1642	BaTiO ₃ /ferrite composites with magnetocapacitance and hard/soft magnetic properties. 2013 , 86, 670-680	15
1641	Synthesis of multiferroic Bi _{0.9} La _{0.1} Fe _{0.95} Mn _{0.05} O ₃ Ba _{0.7} Sr _{0.3} TiO ₃ Ni _{0.8} Zn _{0.2} Fe ₂ O ₄ nanotubes with one closed end using a template-assisted sol-gel process. 2013 , 15, 2147	11
1640	Electrical conductivity of Gd doped BiFeO ₃ -PbZrO ₃ composite. 2013 , 7, 295-301	15
1639	Magnetization, magnetic susceptibility, and effective magnetic moment of the Fe ³⁺ ions in Bi ₂ Fe ₄ O ₉ . 2013 , 49, 616-620	13
1638	Magnetic and leakage current properties of Bi _{1-x} Gd _x FeO ₃ thin films. 2013 ,	
1637	Improved electric behaviors of the Pt/Bi _{1-x} La _x Fe _{0.92} Mn _{0.08} O ₃ /n ⁺ -Si heterostructure for nonvolatile ferroelectric random-access memory. 2013 , 1, 6252	9

1636	Ferroelastic phase transition and switchable dielectric behavior associated with ordering of molecular motion in a perovskite-like architected supramolecular cocrystal. 2013 , 1, 2561	80
1635	High-pressure synthesis, crystal structure, and properties of $\text{In}_2\text{NiMnO}_6$ with antiferromagnetic order and field-induced phase transition. 2013 , 52, 14108-15	23
1634	Oxygen diffusion and nonstoichiometry in BiFeO_3 . 2013 , 52, 12806-10	12
1633	Structural, dielectric and magnetic properties of Pr-, Tb- and Dy-doped $(\text{Bi}_{0.95}\text{RE}_{0.05})(\text{Fe}_{0.95}\text{Mn}_{0.05})\text{O}_3$ ceramics synthesized by solid-state reaction method. 2013 , 03, 1350033	2
1632	Fabrication of Nanoflowers and other Exotic Patterns. 2013 , 201, 159-180	1
1631	Structural, morphological and multiferroic properties of Pr and Co co-substituted BiFeO_3 nanoparticles. 2013 , 90, 152-155	32
1630	Domain walls in a perovskite oxide with two primary structural order parameters: First-principles study of BiFeO_3 . 2013 , 87,	59
1629	Effect of chemical substitution on the morphology and optical properties of $\text{Bi}_{1-x}\text{Ca}_x\text{FeO}_3$ films grown by pulsed-laser deposition. 2013 , 24, 248-252	21
1628	Enhancement of Magnetic and Dielectric Properties in Chemically Modified Multiferroic $(0.90)\text{BiFe}_{1-x}\text{Cr}_x\text{O}_3/(0.10)\text{BaTiO}_3$ Nanocomposite. 2013 , 26, 397-402	5
1627	Homologous series of layered perovskites $\text{A}_{(n+1)}\text{B}_{(n)}\text{O}_{(3n-1)}\text{Cl}$: crystal and magnetic structure of a new oxychloride $\text{Pb}_4\text{BiFe}_4\text{O}_{11}\text{Cl}$. 2013 , 52, 2208-18	6
1626	Lattice dynamics of multiferroic BiFeO_3 studied by inelastic x-ray scattering. 2013 , 25, 102201	19
1625	Microscopical and physical characterization of microwave and microwave-hydrothermal synthesis products. 2013 , 44, 21-44	58
1624	High temperature dielectric and magnetic response of Ti and Pr doped BiFeO_3 ceramics. 2013 , 39, 8113-8121	32
1623	Synthesis and characterization of $\text{Bi}_{1-x}\text{Nd}_x\text{FeO}_3$ thin films deposited using a high throughput physical vapour deposition technique. 2013 , 531, 56-60	9
1622	Gd-doped BiFeO_3 nanoparticles [A novel material for highly efficient dye-sensitized solar cells. 2013 , 574, 71-77	36
1621	Exchange bias in polycrystalline $\text{Bi}_{1-x}\text{La}_x\text{FeO}_3/\text{NiFe}$ bilayers. 2013 , 161, 9-12	11
1620	Charge defects-induced electrical properties in bismuth ferrite bilayered thin films. 2013 , 48, 2973-2977	10
1619	Piezoelectric domains in BiFeO_3 films grown via MOCVD: Structure/property relationship. 2013 , 230, 168-173	9

1618	Enhanced magnetization and improved leakage in Er-doped BiFeO ₃ nanoparticles. 2013 , 210, 809-813	37
1617	Peculiar magnetism of BiFeO ₃ nanoparticles with size approaching the period of the spiral spin structure. 2013 , 3, 2907	196
1616	Gadolinium substitution induced defect restructuring in multiferroic BiFeO ₃ : case study by positron annihilation spectroscopy. 2013 , 46, 495309	18
1615	Multiferroic properties of BiFeO ₃ -(K _{0.5} Bi _{0.5})TiO ₃ ceramics. 2013 , 94, 172-175	28
1614	Influence of transition elements doping on structural, optical and magnetic properties of BiFeO ₃ films fabricated by magnetron sputtering. 2013 , 111, 123-125	35
1613	Structural, Raman and dielectric behavior in Bi _{1-x} Sr _x FeO ₃ multiferroic. 2013 , 1038, 242-249	39
1612	Structural and electrical properties of sol-gel-derived Al-doped bismuth ferrite thin films. 2013 , 39, S461-S464	17
1611	Epitaxial integration of perovskite-based multifunctional oxides on silicon. 2013 , 61, 2734-2750	85
1610	Influence of Co doping on structural, optical and magnetic properties of BiFeO ₃ films deposited on quartz substrates by sol-gel method. 2013 , 268, 146-150	56
1609	Enhancement in magnetic and dielectric properties of La and Pr co substituted BiFeO ₃ . 2013 , 552, 336-344	43
1608	Stabilization of dielectric anomaly near the magnetic phase transition in Ca ²⁺ doped BiFeO ₃ multifunctional ceramics. 2013 , 564, 151-157	37
1607	Structural, vibrational, optical, magnetic and dielectric properties of Bi _{1-x} Ba _x FeO ₃ nanoparticles. 2013 , 39, 6399-6405	83
1606	A new class of room-temperature multiferroic thin films with bismuth-based supercell structure. <i>Advanced Materials</i> , 2013 , 25, 1028-32	24 66
1605	Phase and morphology evolution of bismuth ferrites via hydrothermal reaction route. 2013 , 48, 1694-1699	36
1604	Sol-gel preparation of La-doped bismuth ferrite thin film and its low-temperature ferromagnetic and ferroelectric properties. 2013 , 31, 60-64	14
1603	Synthesis of high-quality inverse opals based on magnetic complex oxides: yttrium iron garnet (Y ₃ Fe ₅ O ₁₂) and bismuth ferrite (BiFeO ₃). 2013 , 1, 2975	8
1602	On the microscopic mechanism for the stabilization of structural and ferroic states in displacive multiferroics. 2013 , 113, 114105	9
1601	Composition- and temperature-driven structural transitions in Bi(1-x)Ca(x)FeO ₃ multiferroics: a neutron diffraction study. 2013 , 25, 135902	27

1600	Nanostructures of Sr ²⁺ doped BiFeO ₃ multifunctional ceramics with tunable photoluminescence and magnetic properties. 2013 , 25, 055303	30
1599	Structure and multiferroic properties of Bi(1-x)Dy _x Fe _{0.90} Mg _{0.05} Ti _{0.05} O ₃ solid solution. 2013 , 113, 054102	12
1598	Magnetic switching of ferroelectric domains at room temperature in multiferroic PZTFT. 2013 , 4, 1534	134
1597	Room-temperature single phase multiferroic magnetoelectrics: Pb(Fe, M) _x (Zr,Ti)(1-x)O ₃ [M = Ta, Nb]. 2013 , 113, 074105	89
1596	Bulk interface engineering for enhanced magnetization in multiferroic BiFeO ₃ compounds. 2013 , 102, 072907	16
1595	Magnetic properties and origins of ferroelectric polarization in multiferroic CaMn ₇ O ₁₂ . 2013 , 87,	25
1594	Study of 0.9 BaTiO ₃ -0.1 Ni _x Zn _{1-x} Fe ₂ O ₄ magneto-electric composite ceramics. 2013 , 113, 114107	29
1593	Improved multiferroic behavior in [111]-oriented BiFeO ₃ /BiAlO ₃ superlattice. 2013 , 113, 123703	10
1592	Ferromagnetic and photocatalytic behaviors observed in Ca-doped BiFeO ₃ nanofibres. 2013 , 113, 146101	52
1591	Development of a bond-valence based interatomic potential for BiFeO ₃ for accurate molecular dynamics simulations. 2013 , 25, 102202	34
1590	BiFeO ₃ single crystal as resistive switching element for application in microelectronic devices. 2013 , 86, 284-289	5
1589	Effect of crystallite size and clustering in influencing the stability of phases of a very large tetragonality ferroelectric system 0.6BiFeO ₃ 0.4PbTiO ₃ . 2013 , 160, 56-60	5
1588	Experimentally determining the intrinsic center point of Bi ₂ O ₃ -Fe ₂ O ₃ phase diagram for growing pure BiFeO ₃ crystals. 2013 , 15, 4900	8
1587	The multiferroic perovskite YFeO ₃ . 2013 , 102, 062903	114
1586	Ligand-directed control over crystal structures of inorganic-organic frameworks and formation of solid solutions. 2013 , 52, 5544-7	29
1585	Direct mechanosynthesis of pure BiFeO ₃ perovskite nanoparticles: reaction mechanism. 2013 , 1, 3551	41
1584	Crafting the magnonic and spintronic response of BiFeO ₃ films by epitaxial strain. 2013 , 12, 641-6	256
1583	Weak ferromagnetic behavior of BiFeO ₃ at low temperature. 2013 , 113, 17D921	17

1582	Raman spectroscopy of nanocrystalline Mn-doped BiFeO ₃ thin films. 2013 , 8, 261-266		22
1581	Interplay of octahedral tilts and polar order in BiFeO ₃ films. <i>Advanced Materials</i> , 2013 , 25, 2497-504	24	94
1580	Controlling magnetism of multiferroic (Bi _{0.9} La _{0.1}) ₂ FeCrO ₆ thin films by epitaxial and crystallographic orientation strain. 2013 , 102, 192911		11
1579	Structural transformation and enhancement in magnetic properties of single-phase Bi _{1-x} Pr _x FeO ₃ nanoparticles. 2013 , 113, 203917		52
1578	First principle study on structural, elastic and electronic properties of cubic BiFeO ₃ . 2013 , 39, S283-S286		20
1577	Field-induced phase transitions and phase diagrams in BiFeO ₃ -like multiferroics. 2013 , 87,		28
1576	Applications of high throughput (combinatorial) methodologies to electronic, magnetic, optical, and energy-related materials. 2013 , 113, 231101		170
1575	Origin of magnetization reversal and exchange bias phenomena in solid solutions of BiFeO ₃ -BiMnO ₃ : intrinsic or extrinsic?. 2013 , 52, 2015-21		34
1574	Effect of Substrate on Structure and Multiferrocity of (La, Mn) CoSubstituted BiFeO ₃ Thin Films. 2013 , 96, 2531-2536		6
1573	Photovoltaic property of sputtered BiFeO ₃ thin films. 2013 , 574, 402-406		26
1572	Room temperature ferromagnetism with large magnetic moment at low field in rare-earth-doped BiFeO ₃ thin films. 2013 , 25, 206003		5
1571	Evidences of magneto-electric coupling in BFOBT solid solutions. 2013 , 577, 222-227		48
1570	Experimental visualization of the Bi-O covalency in ferroelectric bismuth ferrite (BiFeO ₃) by synchrotron X-ray powder diffraction analysis. 2013 , 15, 6779-82		42
1569	Effects of La substitution for BiFeO ₃ epitaxial thin films. 2013 , 62, 1069-1072		1
1568	Photoluminescence and time-resolved spectroscopy in multiferroic BiFeO ₃ : Effects of electric fields and sample aging. 2013 , 102, 222901		35
1567	Four-states multiferroic memory embodied using Mn-doped BaTiO ₃ nanorods. 2013 , 7, 5522-9		66
1566	Magnetic memory effect in multiferroic K ₃ Fe ₅ F ₁₅ and K ₃ Cr ₂ Fe ₃ F ₁₅ . 2013 , 102, 242410		12
1565	Magnetoelectric coupling in multiferroic BiFeO ₃ nanowires. 2013 , 579, 78-84		19

- 1564 Theory of spin-orbit enhanced electric-field control of magnetism in multiferroic BiFeO₃. **2013**, 110, 267202 24
- 1563 Electromechanical coupling among edge dislocations, domain walls, and nanodomains in BiFeO₃ revealed by unit-cell-wise strain and polarization maps. **2013**, 13, 1410-5 65
- 1562 Synthesis peculiarities of BiVO₃ perovskite. **2013**, 39, 5963-5966 8
- 1561 Effect of low-temperature high-pressure sintering on BiFeO₃ density, electrical magnetic and structural properties. **2013**, 86, 1104-1114 4
- 1560 Synthesis and Characteristics of Superparamagnetic Co_{0.6}Zn_{0.4}Fe₂O₄ Nanoparticles by a Modified Hydrothermal Method. **2013**, 96, 2245-2251 17
- 1559 The effect of polarization fatigue process and light illumination on the transport behavior of Bi_{0.9}La_{0.1}FeO₃ sandwiched capacitor. **2013**, 113, 183510 14
- 1558 Pressure induced para-antiferromagnetic switching in BiFeO₃/BaTiO₃ as determined using in-situ neutron diffraction. **2013**, 113, 183910 14
- 1557 Mn substitution-modified polar phase in the Bi_{1-x}NdxFeO₃ multiferroics. **2013**, 113, 214112 19
- 1556 Phase transition and huge ferroelectric polarization observed in BiFe_{1-x}GaxO₃ thin films. **2013**, 102, 222906 36
- 1555 Multiferroic properties of La and Mn co-doped BiFeO₃ nanofibers by sol-gel and electrospinning technique. **2013**, 90, 45-48 57
- 1554 Fabrication of multiferroic Ba_{0.7}Sr_{0.3}TiO₃/Ni_{0.8}Zn_{0.2}Fe₂O₄ composite nanofibers by electrospinning. **2013**, 91, 55-58 14
- 1553 Tunable dielectric characteristics of Mn-doped BiFeO₃ multiferroic ceramics. **2013**, 68, 305-308 12
- 1552 Phase-dependent multiferroism in Dy-doped BiFeO₃ nanowires. **2013**, 53, 184-194 31
- 1551 Intrinsic Compositional Inhomogeneities in Bulk Ti-Doped BiFeO₃: Microstructure Development and Multiferroic Properties. **2013**, 25, 1533-1541 83
- 1550 Magnetic and electric properties of CaMn₇O₁₂ based multiferroic compounds: effect of electron doping. **2013**, 25, 246001 19
- 1549 Epitaxial strontium titanate films grown by atomic layer deposition on SrTiO₃-buffered Si(001) substrates. **2013**, 31, 01A136 38
- 1548 Room-temperature multiferroic magnetoelectrics. **2013**, 5, e72-e72 207
- 1547 Structural, spectroscopic, and dielectric characterizations of Mn-doped 0.67BiFeO₃-0.33BaTiO₃ multiferroic ceramics. **2013**, 2, 252-259 25

1546	Recent Progress in Ferroelectric Diodes: Explorations in Switchable Diode Effect. 2013 , 5, 81-87	16
1545	Investigation of wide range magnetoresistance in $\text{La}_{0.7}\text{Ca}_{0.3-x}\text{Ag}_x\text{MnO}_3$ ($0 \leq x \leq 0.2$) system. 2013 , 24, 1141-1145	7
1544	Overlap of the intrinsic and extrinsic magnetoelectric effects in BiFeO_3 - PbTiO_3 compounds: Potentialities for magnetic-sensing applications. 2013 , 113, 034102	12
1543	A strategy to fabricate bismuth ferrite (BiFeO_3) nanotubes from electrospun nanofibers and their solar light-driven photocatalytic properties. 2013 , 3, 23737	42
1542	Effects of external magnetic field on the morphology and magnetic property of BiFeO_3 particles prepared by hydrothermal synthesis. 2013 , 102, 082901	13
1541	Multiferroic and structural transition properties of $\text{Bi}_{1-x}\text{Pr}_x\text{Fe}_{0.95}\text{Mn}_{0.05}\text{O}_3$ thin films. 2013 ,	
1540	Periodic elastic nanodomains in ultrathin tetragonal-like BiFeO_3 films. 2013 , 88,	20
1539	Electric field-controlled magnetization in exchange biased $\text{IrMn}/\text{Co}/\text{PZT}$ multilayers. 2013 , 4, 025017	8
1538	Swift heavy ion irradiation induced modification of structure and surface morphology of BiFeO_3 thin film. 2013 , 36, 813-818	14
1537	Study of site-disorder in epitaxial magneto-electric GaFeO_3 thin films. 2013 , 102, 212401	29
1536	Room temperature multiferroic properties of $\text{Pb}(\text{Fe}_{0.5}\text{Nb}_{0.5})\text{O}_3/\text{Co}_{0.65}\text{Zn}_{0.35}\text{Fe}_2\text{O}_4$ composites. 2013 , 114, 234106	38
1535	Preparation of BiFeO_3 -Graphene Nanocomposites and Their Enhanced Photocatalytic Activities. 2013 , 2013, 1-5	12
1534	STRUCTURAL AND MAGNETIC PHASE TRANSITIONS OF BiFeO_3 INDUCED BY PRESSURE. 2013 , 06, 1350026	1
1533	Novel Nanoscale Twinned Phases in Perovskite Oxides. 2013 , 23, 234-240	81
1532	Bifurcated Polarization Rotation in Bismuth-Based Piezoelectrics. 2013 , 23, 185-190	127
1531	Novel Nanorod Precipitate Formation in Neodymium and Titanium Codoped Bismuth Ferrite. 2013 , 23, 683-689	26
1530	Microstructural and electrical properties of single phase multiferroic BiFeO_3 nanoparticles. 2013 ,	
1529	Heterometallic Complexes with Rhenium- and Iron-Bismuth Bonds. 2013 , 68, 561-568	9

1528	Structural, magnetic, and nanoscale switching properties of BiFeO ₃ thin films grown by pulsed electron deposition. 2013 , 31, 032801	4
1527	Magnetic properties of proton irradiated BiFeO ₃ . 2013 , 113, 17E152	1
1526	Effect of reduced size and Ba doping on multiferroic properties of BiFeO ₃ nanoparticles. 2013 ,	
1525	Competing antiferromagnetism and local magnetic order in the bulk ceramic PZT/PFW multiferroic system: searching for the most promising ratio between PZT and PFW. 2013 , 46, 455001	6
1524	Synthesis and optical properties of the (La, Mn)-codoped BiFeO ₃ films on n-Si(100) substrates. 2013 ,	
1523	Density Functional Theory Study on How Electron Spin Configuration of Co ³⁺ Ion Affects the Structure and Magnetism of Co-Doped Bismuth Ferrite. 2013 , 52, 09KB01	2
1522	A training effect on electrical properties in nanoscale BiFeO ₃ . 2013 , 24, 135705	2
1521	Ultrafast Photostriction in Thin Film Bismuth Ferrite and its Correlation to Electronic Dynamics. 2013 , 1528, 1	
1520	Novel magnetic arrangement and structural phase transition induced by spin-lattice coupling in multiferroics. 2013 , 3, 213-218	3
1519	Preparation of BiFe _{1-x} Co _x O ₃ Ceramics via a Simple Solid Method and Enhanced Multiferroic Properties. 2013 , 631-632, 452-457	1
1518	Effect of Oxygen Pressure on Electrical Properties of BiFe _{0.9} Co _{0.1} O ₃ Thin Films Prepared by Pulsed Laser Deposition. 2013 , 52, 09KD09	
1517	Spin transfer in ultrathin BiFeO ₃ film under external electric field. 2013 , 101, 67007	9
1516	Effect of Poly Sodium-p-Styrenesulfonate on the Phase Formation and Morphology of the Hydrothermally Synthesized Bismuth Ferrite Powders. 2013 , 745-746, 393-397	
1515	Strain modulated optical properties in BiFeO ₃ thin films. 2013 , 103, 181907	31
1514	Structural and Dielectric Properties of Bi _{0.9} Pr _{0.1} Fe _{1-x} Ti _x O ₃ Ceramics. 2013 , 785-786, 697-700	
1513	Prospects for Ferroelectrics: 2012-2022. 2013 , 2013, 1-24	27
1512	Electric and Magnetic Properties of Sputter Deposited BiFeO ₃ Films. 2013 , 2013, 1-6	4
1511	Grain size effect on site-disorder and magnetic properties of multiferroic GaFeO ₃ nanoparticles. 2013 , 103, 232405	14

1510	Growth and Characterization of Na _{0.5} Bi _{0.5} TiO ₃ Thin Films with BaTiO ₃ Buffer Layer (Study of Au/Na _{0.5} Bi _{0.5} TiO ₃ /BaTiO ₃ /Pt Capacitor). 2013 , 447, 46-55	5
1509	Uncompensated spins in exchange-biased BiFeO ₃ /Fe ₂ O ₃ core/shell-like thin films. 2013 , 114, 103902	6
1508	A giant polarization value of Zn and Mn co-modified bismuth ferrite thin films. 2013 , 102, 052904	44
1507	Photo-induced modulation of ferroelectric polarization in multiferroic TbMnO ₃ . 2013 ,	
1506	Pressure effect on structural and vibrational properties of Sm-substituted BiFeO ₃ . 2013 , 114, 154110	13
1505	Magnetic Relaxation in Bismuth Ferrite Micro-Cubes. 2013 , 448, 58-70	5
1504	High quality multiferroic BiFeO ₃ films prepared by pulsed laser deposition on glass substrates at reduced temperatures. 2013 , 113, 17D917	11
1503	Untilting BiFeO ₃ : The influence of substrate boundary conditions in ultra-thin BiFeO ₃ on SrTiO ₃ . 2013 , 1, 052102	18
1502	Electrical Properties of Stoichiometric BiFeO ₃ Prepared by Mechano-synthesis with Either Conventional or Spark Plasma Sintering. 2013 , 96, 1220-1227	47
1501	Ferroelectric Behavior and Magnetocapacitance Effect Caused by Fe ²⁺ in Ho ₃ Fe ₅ O ₁₂ Ceramics. 2013 , 448, 71-76	8
1500	Pressure-induced phase transitions of multiferroic BiFeO ₃ . 2013 , 37, 128001	4
1499	Optical Study of Sol-gel Processed Nd-doped BiFeO ₃ Multiferroic Films by Spectroscopic Ellipsometry. 2013 , 454, 78-83	6
1498	PREPARATION AND ELECTRICAL PROPERTIES OF BiFeO ₃ /La _{0.7} Sr _{0.3} MnO ₃ MULTILAYERS. 2013 , 27, 1350128	
1497	Electrical properties of ferroelectric BiMnO ₃ /BiTiO ₃ under tailored synthesis and ceramic processing. 2013 , 86, 681-694	12
1496	Local probing of magnetoelectric coupling and magnetoelastic control of switching in BiFeO ₃ -CoFe ₂ O ₄ thin-film nanocomposite. 2013 , 103, 042906	26
1495	Photocurrent Properties of BiFeO ₃ Thin Films Prepared by Chemical Solution Deposition. 2013 , 453, 20-25	3
1494	Strain induced changes in magnetization of amorphous Co ₉₅ Zr ₅ based multiferroic heterostructures. 2013 , 3, 022113	12
1493	Ligand-Directed Control over Crystal Structures of Inorganic/Organic Frameworks and Formation of Solid Solutions. 2013 , 125, 5654-5657	11

1492	Family Value(s). <i>Advanced Materials</i> , 2013 , 25, 10-12	24	1
1491	Anomalous capacitance response induced by the superconducting gap in an Au/BiFeO ₃ /La _{1.84} Sr _{0.16} CuO ₄ /LaSrAlO ₄ heterostructure. 2013 , 103, 153507		5
1490	Multiferroic Properties In Complex Oxides. 2013 , 3, 70-74		
1489	First-Principles Study of Ferroelectric-Ferromagnetic Coupling in Multiferroic BiFeO ₃ . 2014 , 63, 168-173		1
1488	Preparation of Mn-doped (Bi _{0.5} K _{0.5})TiO ₃ -Bi(Mg _{0.5} Ti _{0.5})O ₃ -BiFeO ₃ Ceramics Using BiFeO ₃ Particle Synthesized by Hydrothermal Method and Their Piezoelectric Properties. 2014 , 39, 137-140		1
1487	Degradation of ferroelectric and weak ferromagnetic properties of BiFeO ₃ films due to the diffusion of silicon atoms. 2014 , 23, 077504		4
1486	Synthesis and characterization of coprecipitation-prepared La-doped BiFeO ₃ nanopowders and their bulk dielectric properties. 2014 , 53, 06JG13		8
1485	Emerging Multiferroic Memories. 2014 , 103-166		2
1484	Suppression of grain boundary relaxation in Zr-doped BiFeO ₃ thin films. 2014 , 115, 204102		7
1483	Strain relaxation and enhanced perpendicular magnetic anisotropy in BiFeO ₃ :CoFe ₂ O ₄ vertically aligned nanocomposite thin films. 2014 , 104, 062402		42
1482	Enhanced ferroelectricity and ferromagnetism in Bi _{0.9} Ba _{0.1} FeO ₃ /La _{2/3} Sr _{1/3} MnO ₃ heterostructure grown by pulsed laser deposition. 2014 , 23, 117703		
1481	Surface double-layer structure in (110) oriented BiFeO ₃ thin film. 2014 , 105, 202901		7
1480	The multiferroic properties of polycrystalline Bi _{1-x} Y _x FeO ₃ films. 2014 , 115, 17D902		11
1479	Uniform bipolar resistive switching behaviors in BiFeO ₃ thin films on Fe-doped LaNiO ₃ electrodes. 2014 , 7, 095801		5
1478	Transport properties and anomalous fatigue effect of Ag/Bi _{0.9} La _{0.1} FeO ₃ /La _{0.7} Sr _{0.3} MnO ₃ heterostructures. 2014 , 23, 097702		3
1477	Enhanced Magnetic and Electric Properties of Nanocrystalline Ce Modified BFO Thin Films. 2014 , 470, 272-279		10
1476	The principles of creating new-generation magnetic memory. 2014 , 84, 407-412		
1475	Effects of isothermal treatments on non-stoichiometrical preparation for the optimized perovskite structure of BiFeO ₃ bulk ceramics. 2014 , 115, 1342-1350		

1474	Interface control of a morphotropic phase boundary in epitaxial samarium modified bismuth ferrite superlattices. 2014 , 90,	19
1473	Structural, magnetic, and magnetodielectric studies of metamagnetic DyFe _{0.5} Cr _{0.5} O ₃ . 2014 , 115, 17D728	22
1472	Spontaneous magnetization in the polar phase of Bi _{1-x} CaxFeO _{3-x/2} /x perovskites: The role of anion vacancies. 2014 , 116, 214105	15
1471	Orientations of low-energy domain walls in perovskites with oxygen octahedral tilts. 2014 , 90,	24
1470	Effect of oxygen annealing on the multiferroic properties of Ca ²⁺ doped BiFeO ₃ nanoceramics. 2014 , 116, 244105	25
1469	Magnetic Properties of Bismuth Ferrite Nanopowder Obtained by Mechanochemical Synthesis. 2014 , 126, 1029-1031	6
1468	Electric Conductivity of (Bi _{1-x} La _x FeO ₃) _{0.5} (PbTiO ₃) _{0.5} Ceramics Obtained from Mechanosynthesized Nanopowders. 2014 , 126, 971-974	1
1467	Effects of Interfaces on the Structure and Novel Physical Properties in Epitaxial Multiferroic BiFeO ₃ Ultrathin Films. 2014 , 7, 5403-5426	8
1466	XRD and Raman spectroscopy studies of (Bi _{1-x} La _x FeO ₃) _{0.5} (PbTiO ₃) _{0.5} solid solution. 2014 , 87, 909-921	5
1465	Structural, dielectric and magnetic properties of La and Sc codoped BiFeO ₃ . 2014 , 29, 237-240	1
1464	Structural, electrical and magnetic properties of Bi _{0.90} La _{0.10} Fe _{0.90} Co _{0.10} O ₃ ceramics. 2014 ,	1
1463	Temperature dependent photoexcited carrier dynamics in multiferroic BiFeO ₃ film: A hidden phase transition. 2014 , 104, 151902	8
1462	Uniaxial pressure induced phase transitions in multiferroic materials BiCoO ₃ . 2014 , 4, 64601-64607	6
1461	Engineering 180° ferroelectric domains in epitaxial PbTiO ₃ thin films by varying the thickness of the underlying (La,Sr)MnO ₃ layer. 2014 , 105, 132903	5
1460	Self-assembled nanoscale capacitor cells based on ultrathin BiFeO ₃ films. 2014 , 104, 182903	12
1459	Magnetoelectric Characterization of Multiferroic Nanostructure Materials. 2014 , 473, 137-153	9
1458	Chemical solution deposition derived (001)-oriented epitaxial BiFeO ₃ thin films with robust ferroelectric properties using stoichiometric precursors (invited). 2014 , 116, 066810	19
1457	Magnetic Properties of Polycrystalline Bismuth Ferrite Thin Films Grown by Atomic Layer Deposition. 2014 , 5, 4319-23	21

1456	Multiferroism and enhancement of material properties across the morphotropic phase boundary of BiFeO ₃ -PbTiO ₃ . 2014 , 115, 104104	49
1455	Local polar structure and multiferroic properties of (1-x)Bi _{0.9} Dy _{0.1} FeO ₃ -PbTiO ₃ solid solution. 2014 , 116, 066809	14
1454	Spin-phonon coupling, high-pressure phase transitions, and thermal expansion of multiferroic GaFeO ₃ : A combined first principles and inelastic neutron scattering study. 2014 , 90,	11
1453	Electric field control of magnetism using BiFeO ₃ -based heterostructures. 2014 , 1, 021303	200
1452	Weak ferromagnetism and nanodimensional ferroelectric domain structure stabilized in the polar phase of Bi _{1-x} NdxFeO ₃ multiferroics via Ti doping. 2014 , 115, 164101	18
1451	Photoconductivity and photo-detection response of multiferroic bismuth iron oxide. 2014 , 104, 132910	19
1450	Probing the domain structure of BiFeO ₃ epitaxial films with three-dimensional reciprocal space mapping. 2014 , 104, 182901	15
1449	Dynamic magnetic interaction in La _{2/3} Sr _{1/3} MnO ₃ /BiFeO ₃ heterostructure. 2014 , 105, 112406	6
1448	Strain mediated coupling in magnetron sputtered multiferroic PZT/Ni-Mn-In/Si thin film heterostructure. 2014 , 116, 114103	15
1447	Exchange bias and crystal structure of epitaxial (111) FePt/BiFeO ₃ sputtered thin films. 2014 , 115, 17D903	1
1446	Room temperature ferroelectric properties and leakage current characteristics of Bi ₂ FeMnO ₆ /SrTiO ₃ bilayered thin films by chemical solution deposition. 2014 , 211, 1499-1502	1
1445	Anomalous properties of hexagonal rare-earth ferrites from first principles. 2014 , 89,	40
1444	Effect of cobalt doping on site-disorder and magnetic behavior of magnetoelectric GaFeO ₃ nanoparticles. 2014 , 105, 212407	18
1443	Focused-ion-beam induced damage in thin films of complex oxide BiFeO ₃ . 2014 , 2, 022109	14
1442	Phase transformations in multiferroic Bi _{1-x} LaxFe _{1-y} TiyO ₃ ceramics probed by temperature dependent Raman scattering. 2014 , 116, 164103	5
1441	Molten Salt Synthesis of Bismuth Ferrite Nano- and Microcrystals and their Structural Characterization. 2014 , 97, 2223-2232	22
1440	Multifunctionalities driven by ferroic domains. 2014 , 116, 066801	9
1439	Structural, Raman, and Dielectric Studies on Multiferroic Mn-doped Bi _{1-x} LaxFeO ₃ Ceramics. 2014 , 97, 2323-2330	32

1438	Two-Phase Coexistence and Multiferroic Properties of Cr-Doped BiFeO ₃ Thin Films. 2014 , 27, 2765-2772	15
1437	Photoinduced electrical properties of Mn-doped BiFeO ₃ thin films prepared by chemical solution deposition. 2014 , 53, 09PA17	9
1436	Combined effects of Bi deficiency and Mn substitution on the structural transformation and functionality of BiFeO ₃ films. 2014 , 116, 174102	24
1435	Reversible piezomagnetoelectric switching in bulk polycrystalline ceramics. 2014 , 2, 086105	2
1434	Emerging Non-Volatile Memories. 2014 ,	30
1433	The physical nature of bipolar resistive switching in Pt/BiFe _{0.95} Mn _{0.05} O ₃ /Pt memory devices. 2014 , 211, 191-194	4
1432	Studies of the Room-Temperature Multiferroic Pb(FeTa)(ZrTi)O: Resonant Ultrasound Spectroscopy, Dielectric, and Magnetic Phenomena. 2014 , 24, 2993-3002	34
1431	Magnetic and Photocatalytic Behaviors of Ba-Doped BiFeO ₃ Nanofibers. 2014 , 11, 676-680	10
1430	Photo-carrier control of exchange bias in BiFeO ₃ /La ₂ /3Sr ₁ /3MnO ₃ thin films. 2014 , 104, 252407	15
1429	First-principles study of the multimode antiferroelectric transition in PbZrO ₃ . 2014 , 90,	47
1428	Effect of Vegard strains on the extrinsic size effects in ferroelectric nanoparticles. 2014 , 90,	27
1427	Probing bismuth ferrite nanoparticles by hard x-ray photoemission: Anomalous occurrence of metallic bismuth. 2014 , 105, 102910	16
1426	Ho and Ti co-doped BiFeO ₃ multiferroic ceramics with enhanced magnetization and ultrahigh electrical resistivity. 2014 , 23, 037501	9
1425	Enhanced ferroelectric properties in Bi _{0.86} Sm _{0.14} FeO ₃ Based ceramics. 2014 , 105, 192902	25
1424	Mechanism of switchable and nonswitchable short-circuit photocurrent accompanying polarization switching in Bi _{0.9} La _{0.1} FeO ₃ thin films. 2014 , 105, 37008	4
1423	Effects of Thickness and Polarization Field on the Photovoltaic Properties of BiFeO ₃ Thin Films. 2014 , 31, 037304	4
1422	Effect of excess Bi content on the electrical properties of Bi _{0.95} La _{0.05} FeO ₃ thick films. 2014 , 25, 5316-5321	6
1421	Effects of Single-Substitution and Co-Substitution on BiFeO ₃ Nanoparticles. 2014 , 602-603, 23-26	

1420	Size dependent structural, vibrational and magnetic properties of BiFeO ₃ and core-shell structured BiFeO ₃ @SiO ₂ nanoparticles. 2014 ,	2
1419	Exchange bias in BiFeO ₃ /La _{0.67} Sr _{0.33} MnO ₃ bilayers. 2014 , 53, 08NM01	9
1418	Hole conduction and nonlinear current-voltage behavior in multiferroic lanthanum-substituted bismuth ferrite. 2014 , 615, 916-920	15
1417	Thin Film Applications in Advanced Electron Devices. 2014 , 2014, 1-2	12
1416	Enhanced multiferroic and dielectric properties of Sr ²⁺ -doped BiFe _{0.94} (Mn _{0.04} Cr _{0.02})O ₃ thin films. 2014 , 25, 4363-4368	
1415	Metal-Organic Chemical Vapor Deposition of BiFeO ₃ Based Multiferroics. 2014 , 90, 57-65	1
1414	Magneto-dielectric anomaly in (Bi _{0.95} Nd _{0.05})(Fe _{0.97} Mn _{0.03})O ₃ electroceramic. 2014 , 1636, 1	2
1413	Comparative Studies of Multiferroic BiFeO ₃ Powders Prepared by Hydrothermal Method versus Sol-Gel Process. 2014 , 670-671, 113-116	1
1412	Effect of surface modification of BiFeO ₃ on the dielectric, ferroelectric, magneto-dielectric properties of polyvinylacetate/BiFeO ₃ nanocomposites. 2014 , 8, 669-681	38
1411	Metal-Semiconductor-Insulator-Metal Structure Field-Effect Transistors Based on Zinc Oxides and Doped Ferroelectric Thin Films. 2014 , 1633, 131-137	2
1410	Formation of perovskite BiFeO ₃ (001) films on refined Pt(111) electrode layer with reduced thickness on glass substrates. 2014 , 115, 17D912	6
1409	Magneto-optical properties of BiFeO ₃ thin films using surface plasmon resonance technique. 2014 , 448, 120-124	10
1408	Improved ferroelectric and fatigue properties in Ho doped BiFeO ₃ thin films. 2014 , 129, 166-169	11
1407	Magneto-thermal conduction and phonon anomalies across magnetic transitions in multiferroic (poly and nanocrystalline) bismuth ferrite. 2014 , 437, 10-16	2
1406	Atomic-Scale Visualization of Polarization Pinning and Relaxation at Coherent BiFeO ₃ /LaAlO ₃ Interfaces. 2014 , 24, 793-799	31
1405	Synthesis and properties of bismuth ferrite multiferroic flowers. 2014 , 49, 2596-2604	20
1404	Piezoelectric and ferroelectric properties of Ga modified BiFeO ₃ BaTiO ₃ lead-free ceramics with high Curie temperature. 2014 , 25, 196-201	28
1403	Mechanosynthesis, magnetic and Mössbauer characterization of pure and Ti ⁴⁺ -doped cubic phase BiFeO ₃ nanocrystalline particles. 2014 , 226, 143-151	5

1402	Structural, Thermal, and Magnetic Properties of Cu-doped BiFeO ₃ . 2014 , 27, 1239-1243	17
1401	Enhanced Multiferroic and Magnetocapacitive Properties of (1-x)Ba _{0.7} Ca _{0.3} TiO ₃ -BiFeO ₃ Ceramics. 2014 , 97, 816-825	24
1400	Structural, Dielectric, and Electrical Properties of BiFeWO ₆ Ceramic. 2014 , 43, 732-739	17
1399	Prospects for nanostructured multiferroic composite materials. 2014 , 74, 38-43	62
1398	Studies on structural, electrical and optical properties of multiferroic (Ag, Ni and In) codoped Bi _{0.9} Nd _{0.1} FeO ₃ thin films. 2014 , 292, 702-709	10
1397	Comparative study on multiferroic (Bi _{0.9} RE _{0.1})(Fe _{0.97} Co _{0.03})O ₃ (RE=Ce and Ho) thin films: Structural, electrical and optical properties. 2014 , 40, 6247-6254	9
1396	Structural transformation and multiferroic properties of single-phase Bi _{0.89} Tb _{0.11} Fe _{1-x} MnxO ₃ thin films. 2014 , 290, 280-286	26
1395	Dielectric and multiferroic properties of 0.75BiFeO ₃ -0.25BaTiO ₃ solid solution. 2014 , 25, 888-896	23
1394	Effects of oxygen pressure on the microstructural, ferroelectric and magnetic properties of BiFe _{0.95} Mn _{0.05} O ₃ thin films grown on Si substrates. 2014 , 25, 1908-1914	3
1393	Dielectric and electrical properties of 0.5(BiGd _{0.05} Fe _{0.95} O ₃)-0.5(PbZrO ₃) composite. 2014 , 32, 59-65	17
1392	Investigation of Structural and Electrical Properties of B-Site Complex Ion (Mg _{1/3} Nb _{2/3}) ₄₊ -Modified High-Curie-Temperature BiFeO ₃ -BaTiO ₃ Ceramics. 2014 , 43, 755-760	15
1391	Structure transition and multiferroic properties of Mn-doped BiFeO ₃ thin films. 2014 , 25, 723-729	22
1390	Optical properties of BiFeO ₃ epitaxial thin films. 2014 , 59, 102-106	4
1389	Dielectric behavior of hexagonal and orthorhombic YFeO ₃ prepared by modified sol-gel method. 2014 , 32, 187-191	24
1388	BiFeO ₃ /poly(methyl methacrylate) nanocomposite films: A study on magnetic and dielectric properties. 2014 , 104, 042902	32
1387	Structural and magnetic phase transitions in Bi _{1-x} NdxFe _{1-x} MnxO ₃ multiferroics. 2014 , 115, 034102	16
1386	Study of structural, electrical, magnetic and optical properties of 0.65BaTiO ₃ -0.35Bi _{0.5} Na _{0.5} TiO ₃ -BiFeO ₃ multiferroic composite. 2014 , 597, 188-199	48
1385	Effects of (Dy, Zn) co-doping on structural and electrical properties of BiFeO ₃ thin films. 2014 , 40, 2281-2286	44

1384	Effect of Ln (Ln=La, Pr) and Co co-doped on the magnetic and ferroelectric properties of BiFeO ₃ nanoparticles. 2014 , 584, 520-523	76
1383	Structural, dielectric and piezoelectric properties of xBiFeO ₃ (1-x)BaTi _{0.9} Zr _{0.1} O ₃ ceramics. 2014 , 40, 5173-5179	22
1382	Effect of dysprosium substitution on crystal structure and physical properties of multiferroic BiFeO ₃ ceramics. 2014 , 34, 641-651	53
1381	Enhanced magnetic and conductive properties of Ba and Co co-doped BiFeO ₃ ceramics. 2014 , 355, 259-264	75
1380	Charge defects and highly enhanced multiferroic properties in Mn and Cu co-doped BiFeO ₃ thin films. 2014 , 305, 55-61	47
1379	Tuning of dielectric and ferroelectric properties in single phase BiFeO ₃ ceramics with controlled Fe ²⁺ /Fe ³⁺ ratio. 2014 , 40, 5263-5268	26
1378	Cation-ordered A _{1/2} B _{1/2} B ₂ X ₄ magnetic spinels as magnetoelectrics. 2014 , 364, 47-54	13
1377	Giant dielectric response and enhanced thermal stability of multiferroic BiFeO ₃ . 2014 , 600, 118-124	17
1376	Synthesis, phase evolution and properties of phase-pure nanocrystalline BiFeO ₃ prepared by a starch-based combustion method. 2014 , 590, 324-330	35
1375	Magnetization, magnetic susceptibility, effective magnetic moment of Fe ³⁺ ions in Bi ₂₅ FeO ₃₉ ferrite. 2014 , 212, 147-150	46
1374	Magnetic anisotropy and sub-lattice magnetization study of polycrystalline magneto-electric. 2014 , 362, 97-103	14
1373	Enhanced magnetization and improved insulating character in Eu substituted BiFeO ₃ . 2014 , 115, 124110	42
1372	Coercivity and exchange bias of bismuth ferrite nanoparticles isolated by polymer coating. 2014 , 115, 123906	9
1371	Multiferroic BaTiO ₃ /BiFeO ₃ composite thin films and multilayers: strain engineering and magnetoelectric coupling. 2014 , 47, 135303	83
1370	BiFeO ₃ Ceramics: Processing, Electrical, and Electromechanical Properties. 2014 , 97, 1993-2011	288
1369	Strong smearing and disappearance of phase transitions into polar phases due to inhomogeneous lattice strains induced by A-site doping in Bi _{1-x} A _x FeO ₃ (A: La, Sm, Gd). 2014 , 604, 117-129	29
1368	Effect of Pr substitution on structural and electrical properties of BiFeO ₃ ceramics. 2014 , 143, 629-636	33
1367	Variation of the lattice and spin dynamics in Bi _{1-x} Dy _x FeO ₃ nanoparticles. 2014 , 115, 133506	1

1366	High temperature magnetic behavior of multiferroics Bi _{1-x} CaxFeO ₃ . 2014 , 115, 133912	8
1365	Structural phase transitions of robust insulating Bi _{1-x} La _x Fe _{1-y} Ti _y O ₃ multiferroics. 2014 , 115, 123523	17
1364	Defect-mediated ferroelectric domain depinning of polycrystalline BiFeO ₃ multiferroic thin films. 2014 , 104, 092905	34
1363	Switching ferroelectric domain configurations using both electric and magnetic fields in Pb(Zr,Ti)O ₃ -Pb(Fe,Ta)O ₃ single-crystal lamellae. 2014 , 372, 20120450	15
1362	Interfacial coupling in heteroepitaxial vertically aligned nanocomposite thin films: From lateral to vertical control. 2014 , 18, 6-18	87
1361	Polar and antipolar polymorphs of metastable perovskite BiFe _{0.5} Sc _{0.5} O ₃ . 2014 , 89,	42
1360	Linear electro-optic effect in multiferroic BiFeO ₃ thin films. 2014 , 89,	30
1359	Spin-cycloid instability as the origin of weak ferromagnetism in the disordered perovskite Bi _{0.8} La _{0.2} Fe _{0.5} Mn _{0.5} O ₃ . 2014 , 89,	15
1358	Local Crystal Structure of Antiferroelectric BiMnNiO in Commensurate and Incommensurate Phases Described by Pair Distribution Function (PDF) and Reverse Monte Carlo (RMC) Modeling. 2014 , 26, 2218-2232	5
1357	Strain driven structural phase transformations in dysprosium doped BiFeO ₃ ceramics. 2014 , 2, 3345-3360	33
1356	Synthesis and characterization of BiFeO ₃ nanowires and their applications in dye-sensitized solar cells. 2014 , 21, 206-211	41
1355	Interpretation of magnetoelectric phase states using the praphase concept and exchange symmetry. 2014 , 26, 036003	4
1354	Analytical comparison of magnetic and electrical properties using modified Landau theory in bismuth ferrite: Effect of milling. 2014 , 349, 95-99	12
1353	Frequency dependent electrical characteristics of BiFeO ₃ MOS capacitors. 2014 , 583, 476-480	40
1352	Influence of thickness on optical and structural properties of BiFeO ₃ thin films: PLD grown. 2014 , 49, 531-536	49
1351	Reduced leakage current of multiferroic BiFeO ₃ ceramics with microwave synthesis. 2014 , 40, 4247-4250	21
1350	Structural, electrical and magnetic properties of Bi _{0.825} Pb _{0.175} FeO ₃ , and Bi _{0.725} La _{0.1} Pb _{0.175} FeO ₃ multiferroics. 2014 , 49, 345-351	20
1349	Room temperature dielectric and magnetic properties of Gd and Ti co-doped BiFeO ₃ ceramics. 2014 , 115, 024102	79

1348	Magnetic transitions and site-disordered induced weak ferromagnetism in (1-x)BiFeO ₃ -xBaTiO ₃ . 2014 , 89,	43
1347	Study of structural, ferromagnetic and ferroelectric properties of nanostructured barium doped Bismuth Ferrite. 2014 , 353, 57-64	34
1346	A simple, low-cost CVD route to thin films of BiFeO ₃ for efficient water photo-oxidation. 2014 , 2, 2922	72
1345	Effects of γ-ray irradiation on ferroelectric properties of Pr and Mn co-substituted BiFeO ₃ thin films. 2014 , 47, 045310	6
1344	Stabilization of metastable tetragonal phase in a rhombohedral magnetoelectric multiferroic BiFeO ₃ PbTiO ₃ . 2014 , 47, 045004	18
1343	BiFeO ₃ epitaxial thin films and devices: past, present and future. 2014 , 26, 473201	173
1342	Microstructure of highly strained BiFeO ₃ thin films: Transmission electron microscopy and electron-energy loss spectroscopy studies. 2014 , 115, 043526	16
1341	Electronic structure and magnetic properties of PbMO ₃ (M = Fe, Co, Ni) magnetic perovskites: An ab initio study. 2014 , 28, 1450205	11
1340	Measurement of transient photoabsorption and photocurrent of BiFeO ₃ thin films: Evidence for long-lived trapped photocarriers. 2014 , 89,	24
1339	Introducing a large polar tetragonal distortion into Ba-doped BiFeO ₃ by low-temperature fluorination. 2014 , 53, 12572-83	21
1338	Bimodal island size distribution in heteroepitaxial growth. 2014 , 112, 075503	6
1337	Phase transitions and antiferroelectricity in BiFeO ₃ from atomic-level simulations. 2014 , 90,	15
1336	Optimization of excess Bi doping to enhance ferroic orders of spin casted BiFeO ₃ thin film. 2014 , 115, 234105	37
1335	Photovoltaic Property of Multiferroic BiFeO_3 Films With Different Textures on Glass Substrates. 2014 , 50, 1-4	1
1334	Structure and properties of (1-x)BiFeO ₃ -xPbFe ₂ /3W ₁ /3O ₃ (0 ≤ x ≤ 1) solid solutions. 2014 , 50, 1272-1276	
1333	Low-temperature acetone-assisted hydrothermal synthesis and characterization of BiFeO ₃ powders. 2014 , 25, 4039-4045	17
1332	Effect of process condition on the ferroelectric properties in BiFeO ₃ -(Bi,K)TiO ₃ ceramics. 2014 , 65, 382-386	4
1331	Heat capacity and dielectric properties of multiferroics Bi _{1-x} Gd _x FeO ₃ (x = 0.0-0.20). 2014 , 56, 1412-1415	12

- 1330 Weak ferromagnetism and spin density distributions in thin films of $\text{Gd}_{1-x}\text{Bi}_x\text{FeO}_3$ solid solutions. **2014**, 78, 690-693
- 1329 Transformations of Space-Modulated Structures in BiFeO_3 -Like Multiferroics. **2014**, 215, 495-498 1
- 1328 Effects of $\text{Ba}_{0.7}\text{Sr}_{0.3}\text{TiO}_3$ -based buffer layers and La/Mn doping on the crystallization behavior and multiferroic properties of BiFeO_3 thin films. **2014**, 4, 55889-55896 5
- 1327 Effect of lanthanum doping on tetragonal-like BiFeO_3 with mixed-phase domain structures. **2014**, 90, 22
- 1326 Combined structural, electrical, magnetic and optical characterization of bismuth ferrite nanoparticles synthesized by auto-combustion route Peer review under responsibility of The Ceramic Society of Japan and the Korean Ceramic Society. View all notes. **2014**, 2, 416-421 58
- 1325 Rapid synthesis, structure and photocatalysis of pure bismuth A-site perovskite of $\text{Bi}(\text{Mg}_{3/8}\text{Fe}_{2/8}\text{Ti}_{3/8})\text{O}_3$. **2014**, 43, 9255-9 5
- 1324 Simple top-down preparation of magnetic $\text{Bi}_{1-x}\text{Fe}_x\text{Ti}_x\text{O}_3$ nanoparticles by ultrasonication of multiferroic bulk material. **2014**, 6, 14336-42 31
- 1323 Synthesis and properties of single crystal TbMn_2O_5 nanostructures. **2014**, 4, 58337-58341 1
- 1322 Effect of Substrates on the Structure and Ferroelectric Properties of Multiferroic BiFeO_3 Films. **2014**, 50, 1-4 1
- 1321 Structural and electric evidence of ferroelectric state in PbMnWO_4 double perovskite system. **2014**, 53, 10283-90 13
- 1320 Mössbauer study of temperature-dependent cycloidal ordering in BiFeO_3 nanoparticles. **2014**, 14, 6061-5 32
- 1319 Structural evolution from $\text{Bi}_{4.2}\text{K}_{0.8}\text{Fe}_2\text{O}_9$ nanobelts to BiFeO_3 nanochains in vacuum and their multiferroic properties. **2014**, 6, 14766-71 8
- 1318 Multiferroic Properties and Piezoelectric Characterizations of Bismuth Ferrite Based Compounds Produced by Spark Plasma Sintering. **2014**, 975, 257-262
- 1317 BiFeO_3 thin films prepared on metallic Ni tapes by chemical solution deposition: effects of annealing temperature and a $\text{La}_{0.5}\text{Sr}_{0.5}\text{TiO}_3$ buffer layer on the dielectric, ferroelectric and leakage properties. **2014**, 4, 32738-32743 13
- 1316 Atmosphere controlled conductivity and Maxwell-Wagner relaxation in $\text{Bi}_{0.5}\text{K}_{0.5}\text{TiO}_3/\text{BiFeO}_3$ ceramics. **2014**, 115, 044104 33
- 1315 Novel behaviors of multiferroic properties in Na-Doped BiFeO_3 nanoparticles. **2014**, 6, 10831-8 60
- 1314 Investigation of continuous changes in the electric-field-induced electronic state in $\text{Bi}_{(1-x)}\text{Ca}_x\text{FeO}_{(3-\delta)}$. **2014**, 16, 17412-6 17
- 1313 Ultrathin oriented BiFeO_3 films from deposition of atomic layers with greatly improved leakage and ferroelectric properties. **2014**, 6, 443-9 23

1312	Jahn-Teller, polarity, and insulator-to-metal transition in BiMnO ₃ at high pressure. 2014 , 112, 075501	37
1311	Temperature-dependent interplay of Dzyaloshinskii-Moriya interaction and single-ion anisotropy in multiferroic BiFeO ₃ . 2014 , 113, 107202	45
1310	Misfit strain driven cation inter-diffusion across an epitaxial multiferroic thin film interface. 2014 , 115, 054103	28
1309	Nanostructured Bi(1-x)Gd(x)FeO ₃ as multiferroic photocatalyst on its sunlight driven photocatalytic activity. 2014 , 4, 16871-16878	59
1308	Ab initio study of multiferroic BiFeO ₃ (110) surfaces. 2014 , 89,	16
1307	Structure and lattice dynamics of solid solutions (1-x)BiFeO ₃ -xANbO ₃ (A = K, Na). 2014 , 56, 1866-1871	2
1306	Structure and magnetism of the A site scandium perovskite (Sc _{0.94} Mn _{0.06})Mn _{0.65} Ni _{0.35} O ₃ synthesized at high pressure. 2014 , 372, 20130012	9
1305	Structural, dielectric and magnetic properties of Gd and Dy doped (Bi _{0.95} RE _{0.05})(Fe _{0.95} Mn _{0.05})O ₃ ceramics synthesized by SSR method. 2014 , 197, 1-5	3
1304	Cyclic Chemical Vapor Deposition of Nickel Ferrite Thin Films Using Organometallic Precursor Combination. 2014 , 3, P345-P352	17
1303	Influence of multi-element co-doping on structure and multiferroic properties of BiFeO ₃ thin films. 2014 , 136, 314-317	5
1302	Enhanced Photovoltaic Performance in Polycrystalline BiFeO ₃ Thin Film/ZnO Nanorod Heterojunctions. 2014 , 118, 15200-15206	25
1301	Enhancement of magnetic and ferroelectric properties of BiFeO ₃ by Er and transition element (Mn, Co) co-doping. 2014 , 188, 26-30	33
1300	Evidence of spin-two phonon coupling and improved multiferroic behavior of Bi _{1-x} Dy _x FeO ₃ nanoparticles. 2014 , 40, 13347-13356	18
1299	Structure and multiferroic properties of Sr substituted Bi _{0.89} Sm _{0.11} Sr _x Fe _{0.94} (Mn _{0.04} Cr _{0.02})O ₃ thin films. 2014 , 40, 13249-13256	10
1298	Element-specific depth profile of magnetism and stoichiometry at the La _{0.67} Sr _{0.33} MnO ₃ /BiFeO ₃ interface. 2014 , 90,	16
1297	Interface strain-induced multiferroicity in a SmFeO ₃ film. 2014 , 6, 7356-62	36
1296	Single phase, electrically insulating, multiferroic La-substituted BiFeO ₃ prepared by mechano-synthesis. 2014 , 2, 8398-8411	40
1295	Control of conductivity and electric field induced strain in bulk Bi _{0.5} K _{0.5} TiO ₃ BiFeO ₃ ceramics. 2014 , 104, 122905	24

1294	Impact of the various spin- and orbital-ordering processes on the multiferroic properties of orthovanadate DyVO ₃ . 2014 , 90,	14
1293	Cation exchange in a 3D perovskite-synthesis of Ni(0.5)TaO ₃ 2014 , 53, 8020-4	9
1292	Conduction mechanism and dielectric properties of BiFeO ₃ /BaTiO ₃ solid solutions. 2014 , 25, 4896-4901	11
1291	Monocrystalline mesoporous metal oxide with perovskite structure: a facile solid-state transformation of a coordination polymer. 2014 , 50, 13849-52	10
1290	Investigation of the dielectric relaxation processes in PbZr _{0.65} Ti _{0.35} O ₃ /BaFe ₁₂ O ₁₉ multiferroic ceramic composites. 2014 , 148, 841-845	
1289	Hierarchically Grown CaMn ₃ O ₆ Nanorods by RF Magnetron Sputtering for Enhanced Visible-Light-Driven Photocatalysis. 2014 , 118, 24127-24135	14
1288	Phase diagram of BiFeO ₃ /LaFeO ₃ superlattices studied by x-ray diffraction experiments and first-principles calculations. 2014 , 90,	9
1287	Multiferroic hexagonal ferrites (h-RFeO ₃ , R = Y, Dy-Lu): a brief experimental review. 2014 , 28, 1430008	50
1286	Theoretical study of stability and electronic structure of the new type of ferroelectric materials XSnO ₃ (X = Mn, Zn, Fe, Mg). 2014 , 28, 1450224	10
1285	Nanoscale Bi ₂ FeO ₆ precipitates in BiFeO ₃ thin films: a metastable Aurivillius phase. 2014 , 49, 6952-6960	8
1284	Exchange-biased hybrid ferromagnetic-multiferroic core-shell nanostructures. 2014 , 6, 7215-20	24
1283	Single-crystalline Bi ₂ Fe ₄ O ₉ synthesized by low-temperature co-precipitation: performance as photo- and Fenton catalysts. 2014 , 4, 27820-27829	40
1282	Photoelectrochemical response and electronic structure analysis of mono-dispersed cuboid-shaped Bi ₂ Fe ₄ O ₉ crystals with near-infrared absorption. 2014 , 4, 28209-28218	24
1281	Tunable multiferroic and bistable/complementary resistive switching properties of dilutely Li-doped BiFeO ₃ nanoparticles: an effect of aliovalent substitution. 2014 , 6, 4735-44	84
1280	Relaxor ferroelectricity and magnetoelectric coupling in ZnO-Co nanocomposite thin films: beyond multiferroic composites. 2014 , 6, 4737-42	29
1279	Structural and electrical characterization of BiFeO ₃ /NaTaO ₃ multiferroic. 2014 , 116, 1833-1840	9
1278	Structural and electrical properties of La-modified BiFeO ₃ /BaTiO ₃ composites. 2014 , 25, 2086-2095	38
1277	Photovoltaic properties of Pt/BiFeO ₃ thin film/fluorine-doped tin oxide capacitor. 2014 , 72, 74-79	6

1276	The acute cytotoxicity of bismuth ferrite nanoparticles on PC12 cells. 2014 , 16, 1	6
1275	Effects of Ho and Ti Doping on Structural and Electrical Properties of BiFeO ₃ Thin Films. 2014 , 97, 235-240	35
1274	Heteroepitaxy of tetragonal BiFeO ₃ on hexagonal sapphire(0001). 2014 , 6, 2639-46	13
1273	Co-existence of tetragonal and monoclinic phases and multiferroic properties for $x \geq 0.30$ in the $(1-x)\text{Pb}(\text{Zr}_{0.52}\text{Ti}_{0.48})\text{O}_3(1-x)\text{BiFeO}_3$ system. 2014 , 614, 165-172	13
1272	Enormous energy harvesting and storage potential in multiferroic epitaxial thin film heterostructures: an unforeseen era. 2014 , 1, 015503	15
1271	Thin film multiferroic nanocomposites by ion implantation. 2014 , 6, 1909-15	11
1270	Room temperature ferromagnetism of nonmagnetic element Ca-doped LiNbO ₃ films. 2014 , 10, 115-118	1
1269	Ferromagnetic magnetization switching by an electric field: A review. 2014 , 56, 865-872	19
1268	Optical properties of epitaxial BiFeO ₃ thin film grown on SrRuO ₃ -buffered SrTiO ₃ substrate. 2014 , 9, 188	26
1267	Giant ultrafast photo-induced shear strain in ferroelectric BiFeO ₃ . 2014 , 5, 4301	105
1266	Single-crystalline BiMnO ₃ studied by temperature-dependent x-ray diffraction and Raman spectroscopy. 2014 , 89,	11
1265	Ab Initio Studies on the Structural and Electronic Properties of Bismuth Ferrite Based on Ferroelectric Hexagonal Phase and Paraelectric Orthorhombic Phase. 2014 , 155, 134-142	10
1264	Development of an Atomic Level Model for BiFeO ₃ from First-Principles. 2014 , 461, 61-67	2
1263	A comparative investigation on structure and multiferroic properties of bismuth ferrite thin films by multielement co-doping. 2014 , 60, 596-603	4
1262	Enhanced electric and magnetic properties in Ce/Er co-doped bismuth ferrite nanostructure. 2014 , 136, 441-444	18
1261	Tuning phase stability of complex oxide nanocrystals via conjugation. 2014 , 14, 3314-20	11
1260	Tetragonal-tetragonal-monoclinic-rhombohedral transition: Strain relaxation of heavily compressed BiFeO ₃ epitaxial thin films. 2014 , 104, 052908	15
1259	Ab Initio calculations of the lattice dynamics and the ferroelectric instability of the BiFeO ₃ multiferroic. 2014 , 56, 1799-1805	8

1258	Electronic and magnetic properties of BiFeO ₃ with intrinsic defects: First-principles prediction. 2014 , 23, 067102	4
1257	Visible-Light Photocatalysis in Ca _{0.6} Ho _{0.4} MnO ₃ Films Deposited by RF-Magnetron Sputtering Using Nanosized Powder Compacted Target. 2014 , 118, 590-597	12
1256	Localized excited charge carriers generate ultrafast inhomogeneous strain in the multiferroic BiFeO ₃ . 2014 , 112, 097602	80
1255	Crystallographic and magnetic structure of the perovskite-type compound BaFeO _{2.5} : unrivaled complexity in oxygen vacancy ordering. 2014 , 53, 5911-21	36
1254	Experimental evidence of enhanced ferroelectricity in Ca doped BiFeO ₃ . 2014 , 144, 476-483	34
1253	Effect of cooling oxygen pressure on the photoconductivity in Bi _{0.9} La _{0.1} FeO ₃ thin films. 2014 , 591, 346-350	17
1252	Enhanced magnetization and magnetoelectric coupling in 1 \times (BiFeO ₃)/x(La ₂ /3Sr ₁ /3MnO ₃) composites. 2014 , 69, 1-9	12
1251	Effects of La content on the magnetic, electric and structural properties of BiFeO ₃ . 2014 , 354, 184-189	39
1250	Phase transition and enhanced multiferroic properties of (Sm, Mn and Cr) co-doped BiFeO ₃ thin films. 2014 , 40, 12179-12185	21
1249	Comparative study of room temperature and low temperature magnetization and magnetoelectric coupling behavior of Ti and Pr doped BiFeO ₃ . 2014 , 67, 233-241	11
1248	Structural, electrical and magnetic properties of (Bi _{0.9} RE _{0.1})(Fe _{0.97} Co _{0.03})O ₃ (RE=Nd and Gd) thin films. 2014 , 52, 143-150	7
1247	Piezoelectric, ferroelectric properties of multiferroic YMnO ₃ epitaxial film studied by piezoresponse force microscopy. 2014 , 390, 56-60	6
1246	The oxygen octahedral distortion induced magnetic enhancement in multiferroic Bi _{1-x} YbxFe _{0.95} Co _{0.05} O ₃ powders. 2014 , 604, 327-330	18
1245	Effects of gamma-ray irradiation on interface states and series-resistance characteristics of BiFeO ₃ MOS capacitors. 2014 , 319, 44-47	18
1244	Ferroelectric and ferromagnetic properties of Bi _{7-x} La _x Fe _{1.5} Co _{1.5} Ti ₃ O ₂₁ ceramics prepared by the hot-press method. 2014 , 600, 168-171	35
1243	Effect of structural transition on magnetic and optical properties of Ca and Ti co-substituted BiFeO ₃ ceramics. 2014 , 584, 566-572	89
1242	Preparation and characterization of Bi-doped LuFeO ₃ thin films grown on LaNiO ₃ substrate. 2014 , 387, 6-9	7
1241	Magnetoelectric Devices for Spintronics. 2014 , 44, 91-116	261

1240	Structure, conduction mechanisms and multiferroic properties of (Sm, Cr) co-doped Bi _{0.89} Sm _{0.11} Fe _{0.97} Cr _{0.03} O ₃ /NiFe ₂ O ₄ composition thin films. 2014 , 25, 3389-3395	4
1239	Control of ferroelectricity and magnetism in multi-ferroic BiFeO ₃ by epitaxial strain. 2014 , 372, 20120438	28
1238	Ce-doped bismuth ferrite thin films with improved electrical and functional properties. 2014 , 49, 5355-5364	39
1237	The preparation and characterization of 1D multiferroic BFO/P(VDF-TrFE) composite nanofibers using electrospinning. 2014 , 130, 157-159	13
1236	Effect of Tb/Mn substitution on the magnetic and electrical properties of BiFeO ₃ ceramics. 2014 , 364, 60-67	15
1235	Defect thermodynamics and kinetics in thin strained ferroelectric films: The interplay of possible mechanisms. 2014 , 89,	25
1234	Chiral Properties of BiFeO ₃ Inferred from Resonant X-ray Bragg Diffraction. 2014 , 83, 013706	3
1233	Structure, ferroelectric and piezoelectric properties of Bi _{0.5} (Na _{0.8} K _{0.2}) _{0.5} TiO ₃ modified BiFeO ₃ /BaTiO ₃ lead-free piezoelectric ceramics. 2014 , 25, 3753-3761	10
1232	Structure, leakage mechanism and multiferroic properties of (Mn, Cr) co-doped BiFe _{0.93} Mn _{0.04} Cr _{0.03} O ₃ /NiFe ₂ O ₄ bilayer film by sol-gel. 2014 , 72, 186-193	6
1231	Possibility of room-temperature multiferroism in Mg-doped ZnO. 2014 , 114, 453-457	39
1230	Interfaces and Nanostructures of Functional Oxide Octahedral Framework Structures. 2014 , 1,	2
1229	Phase Transition of BiFe _{1-x} Al _x O ₃ Films Prepared by Chemical Solution Deposition. 2014 , 61, S321-S323	3
1228	Electric Field-Induced Oxidation of Ferromagnetic/Ferroelectric Interfaces. 2014 , 24, 71-76	24
1227	A new chiral phase of BiFeO ₃ evidenced from resonant x-ray Bragg diffraction. 2014 , 519, 012012	
1226	Temperature dependence of magnetic and magnetotransport properties in BiFeO ₃ thin films by pulsed laser deposition. 2014 , 1636, 1	
1225	The Influence of La and Ho Substitution on Structural, Micro Structural and Magnetic Properties of BiFeO ₃ Nanopowders. 2015 , 11, 238-241	3
1224	Multiferroic Thin Films. 2015 , 1-15	
1223	First-Principles Materials Design of High-Performing Bulk Photovoltaics with the LiNbO ₃ Structure. 2015 , 4,	26

1222	Exploiting interfacial and size effects to construct oxide superlattices with robust and tunable magnetoelectric properties at room temperature. 2015 , 91,	3
1221	Ferroelectric soft mode of polar ZnTiO ₃ investigated by Raman spectroscopy at high pressure. 2015 , 91,	11
1220	Pressure-driven metal-insulator transition in BiFeO ₃ from dynamical mean-field theory. 2015 , 92,	19
1219	Linear antiferrodistortive-antiferromagnetic effect in multiferroics: Physical manifestations. 2015 , 92,	12
1218	Anisotropic optical properties of rhombohedral and tetragonal thin film BiFeO ₃ phases. 2015 , 92,	21
1217	Cycloid manipulation by electric field in BiFeO ₃ films: Coupling between polarization, octahedral rotation, and antiferromagnetic order. 2015 , 92,	17
1216	Magnetic structure of an incommensurate phase of La-doped BiFe _{0.5} Sc _{0.5} O ₃ : Role of antisymmetric exchange interactions. 2015 , 92,	12
1215	Driving Spin Excitations by Hydrostatic Pressure in BiFeO ₃ . 2015 , 115, 267204	34
1214	Exchange-striction induced giant ferroelectric polarization in copper-based multiferroic material Bi ₂ VO ₇ . 2015 , 91,	35
1213	Successive Magnetic-Field-Induced Transitions and Colossal Magnetoelectric Effect in Ni ₃ TeO ₆ . 2015 , 115, 137201	40
1212	Giant optical enhancement of strain gradient in ferroelectric BiFeO ₃ thin films and its physical origin. 2015 , 5, 16650	27
1211	Electroelastic fields in artificially created vortex cores in epitaxial BiFeO ₃ thin films. 2015 , 107, 052903	23
1210	Switchable photovoltaic and polarization modulated rectification in Si-integrated Pt/(Bi _{0.9} Sm _{0.1})(Fe _{0.97} Hf _{0.03})O ₃ /LaNiO ₃ heterostructures. 2015 , 107, 162904	31
1209	Structural, electrical and magnetic properties of multiferroic Bi _{1-x} GdxFeO ₃ (x = 0.00 and 0.15). 2015 ,	
1208	Stabilisation of Fe ₂ O ₃ -rich Perovskite Nanophase in Epitaxial Rare-earth Doped BiFeO ₃ Films. 2015 , 5, 13066	7
1207	Tetragonal BiFeO ₃ on yttria-stabilized zirconia. 2015 , 3, 116104	6
1206	Unraveling the magnetic properties of BiFe _{0.5} Cr _{0.5} O ₃ thin films. 2015 , 3, 116107	11
1205	Abnormal variation of band gap in Zn doped Bi _{0.9} La _{0.1} FeO ₃ nanoparticles: Role of Fe-O-Fe bond angle and Fe-O bond anisotropy. 2015 , 107, 042905	10

1204	Crystallization engineering as a route to epitaxial strain control. 2015 , 3, 106102	10
1203	A bridge for accelerating materials by design. 2015 , 1,	33
1202	Rotomagnetic couplings influence on the magnetic properties of antiferrodistortive antiferromagnets. 2015 , 118, 144101	8
1201	Near room temperature giant magnetodielectricity in BiFeO ₃ /CoFe ₂ O ₄ composite. 2015 ,	
1200	Impedance and AC conductivity study of nano crystalline, fine grained multiferroic bismuth ferrite (BiFeO ₃), synthesized by microwave sintering. 2015 , 5, 097164	46
1199	Atomic layer deposition of perovskite oxides and their epitaxial integration with Si, Ge, and other semiconductors. 2015 , 2, 041301	64
1198	Effect of substrates on magnetization of BiFeO ₃ films. 2015 , 118, 075303	6
1197	Synthesis and characterization of BiFeO ₃ for photocatalytic degradation of azo dye. 2015 ,	
1196	Long-time relaxation of photo-induced influence on BiFeO ₃ thin films. 2015 , 118, 204103	11
1195	Magnetoresistance of galferol-based magnetic tunnel junction. 2015 , 5, 127128	1
1194	Rare earth (La) and metal ion (Pb) substitution induced structural and multiferroic properties of bismuth ferrite. 2015 , 4, 292-299	9
1193	Strain Localization in Thin Films of Bi(Fe,Mn)O ₃ Due to the Formation of Stepped Mn(4+)-Rich Antiphase Boundaries. 2015 , 10, 407	11
1192	Low Temperatures Dielectric Anomaly in BiFeO ₃ -Based Multiferroic Ceramics. 2015 , 77-86	
1191	Thermodynamic analysis of defect formation in BiFeO ₃ . 2015 , 12, 117-119	2
1190	Magnetic and dielectric properties of [N(C ₂ H ₅) ₄] ₂ CoClBr ₃ solid solution: A new potential multiferroic. 2015 , 252, 1778-1782	5
1189	Electric-Field-Induced Domain Switching and Domain Texture Relaxations in Bulk Bismuth Ferrite. 2015 , 98, 3884-3890	23
1188	High-Performance Lead-Free Piezoceramics with High Curie Temperatures. <i>Advanced Materials</i> , 2015 , 27, 6976-82	24 283
1187	A Facile Chemical Solution-Based Method for Epitaxial Growth of Thick Ferrite Films. 2015 , 1, 1500102	2

1186	Facile Synthesis of Highly Efficient p-n Heterojunction CuO/BiFeO ₃ Composite Photocatalysts with Enhanced Visible-Light Photocatalytic Activity. 2015 , 7, 3279-3289	77
1185	Structural and Ferroic Properties of La, Nd, and Dy Doped BiFeO ₃ Ceramics. 2015 , 2015, 1-8	9
1184	Polar Order Evolutions near the Rhombohedral to Pseudocubic and Tetragonal to Pseudocubic Phase Boundaries of the BiFeO ₃ -BaTiO ₃ System. 2015 , 8, 8355-8365	14
1183	Double crystal symmetries in morphotropic phase boundary of substituted BiFeO ₃ ceramics. 2015 ,	
1182	Size effect on the magnetic properties of oleic acid stabilized substrate free BiFeO ₃ nanocrystals. 2015 , 70, 10601	1
1181	Epitaxial Growth and Multiferroic Properties of (001)-Oriented BiFeO ₃ -YMnO ₃ Films. 2015 , 2, 157-162	4
1180	Characterization of Multiferroic Domain Structures in Multiferroic Oxides. 2015 , 2015, 1-8	5
1179	Preparation and characterization of Bi _{1-x} NdxFeO ₃ ceramics. 2015 , 88, 817-824	
1178	Strain-mediated electric-field control of exchange bias in a Co ₉₀ Fe ₁₀ /BiFeO ₃ /SrRuO ₃ /PMN-PT heterostructure. 2015 , 5, 8905	46
1177	Magnetic interactions in BiFeO ₃ /MnO ₂ films and BiFeO ₃ /BiMnO ₃ superlattices. 2015 , 5, 9093	35
1176	High density array of multiferroic nanoislands in a large area. 2015 , 3, 2237-2243	11
1175	Texture control of multiferroic BiFeO ₃ polycrystalline films on glass substrates with various metal electrode underlayers. 2015 , 117, 17C713	2
1174	Formation of BiFeO ₃ (110) films on ferromagnetic CoPt(111) electrode layer on glass substrates at reduced temperatures. 2015 , 117, 17C721	5
1173	Low-energy phases, electronic and optical properties of Bi _{1-x} La _x FeO ₃ solid solution: Ab-initio LDA+U studies. 2015 , 41, 10940-10948	14
1172	The abnormal electrical and optical properties in Na and Ni codoped BiFeO ₃ nanoparticles. 2015 , 117, 174106	18
1171	Tunable magnetic and electrical behaviors in perovskite oxides by oxygen octahedral tilting. 2015 , 58, 302-312	22
1170	Structural and optical properties of the BiFeO ₃ system multiferroic films prepared by a sol-gel method. 2015 , 41, S361-S364	2
1169	Effect of Ba substitution on the multiferroic properties of BiFeO ₃ films on glass substrates. 2015 , 117, 17C734	9

1168	Structural, Dielectric, and Magnetic Properties of Ba-Doped Multiferroic Bismuth Ferrite. 2015 , 28, 958-964	14
1167	Versatility of electrospinning in the fabrication of fibrous mat and mesh nanostructures of bismuth ferrite (BiFeO ₃) and their magnetic and photocatalytic activities. 2015 , 17, 17745-54	55
1166	Novel behaviors of single-crystalline BiFeO ₃ nanorods hydrothermally synthesized under magnetic field. 2015 , 3, 6924-6931	32
1165	Multiferroic oxide thin films and heterostructures. 2015 , 2, 021304	112
1164	Static and dynamic strain coupling behaviour of ferroic and multiferroic perovskites from resonant ultrasound spectroscopy. 2015 , 27, 263201	48
1163	Strain correlated effect on structural, magnetic, and dielectric properties in Ti ⁴⁺ substituted Bi _{0.8} Ba _{0.2} Fe _{1-x} Ti _x O ₃ . 2015 , 46, 71-79	3
1162	Superior electro-optic response in multiferroic bismuth ferrite nanoparticle doped nematic liquid crystal device. 2015 , 5, 10845	37
1161	Structural, optical and vibrational properties of self-assembled Pbn+1(Ti1-x Fex)nO(3n+1)- \square Ruddlesden-Popper superstructures. 2015 , 5, 7719	6
1160	Magnetoelastic interaction in a ferromagnet-multiferroic system. 2015 , 57, 924-928	2
1159	Transport properties of Ba-doped BiFeO ₃ multiferroic nanoparticles. 2015 , 26, 6793-6800	17
1158	Effect of isovalent non-magnetic Fe-site doping on the electronic structure and spontaneous polarization of BiFeO ₃ . 2015 , 117, 184104	8
1157	Dielectric and Electrical Properties of BiFeO ₃ /LiTaO ₃ Systems. 2015 , 44, 2359-2368	8
1156	Synthesis and characterization of Bismuth ferrite (BiFeO ₃) nanoparticles by solution evaporation method. 2015 , 393, 269-272	25
1155	In situ electron microscopy of ferroelectric domains. 2015 , 40, 53-61	10
1154	Spin and lattice excitations of a BiFeO ₃ thin film and ceramics. 2015 , 91,	21
1153	Dielectric and magnetic properties of (Bi _{1-x} La _x FeO ₃) _{0.5} (PbTiO ₃) _{0.5} ceramics prepared by high energy mechanochemical technique. 2015 , 35, 33-44	4
1152	Enhanced Multiferroic Properties of Eu-Doped BiFeO ₃ Thin Films Derived from Rhombohedral \square Tetragonal Phase Boundary. 2015 , 44, 3752-3760	5
1151	Electric-field-induced structural and magnetic transformations in BiFeO ₃ multiferroics. 2015 , 57, 933-942	7

1150	Epitaxial growth of magnetic-oxide thin films. 2015 , 129-172	2
1149	Phase transition and enhanced magneto-dielectric response in BiFeO ₃ -DyMnO ₃ multiferroics. 2015 , 117, 144103	36
1148	Enhancement of photoinduced electrical properties of Al-doped ZnO/BiFeO ₃ layered thin films prepared by chemical solution deposition. 2015 , 54, 10NA05	7
1147	Understanding Strain-Induced Phase Transformations in BiFeO Thin Films. 2015 , 2, 1500041	14
1146	Self-interaction corrected LDA + U investigations of BiFeO ₃ properties: plane-wave pseudopotential method. 2015 , 2, 116101	24
1145	Multiferroic materials and magnetoelectric physics: symmetry, entanglement, excitation, and topology. 2015 , 64, 519-626	486
1144	The facile synthesis, characterization and evaluation of photocatalytic activity of bimetallic FeBiO ₃ in natural sunlight exposure. 2015 , 5, 102663-102673	16
1143	Structure and Mössbauer spectroscopy studies of mechanically activated (BiFeO ₃) _{1-x} (BaTiO ₃) _x solid solutions. 2015 , 60, 109-114	2
1142	Multiferroic properties of Bi _{0.5} K _{0.5} TiO ₃ /BiFe _{1-x} CoxO ₃ (0 ≤ x ≤ 0.2) solid solution. 2015 , 5, 104210-104215	2
1141	Effects of Interface Layers and Domain Walls on the Ferroelectric-Resistive Switching Behavior of Au/BiFeO ₃ /La _{0.6} Sr _{0.4} MnO ₃ Heterostructures. 2015 , 7, 26036-42	23
1140	Structure and local polar domains of Dy-modified BiFeO ₃ /PbTiO ₃ multiferroic solid solutions. 2015 , 3, 12450-12456	19
1139	Sintering behavior and dielectric properties of Bi ³⁺ -substituted Nd(Zn _{0.5} Ti _{0.5})O ₃ microwave ceramics. 2015 , 29, 1550233	1
1138	Magnetoelectronics--electric field control of magnetism in the solid state. 2015 , 27, 500301	1
1137	Ferroelectric and Magnetic Properties of SrO-B ₂ O ₃ -SiO ₂ Glass-Doped BiFeO ₃ Ceramics. 2015 , 489, 43-50	5
1136	The Multiferroic Properties of BiFeO ₃ /Na _{0.5} Bi _{0.5} TiO ₃ Solid Solution Ceramics. 2015 , 51, 1-4	3
1135	The Electrical and Enhanced Magnetic Properties of (Ce, Co) Doped BiFeO ₃ Particles Synthesized Via Sol-Gel Method. 2015 , 489, 73-80	4
1134	AlFeO ₃ nanoparticles: An efficient perovskite material for low operating bias memristive devices. 2015 ,	
1133	Effect of La Substitution on Structural, Electrical and Magnetic Properties in BF-BCZT Ceramics. 2015 , 489, 88-95	2

1132	Studies of structural, dielectric, electrical and ferroelectric characteristics of BiFeO ₃ and (Bi _{0.5} K _{0.5})(Fe _{0.5} Ta _{0.5})O ₃ . 2015 , 26, 9640-9648	6
1131	Magneto-dielectricity in Li _{0.05} Ti _{0.02} Ni _{0.93} O at room temperature. 2015 , 2, 096101	1
1130	New complex bismuth oxides in the Bi ₂ O ₃ -NiO-Sb ₂ O ₅ system and their properties. 2015 , 225, 97-104	11
1129	The microstructure and ferroelectric property of Nd-doped multiferroic ceramics Bi _{0.85} Nd _{0.15} FeO ₃ . 2015 , 41, 5498-5504	10
1128	Effect of film thickness and bottom electrode material on the ferroelectric and photovoltaic properties of sputtered polycrystalline BiFeO ₃ films. 2015 , 139, 325-328	26
1127	Multiferroic and magnetoelectric properties of BiFeO ₃ -CrO ₃ ceramics at the rhombohedral-orthorhombic phase boundary. 2015 , 141, 168-171	4
1126	Fast synthesis of rare-earth (Pr ³⁺ , Sm ³⁺ , Eu ³⁺ and Gd ³⁺) doped bismuth ferrite powders with enhanced magnetic properties. 2015 , 629, 62-68	51
1125	Magnetic, ferroelectric and leakage current properties of gadolinium doped bismuth ferrite thin films by sol-gel method. 2015 , 381, 127-130	9
1124	Magnetoelectricity in BiFeO ₃ and BiFe _{0.98} Co _{0.02} O ₃ nano particles. 2015 , 628, 32-38	14
1123	High field studies on BiFeO ₃ single crystals grown by the laser-diode heating floating zone method. 2015 , 383, 259-261	6
1122	Synthesis, phase diagram and magnetic properties of (1-x)BiFeO ₃ -LaMnO ₃ Solid Solution. 2015 , 634, 142-147	9
1121	In-field ⁵⁷ Fe Mössbauer study of multiferroic Ba _{0.5} Sr _{1.5} Zn ₂ Fe ₁₂ O ₂₂ Y-type hexaferrite. 2015 , 384, 27-32	7
1120	Microstructural and optical properties tuning of BiFeO ₃ thin films elaborated by magnetron sputtering. 2015 , 26, 3316-3323	5
1119	Electric polarization and diode-like conduction in hydrothermally grown BiFeO ₃ thin films. 2015 , 622, 734-737	6
1118	Oxygen-vacancy and charge hopping related dielectric relaxation and conduction process in orthorhombic Gd doped YFe _{0.6} Mn _{0.4} O ₃ multiferroics. 2015 , 628, 379-389	41
1117	Composition- and pressure-induced ferroelectric to antiferroelectric phase transitions in Sm-doped BiFeO ₃ system. 2015 , 106, 012903	43
1116	Synthesis, structures and magnetic properties of the dimorphic Mn ₂ CrSbO ₆ oxide. 2015 , 44, 10665-72	34
1115	The local distortion and electronic behavior in Mn doped BiFeO ₃ . 2015 , 633, 216-219	30

1114	Neutron inelastic scattering measurements of low-energy phonons in the multiferroic BiFeO ₃ . 2015 , 91,	12
1113	Enhanced unipolar resistive switching in substituted Bi(Fe _{0.95} Mn _{0.05})O ₃ bilayer films. 2015 , 2, 026402	
1112	Improved multiferroic properties in (Ho, Mn) co-doped BiFeO ₃ thin films prepared by chemical solution deposition. 2015 , 41, 4668-4674	24
1111	Diffuse phase ferroelectric vs. Polomska transition in (1-x) BiFeO ₃ -(x) BaZr _{0.025} Ti _{0.975} O ₃ (0.1 ≤ x ≤ 0.3) solid solutions. 2015 , 117, 024102	8
1110	Ferroelectric domain structures and polarization switching characteristics of polycrystalline BiFeO ₃ thin films on glass substrates. 2015 , 15, 584-587	9
1109	Structural, electrical, and multiferroic properties of (Nd, Zn) co-doped BiFeO ₃ thin films prepared by a chemical solution deposition method. 2015 , 119, 667-672	8
1108	Structural, magnetic and electrical properties of BiFeO ₃ co-substituted with PrMn. 2015 , 65, 224-230	9
1107	Phase transition and piezoelectricity of sol-gel-processed Sm-doped BiFeO ₃ thin films on Pt(111)/Ti/SiO ₂ /Si substrates. 2015 , 3, 2115-2122	48
1106	BiFeO ₃ Thin Films: A Playground for Exploring Electric-Field Control of Multifunctionalities. 2015 , 45, 249-275	60
1105	Mn substitution-induced revival of the ferroelectric antiferromagnetic phase in Bi _{1-x} Ca _x FeO ₃ /2 multiferroics. 2015 , 50, 1740-1745	13
1104	Photovoltaic and magnetic properties of BiFeO ₃ /TiO ₂ heterostructures under epitaxial strain and an electric field. 2015 , 153, 405-409	4
1103	Effect of Ba _{1-x} Nb _x co-doping on the structural, dielectric, magnetic and ferroelectric properties of BiFeO ₃ nanoparticles. 2015 , 41, 6912-6919	53
1102	Ferroelectricity in hexagonal YFeO ₃ film at room temperature. 2015 , 24, 017701	5
1101	Multiferroic behavior of templated BiFeO ₃ -CoFe ₂ O ₄ self-assembled nanocomposites. 2015 , 7, 2263-8	69
1100	Structural evolution and enhanced magnetization of Bi _{1-x} Pr _x FeO ₃ . 2015 , 382, 1-6	15
1099	Identification and mechanical control of ferroelastic domain structure in rhombohedral CaMn ₇ O ₁₂ . 2015 , 91,	6
1098	Enhanced optical properties and the origin of carrier transport in BiFeO ₃ /TiO ₂ heterostructures with 109° domain walls. 2015 , 628, 311-316	11
1097	Magnetic glass/ceramics containing multiferroic BiFeO ₃ crystals. 2015 , 40, 31-35	6

1096	Coupling between an incommensurate antiferromagnetic structure and a soft ferromagnet in the archetype multiferroic BiFeO ₃ /cobalt system. 2015 , 91,	7
1095	Magnetic control of transverse electric polarization in BiFeO ₃ 2015 , 6, 5878	79
1094	Composition-driven structural phase transitions in rare-earth-doped BiFeO ₃ ceramics: a review. 2015 , 62, 62-82	118
1093	Effect of temperature on structural expansion for Bi _{0.8} Pr _x Ba _{0.2} FeO ₃ (x = 0.1) ceramics. 2015 , 602, 74-77	2
1092	Effect of Mn doping on structural, dielectric and magnetic properties of BiFeO ₃ thin films. 2015 , 74, 329-339	28
1091	Effects of Bismuth Oxide Buffer Layer on BiFeO ₃ Thin Film. 2015 , 98, 724-731	18
1090	Dielectric investigations of polycrystalline samarium bismuth ferrite ceramic. 2015 , 106, 012906	22
1089	Intrinsic interfacial phenomena in manganite heterostructures. 2015 , 27, 123001	22
1088	Optical properties of epitaxial BiFeO ₃ thin films grown on LaAlO ₃ . 2015 , 106, 012908	44
1087	Strain effects on multiferroic BiFeO ₃ films. 2015 , 16, 193-203	33
1086	Enhanced ferroelectric and ferromagnetic properties in lead-free multilayer composite films based on ferroelectric (Bi _{0.5} Na _{0.5}) _{0.945} Ba _{0.055} TiO ₃ and multiferroic BiFeO ₃ . 2015 , 117, 064105	3
1085	Hetero-epitaxial BiFeO ₃ /SrTiO ₃ nanolaminates with higher piezoresponse performance over stoichiometric BiFeO ₃ films. 2015 , 106, 022905	11
1084	Mesoporous bismuth ferrite with amplified magnetoelectric coupling and electric field-induced ferrimagnetism. 2015 , 6, 6562	51
1083	Vogel-Bulcher analysis of relaxor dielectrics with the tetragonal tungsten bronze structure: Ba ₆ MNb ₉ O ₃₀ (M = Ga, Sc, In). 2015 , 120, 1249-1259	22
1082	Effect of rhombohedral to orthorhombic transition on magnetic and dielectric properties of La and Ti co-substituted BiFeO ₃ . 2015 , 24, 045028	44
1081	Templated assembly of BiFeO ₃ nanocrystals into 3D mesoporous networks for catalytic applications. 2015 , 7, 5737-43	34
1080	Electrical, magnetic and magnetoelectric properties of 0.6BaTiO ₃ -0.4BiFeO ₃ /CoFe ₂ O ₄ particulate composites. 2015 , 26, 3370-3374	4
1079	Bismuth-based perovskites as multiferroics. 2015 , 16, 182-192	18

1078	Irreversible electrical manipulation of magnetization on BiFeO ₃ -based heterostructures. 2015 , 117, 17D707	3
1077	High-pressure synthesis, crystal structure and magnetic properties of TlCrO ₃ perovskite. 2015 , 44, 10785-94	13
1076	Effect of cobalt substitution on the optical properties of bismuth ferrite thin films. 2015 , 34, 109-113	16
1075	Piezoelectric ceramic materials for power ultrasonic transducers. 2015 , 101-125	4
1074	Synthesis of Pt/BiFeO ₃ heterostructured photocatalysts for highly efficient visible-light photocatalytic performances. 2015 , 143, 386-396	98
1073	Two-Dimensional Superlattices of Bi Nanoclusters Formed on a Au(111) Surface Using Porous Supramolecular Templates. 2015 , 9, 8547-53	23
1072	Effect of Ho substitution on structure and magnetic property of BiFeO ₃ prepared by sol-gel method. 2015 , 40, 787-795	16
1071	Enhanced multiferroic properties of Nd and Co co-doped BiFeO ₃ ceramics. 2015 , 26, 6907-6912	6
1070	Properties of Bi _{0.8} Ln _{0.2} FeO ₃ (Ln=La, Gd, Ho) multiferroic ceramics. 2015 , 41, 14718-14726	18
1069	Multiferroic properties of (Bi, Ca)FeO ₃ films on glass substrates. 2015 , 355, 121-126	5
1068	Functional properties of Sm ₂ NiMnO ₆ multiferroic ceramics prepared by spark plasma sintering. 2015 , 649, 151-158	17
1067	Photothermal Electrical Resonance Spectroscopy of Physisorbed Molecules on a Nanowire Resonator. 2015 , 15, 5658-63	14
1066	Magnetoelectric coupling of LaFeO ₃ /BiFeO ₃ heterostructures. 2015 , 41, 13126-13134	12
1065	Structural, magnetic and photocatalytic properties of La and alkaline co-doped BiFeO ₃ nanoparticles. 2015 , 40, 796-802	31
1064	Ti doping-driven magnetic and morphological changes in multiferroic ceramics of Bi _{0.9} La _{0.1} FeO ₃ . 2015 , 48, 345001	11
1063	Magnetic Augment in the Nitrogen Substituted Bismuth Ferrite. 2015 , 51, 1-3	5
1062	Dissipationless multiferroic magnonics. 2015 , 114, 157203	34
1061	Ab Initio Study of BiFeO ₃ : Thermodynamic Stability Conditions. 2015 , 6, 2847-51	38

1060	Ferroelectric control of magnetism in P(VDF-TrFE)/Co heterostructure. 2015 , 26, 7502-7506	9
1059	Synthesis of nano-structured Bi _{1-x} BaxFeO ₃ ceramics with enhanced magnetic and electrical properties. 2015 , 162, 106-112	21
1058	Structural and magnetic studies of the nickel doped CoFe ₂ O ₄ ferrite nanoparticles synthesized by the chemical co-precipitation method. 2015 , 394, 379-384	67
1057	Destructive Interactions between Pore Forming Agents and Matrix Phase during the Fabrication Process of Porous BiFeO ₃ Ceramics. 2015 , 31, 798-805	13
1056	Ultrafast microwave hydrothermal synthesis and characterization of Bi _{1-x} LaxFeO ₃ micronized particles. 2015 , 162, 69-75	15
1055	Effect of metamagnetism on multiferroic property in double perovskite Sm ₂ CoMnO ₆ . 2015 , 117, 17D914	16
1054	Structural evolution and physical properties of multiferroic Bi _{0.9-x} La _{0.1} PbxFeO _{3-x/2} ceramics. 2015 , 48, 305004	5
1053	Electronic Structure of BiFeO ₃ in Different Crystal Phases. 2015 , 127, 266-268	6
1052	First-principles study of structural, electronic, and ferroelectric properties of rare-earth-doped BiFeO ₃ . 2015 , 50, 6227-6235	26
1051	Structural, Electrical, and Magnetic Properties of Mechanosynthesized (1-x)BiFeO ₃ -xBaMnO ₃ (0 ≤ x ≤ 1.5) Multiferroic System. 2015 , 44, 3811-3818	4
1050	Enhanced magnetic response in single-phase Bi _{0.80} La _{0.15} A _{0.05} FeO ₃ (A=Ca, Sr, Ba) ceramics. 2015 , 220, 6-11	9
1049	Utilizing the anti-ferromagnetic functionality of a multiferroic shell to study exchange bias in hybrid core-shell nanostructures. 2015 , 7, 13398-403	15
1048	Structural modification and enhanced magnetic properties with two phonon modes in Ca _{1-x} Co _x BiFeO ₃ nanoparticles. 2015 , 41, 14306-14314	9
1047	Studying the Polarization Switching in Polycrystalline BiFeO ₃ Films by 2D Piezoresponse Force Microscopy. 2015 , 5, 12237	26
1046	Conduction mechanisms and enhanced multiferroic properties of Sr doped Bi _{0.85-x} Pr _{0.15} SrxFe _{0.97} Mn _{0.03} O ₃ thin films. 2015 , 26, 7407-7414	3
1045	Enhanced multiferroic properties in epitaxial Yb-doped BiFeO ₃ thin films. 2015 , 11, 609-613	9
1044	X-Ray Diffraction, Mössbauer Spectroscopy, and Magnetoelectric Effect Studies of Multiferroic Bi ₅ Ti ₃ FeO ₁₅ Ceramics. 2015 , 127, 296-299	16
1043	Nanoscale study of perovskite BiFeO ₃ /spinel (Fe,Zn) ₃ O ₄ co-deposited thin film by electrical scanning probe methods. 2015 , 351, 531-536	7

1042	Dielectric and piezoelectric properties of BiFeO ₃ from molecular dynamics simulations. 2015 , 218, 10-13	18
1041	Tuning Magnetic Properties of BiFeO ₃ Thin Films by Controlling Rare-Earth Doping: Experimental and First-Principles Studies. 2015 , 150616125012002	28
1040	Structural, magnetic and ferroelectric properties of Pr doped multiferroics bismuth ferrites. 2015 , 394, 385-390	43
1039	Epitaxial multiferroic heterostructures. 2015 , 87-101	
1038	Effect of sintering temperature on structure and multiferroic properties of Bi _{0.825} Sm _{0.175} FeO ₃ ceramics. 2015 , 162, 469-476	19
1037	Investigation of electrical properties in La-doped BiFeO ₃ /PbTiO ₃ thin films prepared by sol-gel method. 2015 , 76, 220-226	4
1036	Structure, piezoelectric and multiferroic properties of Bi(Ni _{0.5} Mn _{0.5})O ₃ -modified BiFeO ₃ /BaTiO ₃ ceramics. 2015 , 26, 9451-9462	6
1035	Strain-based scanning probe microscopies for functional materials, biological structures, and electrochemical systems. 2015 , 1, 3-21	87
1034	Magnetic properties of solid solutions between BiCrO and BiGaO with perovskite structures. 2015 , 16, 026003	10
1033	Thickness-dependent phase boundary in Sm-doped BiFeO ₃ piezoelectric thin films on Pt/Ti/SiO ₂ /Si substrates. 2015 , 17, 19759-65	15
1032	Oxygen octahedra distortion induced structural and magnetic phase transitions in Bi _{1-x} CaxFe _{1-x} MnxO ₃ ceramics. 2015 , 117, 194103	86
1031	Enhancement in magnetic properties of magnesium substituted bismuth ferrite nanoparticles. 2015 , 117, 224101	11
1030	Enhanced ferromagnetism in N-doped BiFeO ₃ : A first-principles prediction. 2015 , 644, 30-39	10
1029	Current rectifying and resistive switching in high density BiFeO ₃ nanocapacitor arrays on Nb-SrTiO ₃ substrates. 2015 , 5, 9680	59
1028	Structural, dielectric, vibrational and magnetic properties of Sm doped BiFeO ₃ multiferroic ceramics prepared by a rapid liquid phase sintering method. 2015 , 41, 9285-9295	76
1027	Mechanical Switching of Nanoscale Multiferroic Phase Boundaries. 2015 , 25, 3405-3413	33
1026	Gas-sensing and electrical properties of perovskite structure p-type barium-substituted bismuth ferrite. 2015 , 5, 29618-29623	78
1025	Phase transition and enhanced electrical properties in 0.725BiFeO ₃ -0.275Ba _{0.85} Ca _{0.15} Ti _{0.9} Zr _{0.1} SnxO ₃ multiferroic ceramics. 2015 , 637, 137-142	6

1024	Structural, vibrational, electrical and magnetic properties of $\text{Bi}_{1-x}\text{Pr}_x\text{FeO}_3$. 2015 , 41, 8511-8519	21
1023	Structural, electrical and multiferroic properties of La-doped mullite $\text{Bi}_2\text{Fe}_4\text{O}_9$ thin films. 2015 , 70, 279-283	18
1022	Enhanced switching characteristics and piezoelectric response in epitaxial $\text{BiFeO}_3/\text{PbMnO}_3$ thin films. 2015 , 466-467, 11-15	4
1021	First-principles study on ferromagnetism in Mn-doped tetragonal BiFeO_3 . 2015 , 105, 1-5	16
1020	Structural, electrical and magnetic properties of rare-earth and transition element co-doped bismuth ferrites. 2015 , 641, 205-209	35
1019	Mechanism of ferroelectric resistive switching in $\text{Bi}_{0.9}\text{La}_{0.1}\text{FeO}_3$ thin films. 2015 , 583, 13-18	6
1018	The multiferroic properties of $\text{BiFe}_{0.5}\text{Mn}_{0.5}\text{O}_3$ and $\text{BiFeO}_3/\text{BiMnO}_3$ superlattice films. 2015 , 117, 17D911	6
1017	Investigation of phase coexistence and correlation in $\text{La}_{1-x}\text{Bi}_x\text{MnO}_3$ ($x = 0.4$ and 0.6). 2015 , 2, 046105	6
1016	Room temperature polarization in the ferrimagnetic $\text{Ga}_{2-x}\text{Fe}_x\text{O}_3$ ceramics. 2015 , 35, 2277-2281	11
1015	Effect of local structural distortion on magnetic and dielectric properties in BiFeO_3 with Ba, Ti co-doping. 2015 , 468-469, 81-84	12
1014	First principles prediction of interfacial magnetoelectric coupling in tetragonal $\text{La}_{2/3}\text{Sr}_{1/3}\text{MnO}_3/\text{BiFeO}_3$ multiferroic superlattices. 2015 , 17, 13647-53	5
1013	Domains and domain walls in multiferroics. 2015 , 16, 227-240	16
1012	Enhanced magnetization with unusual low temperature magnetic ordering behaviour and spin reorientation in holmium-modified multiferroic BiFeO_3 perovskite ceramics. 2015 , 48, 205001	15
1011	Residual tensile stress in robust insulating rhombohedral $\text{Bi}_{1-x}\text{La}_x\text{Fe}_{1-x}\text{Ti}_x\text{O}_3$ multiferroic ceramics and its ability to pin ferroelectric polarization switching. 2015 , 106, 112907	20
1010	Enhancement of ferromagnetic and ferroelectric properties in calcium doped BiFeO_3 by chemical synthesis. 2015 , 41, 9265-9275	13
1009	BiFeO_3 thin films via aqueous solution deposition: a study of phase formation and stabilization. 2015 , 50, 4463-4476	8
1008	Preparation and magnetic properties of $\text{La}_{0.1}\text{Bi}_{0.9}\text{FeO}_3/\text{NiFe}_2\text{O}_4$ composite powders. 2015 , 26, 2688-2692	
1007	Sol-gel synthesis, characterization and dielectric properties of $\text{Bi}_{1-x}\text{La}_x\text{FeO}_3$. 2015 , 75, 134-140	5

1006	Effect of Rare Earth Doping on Impedance, Modulus and Conductivity Properties of Multiferroic Composites: 0.5(BiLa x Fe)0.5(O3)0.5(PbTiO3). 2015 , 28, 847-857	18
1005	Interfacial Charge Induced Magnetoelectric Coupling at BiFeO3/BaTiO3 Bilayer Interface. 2015 , 7, 8472-9	50
1004	Intriguing photo-control of exchange bias in BiFeO3/La2/3Sr1/3MnO3 thin films on SrTiO3 substrates. 2015 , 10, 125	7
1003	Effects of Zn2+ and Mn4+ co-doping in BiFeO3 thin films. 2015 , 66, 1093-1096	
1002	Enhanced photovoltaic effect in K substituted BiFeO3 films. 2015 , 644, 602-606	13
1001	Influence of Mn dopants on the structure and multiferroic properties of a Bi0.90Ho0.10FeO3 thin film. 2015 , 5, 43594-43600	8
1000	Reactive sintering of (K0.5Bi0.5)TiO3-BiFeO3 lead-free piezoelectric ceramics. 2015 , 66, 1426-1438	4
999	Magnetoelectric effect in layered ferrite/PZT composites. Study of the demagnetizing effect on the magnetoelectric behavior. 2015 , 117, 184102	26
998	Ferroelectric properties and the origin of the magnetism in the Bi6Fe2Ti3O18 thin films. 2015 , 50, 5475-5481	10
997	Phonon thermal transport and phonon-magnon coupling in polycrystalline BiFeO3 systems. 2015 , 48, 115301	8
996	Structural, magnetic and dielectric properties of Sr and V doped BiFeO3 multiferroics. 2015 , 385, 175-181	37
995	Mechanosynthesis and multiferroic properties of the BiFeO3-BiMnO3-PbTiO3 ternary system along its morphotropic phase boundary. 2015 , 3, 2255-2265	26
994	Solution Processed Bismuth Ferrite Thin Films for All-Oxide Solar Photovoltaics. 2015 , 119, 5872-5877	61
993	Enhanced piezoelectric activity in high-temperature Bi1-xSmxLaFeO3 lead-free ceramics. 2015 , 3, 3684-3693	38
992	Effects of Ba and Ti Codoping on Stoichiometric and Nonstoichiometric BiFeO3 Multiferroic Ceramics. 2015 , 815, 154-158	2
991	Enhancement of Oxygen Vacancies Induced Photovoltaic Effects in Bi0.9La0.1FeO3 Thin Films. 2015 , 815, 176-182	2
990	Compliments of confinements: substitution and dimension induced magnetic origin and band-bending mediated photocatalytic enhancements in Bi(1-x)Dy(x)FeO3 particulate and fiber nanostructures. 2015 , 7, 10667-79	59
989	Structural, electrical and magnetic phase evolution of Cr substituted GdMn1-xCr x O3 (0 ≤ x ≤ 0.2) manganites. 2015 , 644, 575-581	28

988	Critical roles of Mn-ions in enhancing the insulation, piezoelectricity and multiferroicity of BiFeO ₃ -based lead-free high temperature ceramics. 2015 , 3, 5811-5824	105
987	Polarization switching at room temperature of undoped BiFeO ₃ thin films crystallized at temperatures between 400 T 500 °C. 2015 , 26, 9373-9386	2
986	Microstructures and electrical properties of a Li ₂ ZnO/BiFeO ₃ double-layered thin film fabricated by a chemical solution deposition method. 2015 , 41, S303-S307	2
985	High-quality single crystal growth and spin flop of multiferroic Co ₄ Nb ₂ O ₉ . 2015 , 420, 90-93	21
984	Possible misleading interpretations on magnetic and transport properties in BiFeO ₃ nanoparticles caused by impurity phase. 2015 , 379, 1549-1553	15
983	Measuring the magnetoelectric effect across scales. 2015 , 38, 25-74	22
982	Synthesis, microstructural characterization, and dielectric properties of BiFeO ₃ microcrystals derived from molten salt method. 2015 , 41, S19-S25	23
981	PZT-like structural phase transitions in the BiFeO ₃ -KNbO ₃ solid solution. 2015 , 44, 10608-13	8
980	Room temperature threshold switching behaviors of Bi _{0.9} Nd _{0.1} Fe _{1-x} CoxO ₃ nanoparticles. 2015 , 3, 4141-4147	9
979	Electrical conductivity and thermopower of (1 - x) BiFeO ₃ - xBi _{0.5} K _{0.5} TiO ₃ (x = 0.1, 0.2) ceramics near the ferroelectric to paraelectric phase transition. 2015 , 17, 9420-8	28
978	Effect of Fuel on Phase Formation of Nanocrystalline Bismuth Ferrite (BiFeO ₃). 2015 , 2, 1923-1926	3
977	Structural, Optical, and Electrical Characterization of Yttrium-Substituted BiFeO ₃ Ceramics Prepared by Mechanical Activation. 2015 , 54, 9876-84	17
976	Prediction of a metal-insulator transition and a two-dimensional electron gas in orthoferrite LaTiO ₃ /tetragonal BiFeO ₃ heterostructures. 2015 , 3, 11066-11075	12
975	SBR/BiFeO ₃ Elastomer Capacitor Films Prepared under Magnetic and Electric Fields Displaying Magnetoelectric Coupling. 2015 , 119, 23319-23328	11
974	Investigation of the properties of BiFeO ₃ /intermediate-layer structures fabricated by magnetron sputtering. 2015 , 57, 1764-1771	
973	Dielectric, impedance and transport characteristics of (Bi _{0.6} Pb _{0.4} Fe _{0.6} Ti _{0.4})O ₃ . 2015 , 26, 10012-10019	3
972	Structural, Dielectric, and Electrical Properties of Bi _{1-x} Pb _x Fe _{1-x} (Zr _{0.5} Ti _{0.5}) _x O ₃ . 2015 , 44, 4794-4803	
971	Annealing temperature effects on (111)-oriented BiFeO ₃ thin films deposited on Pt/Ti/SiO ₂ /Si by chemical solution deposition. 2015 , 3, 10742-10747	18

970	Pursuing the Crystallization of Mono- and Polymetallic Nanosized Crystalline Inorganic Compounds by Low-Temperature Wet-Chemistry and Colloidal Routes. 2015 , 115, 11449-502	46
969	Competing magnetic interactions and low temperature magnetic phase transitions in composite multiferroics. 2015 , 2, 086101	4
968	Effect of local strain fields on the structural, N _B L transition temperature and long range ferroelectric ordering in rare earth substituted Bi _{0.9} R _{0.1} FeO ₃ multiferroic ceramics (where, R = Gd ³⁺ , Tb ³⁺ , Dy ³⁺). 2015 , 26, 8676-8687	7
967	Competition between compressive strain and Mn doping on tuning the structure and magnetic behavior of BiFeO ₃ thin films. 2015 , 08, 1550066	3
966	Structural phase transition and enhanced ferroelectricity in Bi(Fe _{1-x} Mn _x)O ₃ thin films deposited by pulsed laser deposition. 2015 , 594, 80-87	7
965	Characterization of interface defects in BiFeO ₃ metal/oxide/semiconductor capacitors deposited by radio frequency magnetron sputtering. 2015 , 26, 5987-5993	14
964	Magnetic and transport properties assisted by local distortions in Bi ₂ Mn ₄ O ₁₀ and Bi ₂ Fe ₄ O ₉ multiferroic compounds. 2015 , 651, 405-413	8
963	Structure evolution and magnetic property of cobalt-modified Bi _{0.9} Gd _{0.1} FeO ₃ nanocrystal at morphotropic phase boundary. 2015 , 650, 489-493	2
962	Magnetic, magnetoelectric, magnetodielectric and magnetoresistance studies on CuO doped Sr ₂ Bi ₄ Ti ₅ O ₁₈ lead free ferroelectric ceramics. 2015 , 650, 758-767	5
961	Phase transition in orthorhombic perovskite Sm _{1-x} LuxMnO ₃ : Evidenced by the emergence of ferroelectric polarization. 2015 , 117, 17D913	
960	Grain size dependent phase stabilities and presence of a monoclinic (Pm) phase in the morphotropic phase boundary region of (1-x)Bi(Mg _{1/2} Ti _{1/2})O ₃ -xPbTiO ₃ piezoceramics. 2015 , 117, 144102	11
959	Effect of pressure on the magnetic properties of multiferroic BiFeO ₃ . 2015 , 41, 528-533	7
958	Insight on the ferroelectric properties in a (BiFeO ₃) ₂ (SrTiO ₃) ₄ superlattice from experiment and ab initio calculations. 2015 , 107, 042904	10
957	Dielectric and impedance spectroscopy of (Ba, Sm)(Ti, Fe)O ₃ system in the low-medium frequency range. 2015 , 26, 6572-6584	25
956	Effects of ZnO Content on Piezoelectric, Dielectric, and Magnetic Properties of Sr-Modified PZT/BMWBN/(Ni-Co-Cu) ME Composites. 2015 , 44, 3415-3421	1
955	Enhancement of visible-light photocatalytic activity in BiFeO ₃ @carbon-microspheres heterostructures and its mechanism implication. 2015 , 26, 7496-7501	4
954	Solution processed TiO ₂ /BiFeO ₃ /poly(3-hexylthiophene) solar cells. 2015 , 159, 305-308	11
953	Unusual Strong Incommensurate Modulation in a Tungsten-Bronze-Type Relaxor PbBiNb ₅ O ₁₅ . 2015 , 137, 13468-71	30

- 952 Nanostructured hexahedron of bismuth ferrite clusters: delicate synthesis processes and an efficient multiplex catalyst for organic pollutant degradation. **2015**, 5, 86891-86900 16
- 951 Direct observation of magnetodielectric effect in type-I multiferroic $\text{PbFe}_{0.5}\text{Ti}_{0.25}\text{W}_{0.25}\text{O}_3$. **2015**, 15, 1545-1548 2
- 950 Ferromagnetism and enhanced photocatalytic activity in Nd doped BiFeO_3 nanopowders. **2015**, 26, 9929-9940 29
- 949 Enhanced Electrical Properties of Quenched $(1-x)\text{BiFeO}_3-x\text{SmyFeO}_3$ Lead-Free Ceramics. **2015**, 119, 21105-21115 26
- 948 The phase diagram and magnetic properties of Co and Ti co-doped $(1-x)\text{BiFeO}_3-x\text{LaFeO}_3$ solid solutions. **2015**, 650, 878-883 6
- 947 Nanocrystalline Ferroelectric BiFeO_3 Thin Films by Low-Temperature Atomic Layer Deposition. **2015**, 27, 6322-6328 20
- 946 Quantitative phase separation in multiferroic $\text{Bi}_{0.88}\text{Sm}_{0.12}\text{FeO}_3$ ceramics via piezoresponse force microscopy. **2015**, 118, 072004 21
- 945 The effect of sintering temperature on the magneto-transport properties of $\text{Pr}_{0.67}\text{Sr}_{0.33-x}\text{Ag}_x\text{MnO}_3$ ($0 \leq x \leq 0.1$) manganites. **2015**, 26, 6444-6449 10
- 944 Piezoresponse and magnetic properties of multiferroic $(1-x)\text{Bi}_{0.9}\text{Dy}_{0.1}\text{FeO}_3-x\text{PbTiO}_3$ solid solution. **2015**, 118, 072005 8
- 943 Effect of thermal annealing on electric conduction in hydrothermally-grown BiFeO_3 thick films. **2015**, 66, 1627-1630
- 942 Specific features of the evolution of magnetic properties of bismuth ferrite modified with rare-earth element cations. **2015**, 57, 1787-1792 8
- 941 The origin of enhanced optical absorption of the $\text{BiFeO}_3/\text{ZnO}$ heterojunction in the visible and terahertz regions. **2015**, 17, 26930-6 13
- 940 Giant magnetoelectric coupling interaction in $\text{BaTiO}_3/\text{BiFeO}_3/\text{BaTiO}_3$ trilayer multiferroic heterostructures. **2015**, 107, 082908 35
- 939 Synthesis, thermal, structural, and magnetic properties of phase-pure nanocrystalline BiFeO_3 via wet chemical route. **2015**, 121, 681-688 13
- 938 Visible-light driven generation of reactive radicals over $\text{BiFeO}_3/\text{TiO}_2$ nanotube array: experimental evidence and energetic mechanism. **2015**, 17, 1 8
- 937 The magnetic augment in the nitrogen substituted bismuth ferrite. **2015**, 1 1
- 936 High-efficiency and dynamic stable electromagnetic wave attenuation for La doped bismuth ferrite at elevated temperature and gigahertz frequency. **2015**, 5, 77184-77191 56
- 935 Multiferroic heterostructures and tunneling junctions. **2015**, 1, 263-284 26

934	Exchange coupling of a BiFeO ₃ multiferroic nanolayer with a Co _{0.9} Fe _{0.1} ferromagnetic nanolayer. 2015 , 57, 1781-1786	4
933	Integration of BiFeO ₃ thick films onto ceramic and metal substrates by screen printing. 2015 , 35, 4163-4171	13
932	Influence of substrate and Ca substitution on multiferroic BiMnO ₃ thin films. 2015 , 38, 1099-1104	2
931	Nd doping of bismuth ferrite to tune electromagnetic properties and increase microwave absorption by magnetic dielectric synergy. 2015 , 3, 9276-9282	107
930	Heat capacity of nanocrystalline bismuth ferrite. 2015 , 53, 601-604	1
929	Structural Transition and Enhanced Ferromagnetic Properties of La, Nd, Gd, and Dy-Doped BiFeO ₃ Ceramics. 2015 , 44, 4354-4366	8
928	Enhancement of piezoelectric response in Ga doped BiFeO ₃ epitaxial thin films. 2015 , 117, 244107	9
927	Visible-light driven water splitting over BiFeO ₃ photoanodes grown via the LPCVD reaction of [Bi(OtBu)] ₃ and [Fe(OtBu)] ₃ and enhanced with a surface nickel oxygen evolution catalyst. 2015 , 7, 16343-53	47
926	Bismuth Self-Limiting Growth of Ultrathin BiFeO ₃ Films. 2015 , 27, 6508-6515	23
925	The effect of Fe-O-Fe bond angle on modulating multiferroic properties of Ba ²⁺ -codoped BiFeO ₃ nanoparticles. 2015 , 17, 1	13
924	Piezoelectric materials for high temperature transducers and actuators. 2015 , 26, 9256-9267	68
923	Influence of space charge on domain patterns and susceptibility in a rhombohedral ferroelectric film. 2015 , 100, 323-332	2
922	Giant elastic tunability in strained BiFeO ₃ near an electrically induced phase transition. 2015 , 6, 8985	35
921	Influence of Uniaxial Pressure on Dielectric Properties and Aging Effect of BiFeO ₃ Ceramic. 2015 , 485, 116-123	4
920	Antisymmetric exchange in La-substituted BiFe _{0.5} Sc _{0.5} O ₃ system: symmetry adapted distortion modes approach. 2015 , 230, 767-774	15
919	Preparation and characterization of La _{0.1} Bi _{0.9} FeO ₃ /CoFe ₂ O ₄ nanocomposite powders. 2015 , 41, 6079-6083	9
918	Magnetocapacitance and structure properties of Bi _{0.85} La _{0.15} PbxFeO ₃ ceramics. 2015 , 41, 4050-4055	6
917	Thickness dependent magnetic and ferroelectric properties of LaNiO ₃ buffered BiFeO ₃ thin films. 2015 , 15, 194-200	29

916	Effects of nano-sized BiFeO ₃ addition on the properties of high piezoelectric response (1-x)Bi _{0.5} Na _{0.5} TiO ₃ /Bi _{0.5} K _{0.5} TiO ₃ ceramics. 2015 , 50, 2093-2102	3
915	First-principles studies of multiferroic and magnetoelectric materials. 2015 , 60, 156-181	40
914	Investigation of multiferroic properties of doped BiFeO ₃ /BaTiO ₃ composite ceramics. 2015 , 142, 42-44	35
913	Influence of multi-ion co-doping and NiFe ₂ O ₄ layer on the properties of BiFeO ₃ /NiFe ₂ O ₄ composite films by sol-gel. 2015 , 142, 27-29	5
912	Synthesis, structural and spectroscopic properties of acentric triple molybdate Cs ₂ NaBi(MoO ₄) ₃ . 2015 , 225, 53-58	44
911	A high surface area ordered mesoporous BiFeO ₃ semiconductor with efficient water oxidation activity. 2015 , 3, 1587-1593	73
910	Low temperature ferromagnetic ordering and dielectric properties of Bi _{1-x} Dy _x FeO ₃ ceramics. 2015 , 41, 3227-3236	30
909	Covering vertically aligned carbon nanotubes with a multiferroic compound. 2015 , 82, 408-416	
908	Finite-Temperature Properties of Rare-Earth-Substituted BiFeO ₃ Multiferroic Solid Solutions. 2015 , 25, 552-558	55
907	Magnetic hysteresis of cerium doped bismuth ferrite thin films. 2015 , 378, 333-339	12
906	Effect of Ho and Mn co-doping on structural, ferroelectric and ferromagnetic properties of BiFeO ₃ thin films. 2015 , 584, 103-107	23
905	Synthesis and Thermal, Structural, Dielectric, Magnetic and Magnetoelectric Studies of BiFeO ₃ -MgFe ₂ O ₄ Nanocomposites. 2015 , 98, 574-579	15
904	Large magnetoelectric coupling in magnetically short-range ordered Bi _{1-x} Fe _x O ₃ film. 2014 , 4, 5255	120
903	Enhanced ferromagnetic properties and high temperature dielectric anomalies in Bi _{0.9} Ca _{0.05} Sm _{0.05} FeO ₃ prepared by hydrothermal method. 2015 , 62, 5-10	11
902	Enhanced electrical insulation and ferroelectricity in La and Ni co-doped BiFeO ₃ thin films. 2015 , 621, 339-344	38
901	Low magnetic field response single-phase multiferroics under high temperature. 2015 , 2, 232-236	72
900	Investigation of structural and magnetic properties of doped BaFeO ₃ /BaTiO ₃ multiferroic composites. 2015 , 26, 98-102	7
899	Photovoltaic properties of ferroelectric solar cells based on polycrystalline BiFeO ₃ films sputtered on indium tin oxide substrates. 2015 , 58, 1-6	10

898	Effect of samarium doping on the structural, optical and magnetic properties of sol-gel processed BiFeO ₃ thin films. 2015 , 26, 49-58	28
897	A comparative study on the magnetic and electrical properties of Bi _{0.89} Tb _{0.11} FeO ₃ and Bi _{0.89} Tb _{0.11} FeO ₃ /CoFe ₂ O ₄ multiferroic thin films. 2015 , 623, 243-247	6
896	Epitaxial (001) BiFeO ₃ thin-films with excellent ferroelectric properties by chemical solution deposition-the role of gelation. 2015 , 3, 582-595	39
895	First principles study of structural, electronic and magnetic properties of ferromagnetic Bi ₂ Fe ₄ O ₉ . 2015 , 624, 131-136	25
894	Hollandites as a new class of multiferroics. 2014 , 4, 6203	26
893	Nanodomains and nanometer-scale disorder in multiferroic bismuth ferrite single crystals. 2015 , 82, 356-368	21
892	Microstructural evolution of charged defects in the fatigue process of polycrystalline BiFeO ₃ thin films. 2015 , 82, 190-197	15
891	A comparative study of dielectric, ferroelectric and magnetic properties of BiFeO ₃ multiferroic ceramics synthesized by conventional and spark plasma sintering techniques. 2015 , 35, 131-138	53
890	Preparation and microwave absorption properties of Ni _{0.5} Co nanoferrites. 2015 , 618, 222-226	70
889	Barrier enhancement behavior in an Au/BiFeO ₃ /YBa ₂ Cu ₃ O _{7-δ} /SrTiO ₃ heterostructure with the magnetic field effect. 2015 , 619, 505-508	10
888	Structure and properties of chemically synthesized BiFeO ₃ . Influence of fuel and complexing agent. 2015 , 41, 69-77	19
887	Effects of Gd on the magnetic, electric and structural properties of BiFeO ₃ nanstructures synthesized by co-precipitation followed by microwave sintering. 2015 , 375, 38-42	21
886	Structure-Dependent Mechanical Properties of ALD-Grown Nanocrystalline BiFeO ₃ Multiferroics. 2016 , 2016, 1-7	5
885	Structural and Magnetic Properties of Mn Doped BiFeO ₃ Nanomaterials. 2016 , 2016, 1-5	17
884	Multiferroic Materials: Physics and Properties. 2016 ,	8
883	Structural, Magnetic and Optical Properties of BiFe _{1-x} NbxO ₃ . 2016 , 29, 578-584	7
882	Substitution driven structural and magnetic properties and evidence of spin phonon coupling in Sr-doped BiFeO ₃ nanoparticles. 2016 , 6, 68028-68040	21
881	Mullite-hexagonal di-phase multiferroic behavior with enhanced ferromagnetism of (1-x)Bi ₂ Fe ₄ O ₉ -xBaFe ₁₂ O ₁₉ composites. 2016 , 213, 2741-2750	2

880	Optical nonlinearity in multiferroic bismuth ferrite. 2016 , 688, 796-802		4
879	First principles investigation of electronic and magnetic structures of centrosymmetric BiMnO ₃ using an improved approach. 2016 , 243, 65-70		2
878	Self-Poling of BiFeO ₃ Thick Films. 2016 , 8, 19626-34		10
877	Perovskite solid solutions with multiferroic morphotropic phase boundaries and property enhancement. 2016 , 06, 1630004		1
876	Piezopotential-Induced Schottky Behavior of Zn _{1-x} SnO ₃ Nanowire Arrays and Piezophotocatalytic Applications. 2016 , 99, 2593-2600		42
875	Optically modulated resistive switching in BiFeO ₃ thin film. 2016 , 213, 2183-2188		16
874	Interplay between elasticity, ferroelectricity and magnetism at the domain walls of bismuth ferrite. 2016 , 10, 209-217		13
873	Crystallization Behavior and Multiferroic Properties of Bi _{3.15} Nd _{0.85} Ti ₃ O ₁₂ /CoFe ₂ O ₄ Powders Synthesized by Sol-Gel Method. 2016 , 99, 2334-2340		11
872	Multiferroic Heterostructures Integrating Ferroelectric and Magnetic Materials. <i>Advanced Materials</i> , 2016 , 28, 15-39	24	284
871	Spin Structure Change in Co-Substituted BiFeO ₃ . 2016 , 85, 064704		18
870	Molecular Design for Tailoring a Single-Source Precursor for Bismuth Ferrite. 2016 , 55, 7542-9		6
869	Implementing Room-Temperature Multiferroism by Exploiting Hexagonal-Orthorhombic Morphotropic Phase Coexistence in LuFeO ₃ Thin Films. <i>Advanced Materials</i> , 2016 , 28, 7430-5	24	27
868	Structure and multiferroic properties of multi-doped Bi _{1-x} Er _x Fe _{0.96} Mn _{0.02} Co _{0.02} O ₃ thin films. 2016 , 684, 438-444		16
867	Fabrication of high-density BiFeO nanodot and anti-nanodot arrays by anodic alumina template-assisted ion beam etching. 2016 , 27, 485302		14
866	Shift current bulk photovoltaic effect in polar materialsHybrid and oxide perovskites and beyond. 2016 , 2,		142
865	Strain phase separation: Formation of ferroelastic domain structures. 2016 , 94,		23
864	Structure evolution and piezoelectric properties across the morphotropic phase boundary of Sm-substituted BiFeO ₃ ceramics. 2016 , 119, 064104		35
863	Sintering time effect on crystal structure and magnetic properties of Bi _{0.8} La _{0.2} FeO ₃ multiferroics. 2016 ,		0

862	Landau-Ginzburg description of anomalous properties of novel room temperature multiferroics $\text{Pb}(\text{Fe}_{1/2}\text{Ta}_{1/2})_x(\text{Zr}_{0.53}\text{Ti}_{0.47})_{1-x}\text{O}_3$ and $\text{Pb}(\text{Fe}_{1/2}\text{Nb}_{1/2})_x(\text{Zr}_{0.53}\text{Ti}_{0.47})_{1-x}\text{O}_3$. 2016 , 119, 024102	9
861	The appearance of weak ferromagnetism of hexagonal stabilized ErFeO_3 thin film. 2016 ,	1
860	Magnetization switching in the $\text{BiFe}_{0.9}\text{Mn}_{0.1}\text{O}_3$ thin films modulated by resistive switching process. 2016 , 109, 112903	15
859	Fabrication and characterization of nanostructured Ba-doped BiFeO_3 porous ceramics. 2016 , 34, 148-156	3
858	Strain-controlled interfacial magnetization and orbital splitting in $\text{La}_{2/3}\text{Sr}_{1/3}\text{MnO}_3$ /tetragonal BiFeO_3 heterostructures. 2016 , 120, 165303	11
857	Structural, dielectric and ferroelectric properties of La and Ni codoped BiFeO_3 . 2016 ,	2
856	Band-gap tuning and magnetic properties of heterovalent ions (Ba, Sr and Ca) substituted BiFeO_3 nanoparticles. 2016 ,	3
855	Resistive memory effects in BiFeO_3 single crystals controlled by transverse electric fields. 2016 , 108, 162903	5
854	Role of $(\text{Bi}_{1/2}\text{K}_{1/2})\text{TiO}_3$ in the dielectric relaxations of BiFeO_3 - $(\text{Bi}_{1/2}\text{K}_{1/2})\text{TiO}_3$ ceramics. 2016 , 119, 154101	22
853	Flexo-chemo effect in nanoferroics as a source of critical size disappearance at size-induced phase transitions. 2016 , 119, 094109	21
852	Studies on structural, optical, magnetic, and resistive switching properties of doped $\text{BiFe}_{1-x}\text{Cr}_x\text{O}_3$ thin films. 2016 , 120, 194101	5
851	Visible Light Driven Photocatalytic Efficiency of rGO-Ag-BiFeO_3 Ternary Nanohybrids on the Decontamination of Dye-Polluted Water: An Amalgamation of 1D, 2D and 3D Systems. 2016 , 1, 6961-6971	5
850	Structural transition and its effect in La, Zr co-substituted mono-domain BiFeO_3 . 2016 , 120, 214106	15
849	Synthesis, structure and properties of nanostructured materials based on BiFeO_3 . 2016 ,	2
848	Perpendicular Magnetic Anisotropy and High Spin Polarization in Tetragonal $\text{Fe}_4\text{N/BiFeO}_3$ Heterostructures. 2016 , 6,	26
847	Preparation and enhanced ferromagnetic properties in Co doped BiFeO_3 nanoparticles prepared by sol-gel method. 2016 , 505, 123-129	5
846	Size dependent magnetic and electrical properties of Ba-doped nanocrystalline BiFeO_3 . 2016 , 6, 035314	34
845	Collapse and reappearance of magnetic orderings in spin frustrated TbMnO_3 induced by Fe substitution. 2016 , 109, 102401	3

844	Coherent x-ray diffraction imaging of photo-induced structural changes in BiFeO ₃ nanocrystals. 2016 , 18, 093003	9
843	Ultrafast acousto-optic mode conversion in optically birefringent ferroelectrics. 2016 , 7, 12345	32
842	A multiferroic on the brink: Uncovering the nuances of strain-induced transitions in BiFeO ₃ . 2016 , 3, 011106	80
841	Structural, magnetic and electrical properties of samarium substituted multiferroic bismuth ferrite. 2016 ,	
840	Optical spectroscopy study on the photo-response in multiferroic BiFeO ₃ . 2016 , 109, 182903	8
839	Ferroelectric BiFeO ₃ thin-film optical modulators. 2016 , 108, 233502	7
838	Magnetic fingerprint of interfacial coupling between CoFe and nanoscale ferroelectric domain walls. 2016 , 109, 082906	1
837	Dual strain mechanisms in a lead-free morphotropic phase boundary ferroelectric. 2016 , 6, 19630	49
836	Synthesis of BiFeO ₃ thin films on single-terminated Nb : SrTiO ₃ (111) substrates by intermittent microwave assisted hydrothermal method. 2016 , 6, 065117	5
835	Effect of sintering temperature on structural and dielectric properties of (Bi ₂ O ₃ Fe ₂ O ₃) _{0.4} (Nb ₂ O ₅ Nd ₂ O ₃) _{0.6} . 2016 ,	
834	Phase transitions, domain structure, and pseudosymmetry in La- and Ti-doped BiFeO ₃ . 2016 , 119, 054101	20
833	Photoconductivity of transparent perovskite semiconductor BaSnO ₃ and SrTiO ₃ epitaxial thin films. 2016 , 108, 092106	18
832	Effect of (Sr _{0.7} Ca _{0.3})TiO ₃ -substitution on structure, dielectric, ferroelectric, and magnetic properties of BiFeO ₃ ceramics. 2016 , 119, 204102	17
831	Magnetic properties of the multiferroics Bi _{1-x} CaxFe _{1-x} MnxO ₃ and Bi _{1-x} CaxFe _{1-x} TixO ₃ . 2016 , 42, 1122-1125	1
830	Bi deficiency-tuned functionality in multiferroic Bi _{1-x} Fe _{0.95} Mn _{0.05} O ₃ films. 2016 , 6, 19385	9
829	Controllable Synthesis of Bi ₂ Fe ₄ O ₉ Nanocrystal with High Active Facets and the Enhanced Visible Light Photoelectrochemical Property. 2016 , 67, 06045	1
828	Dielectric relaxation in magnetoelectric composite 0.85BiFeO ₃ -0.15MgFe ₂ O ₄ . 2016 , 80, 1092-1096	1
827	Effect of synthesis conditions on the photocatalytic property of multiferroic BiFeO ₃ towards the degradation of phenol red. 2016 ,	2

826	Grain size effect on electrical properties of Mn-modified $0.67\text{BiFeO}_3\text{0.33BaTiO}_3$ lead-free piezoelectric ceramics. 2016 , 42, 8206-8211	23
825	Chemical route derived bismuth ferrite thin films and nanomaterials. 2016 , 4, 4092-4124	99
824	Phase transition, dielectric relaxation and piezoelectric properties of bismuth doped $\text{La}_2\text{Ti}_2\text{O}_7$ ceramics. 2016 , 42, 11453-11458	12
823	A systematic study on multiferroics $\text{Bi}_{1-x}\text{CexFe}_1\text{MnyO}_3$: Structural, magnetic and electrical properties. 2016 , 42, 10373-10379	16
822	Domain switching contribution to the ferroelectric, fatigue and piezoelectric properties of lead-free $\text{Bi}_{0.5}(\text{Na}_{0.85}\text{K}_{0.15})_{0.5}\text{TiO}_3$ films. 2016 , 6, 33834-33842	24
821	Effect of Gd^{3+} co-substitution on structural, magnetic and electrical properties of multiferroic BiFeO_3 . 2016 , 418, 54-61	25
820	Pd cocatalyst on Sm-doped BiFeO_3 nanoparticles: synergetic effect of a Pd cocatalyst and samarium doping on photocatalysis. 2016 , 6, 34574-34587	30
819	Defect dipole-induced poling characteristics and ferroelectricity of quenched bismuth ferrite-based ceramics. 2016 , 4, 6140-6151	55
818	Robust insulating La and Ti co-doped BiFeO_3 multiferroic ceramics. 2016 , 27, 8725-8733	9
817	Multiferroic properties of $\text{Bi}_{1-x}\text{AxFeO}_3$ polycrystalline films on glass substrates (A = Ca, Sr, Ba and $x=0.05\text{0.15}$). 2016 , 683, 427-432	12
816	Tailoring the multiferroic behavior in BiFeO_3 nanostructures by Pb doping. 2016 , 6, 57727-57738	38
815	Bioinformatics Research and Applications. 2016 ,	1
814	Effect of Fe B substitution on phase transformation, optical, electrical and dielectrical properties of BaTiO_3 nanoceramics synthesized by sol-gel auto combustion method. 2016 , 37, 110-120	17
813	Tailoring the magnetic and optical characteristics of BiFeO_3 ceramics by doping with La and Co. 2016 , 179, 186-189	4
812	Magnetically recyclable Bi/Fe-based hierarchical nanostructures via self-assembly for environmental decontamination. 2016 , 8, 12736-46	19
811	One-dimensional BiFeO_3 nanotubes: Preparation, characterization, improved magnetic behaviors, and prospects. 2016 , 384, 368-375	19
810	New modalities of strain-control of ferroelectric thin films. 2016 , 28, 263001	61
809	Effect of heat treatment on the structure and properties of a BiFeO_3 nanopowder. 2016 , 58, 959-966	6

808	Influence of divalent Ni and trivalent Cr ions on the properties of ytterbium modified bismuth ferrite. 2016 , 684, 55-61	18
807	Crystal structure, leakage conduction mechanism evolution and enhanced multiferroic properties in Y-doped BiFeO ₃ ceramics. 2016 , 42, 13395-13403	36
806	Phase transition, leakage conduction mechanism evolution and enhanced ferroelectric properties in multiferroic Mn-doped BiFeO ₃ thin films. 2016 , 27, 3095-3102	19
805	The Multiferroic Properties of Bi _x FeO ₃ and Bi _{1-x} Li _y FeO ₃ . 2016 , 29, 1821-1825	1
804	Synthesis of Dense Fine-Grained Ceramics by Sol-Gel Technique of RE-substituted Bi _{1-x} A _x FeO ₃ Nanopowders (A = La ³⁺ , Y ³⁺ , Dy ³⁺ , Ce ³⁺): Structural, Electrical, and Magnetic Characterization. 2016 , 47, 1720-1728	2
803	Influence of isovalent and heterovalent substitution for Bi ³⁺ and Fe ³⁺ on the properties of Bi ₂ Fe ₄ O ₉ -based solid solutions. 2016 , 52, 361-366	
802	Photoinduced magnetoresistance and magnetic-field-modulated photoelectric response in BiFeO ₃ /Si heterojunctions. 2016 , 122, 1	1
801	Structural and electrical characteristics of (Co, Ti) modified BiFeO ₃ . 2016 , 27, 7115-7123	23
800	Screen-printed BiFeO ₃ thick films on noble metal foils. 2016 , 496, 196-203	1
799	Structural, optical and magnetic properties of multiferroic (1-x)BiFeO ₃ xPbTiO ₃ nanoparticles. 2016 , 683, 133-138	9
798	Current-voltage hysteresis of the composite MoS ₂ -MoO ₃ nanobelts for data storage. 2016 , 679, 47-53	17
797	Structural and electrical properties of multiferroic (1-x)BiFeO ₃ -xBi _{0.5} K _{0.5} TiO ₃ ceramics. 2016 , 678, 228-233	11
796	Improper Ferroelectric Contributions in the Double Perovskite Pb ₂ Mn _{0.6} Co _{0.4} WO ₆ System with a Collinear Magnetic Structure. 2016 , 55, 4381-90	5
795	Quenched bismuth ferrite-barium titanate lead-free piezoelectric ceramics. 2016 , 676, 505-512	38
794	Electronic structure and lattice dynamics of rhombohedral BiAlO ₃ from first-principles. 2016 , 177, 405-412	14
793	Dielectric properties of Bi-Fe _{1.6} Ga _{0.4} O ₃ oxide: A promising magneto-electric material. 2016 , 680, 31-42	23
792	Magnetic and ferroelectric characteristics of Gd ³⁺ and Ti ⁴⁺ co-doped BiFeO ₃ ceramics. 2016 , 39, 593-601	36
791	Refractive index dispersion of swift heavy ion irradiated BFO thin films using Surface Plasmon Resonance technique. 2016 , 379, 126-130	5

790	Influence of lightly Sm-substitution on crystal structure, magnetic and dielectric properties of BiFeO ₃ ceramics. 2016 , 682, 672-678	18
789	Air-stable and highly luminescent bismuth complex nanoparticles. 2016 , 4, 4899-4904	4
788	Fabrication and characterization of flexible films of poly(vinylidene fluoride)/Pb(Fe _{0.5} Ti _{0.5})O ₃ multi-ferroic nano-composite. 2016 , 6, 42892-42898	5
787	Substitution driven structural and magnetic transformation in Ca-doped BiFeO ₃ nanoparticles. 2016 , 6, 43080-43090	46
786	Investigation of dielectric and optical properties of structurally modified bismuth ferrite nanomaterials. 2016 , 42, 11447-11452	9
785	Microwave sintered Bi _{0.90} La _{0.10} Fe _{0.95} Mn _{0.05} O ₃ nanocrystalline ceramics: Impedance and modulus spectroscopy. 2016 , 42, 12914-12921	13
784	Multiferroic iron doped BaTiO ₃ nanoceramics synthesized by sol-gel auto combustion: Influence of iron on physical properties. 2016 , 42, 12441-12451	58
783	Nanocomposites of Bi ₅ FeTi ₃ O ₁₅ with MoS ₂ as novel Pt-free counter electrode in dye-sensitized solar cells. 2016 , 42, 12888-12893	26
782	Microstructural and electrical characteristics of epitaxial BiFeO ₃ thick films sputtered at different Ar/O ₂ flow ratios. 2016 , 18, 4604-4612	7
781	Optical Writing of Magnetic Properties by Remanent Photostriction. 2016 , 117, 107403	37
780	Enhancement in visible light photocatalytic activity of BiFeO ₃ photocatalysts by Pd cocatalyst. 2016 , 122, 1	9
779	Nanostructures and Thin Films Deposited with Sputtering. 2016 , 59-79	
778	Investigating the effect of Cd-Mn co-doped nano-sized BiFeO ₃ on its physical properties. 2016 , 6, 675-682	10
777	Investigation on the effect of Ti doping on dielectric, impedance and magnetic properties of Ba ²⁺ -substituted BiFeO ₃ ceramics. 2016 , 27, 12539-12549	2
776	YCrO ₃ /Al ₂ O ₃ Core-Shell Design: The Effect of the Nanometric Al ₂ O ₃ -Shell on Dielectric Properties. 2016 , 99, 3382-3388	2
775	Room temperature magnetoelectric multiferroic behavior of 50 mol% Fe substituted PbTiO ₃ (PbTi _{0.5} Fe _{0.5} O ₃) nanoparticles. 2016 , 6, 90132-90137	4
774	Well-saturated ferroelectric polarization in PbTiO ₃ /SmFeO ₃ thin films. 2016 , 3, 1473-1479	7
773	Phase transition, interband electronic transitions and enhanced ferroelectric properties in Mn and Sm co-doped bismuth ferrite films. 2016 , 6, 96563-96572	20

772	Multiferroic bismuth ferrite-based materials for multifunctional applications: Ceramic bulks, thin films and nanostructures. 2016 , 84, 335-402	348
771	Effects of high magnetic field annealing on microstructure and multiferroic properties of Bi _{1-x} LaxFeO ₃ ceramics. 2016 , 42, 18785-18790	1
770	Density relative change and interface zone mutual diffusion of BiFeO ₃ films prepared on Si (1 0 0), SiO ₂ and SiO ₂ /Si (1 0 0). 2016 , 384, 106-112	2
769	Special quasirandom structures for perovskite solid solutions. 2016 , 28, 475901	10
768	The effect of substrate clamping on the paraelectric to antiferroelectric phase transition in Nd-doped BiFeO ₃ thin films. 2016 , 616, 767-772	5
767	Effects of Eu and Ca Co-Substitution for the Improvement of Multiferroic Properties of BiFeO ₃ . 2016 , 697, 288-292	
766	Strain-induced electrostatic enhancements of BiFeO ₃ nanowire loops. 2016 , 18, 22772-7	6
765	Structural, transport and magnetic properties of (1-x) BiFeO ₃ -xCo _{0.7} Ni _{0.3} Fe ₂ O ₄ nanocomposite samples (x = 0.0, 0.2, 0.5, 0.8, 1.0). 2020 , 3, 609-620	6
764	Magnetic field effect on the dielectric properties of rare earth doped multiferroic BiFeO ₃ . 2020 , 513, 167101	2
763	Stable electric polarization switching accompanied by magnetization reversal in B-site-substituted multiferroic BiFe _{0.9} Co _{0.1} O ₃ thin films. 2020 , 13, 071001	1
762	Tuning the Structural and the Magnetic Properties of BiFeO ₃ Magnetic Nanoparticles. 2020 , 257, 2000005	1
761	Effect of particle size and morphology on the performance of BiFeO ₃ /PDMS piezoelectric generators. 2020 , 22, 2919-2925	4
760	Electrical Manipulation of Magnetic Anisotropy in a Fe ₈₁ Ga ₁₉ /Pb(Mg _{1/3} Nb _{2/3})O ₃ -Pb(ZrxTi _{1-x})O ₃ Magnetoelectric Multiferroic Composite. 2020 , 13,	8
759	Room temperature magnetoelectric coupling in Fe-doped sodium bismuth titanate ceramics. 2020 , 830, 154679	5
758	Effect of rare-earth Nd/Sm doping on the structural and multiferroic properties of BiFeO ₃ ceramics prepared by spark plasma sintering. 2020 , 46, 15228-15235	11
757	A Review of Thin-Film Magnetoelastic Materials for Magnetoelectric Applications. 2020 , 20,	35
756	Large energy storage density in BiFeO ₃ -BaTiO ₃ -AgNbO ₃ lead-free relaxor ceramics. 2020 , 40, 2929-2935	53
755	Phonon and magnetoelastic coupling in AlGaFeO: Raman, magnetization and neutron diffraction studies. 2020 , 22, 6906-6918	3

- 754 Two-dimensional ligand-functionalized plumbene: A promising candidate for ferroelectric and topological order with a large bulk band gap. **2020**, 120, 114095 4
- 753 Enhanced Electromechanical Properties of 0.65Bi1.05FeO3/0.35BaTiO3 Ceramics through Optimizing Sintering Conditions. **2020**, 217, 1900970 6
- 752 Interplay of negative electronic compressibility and capacitance enhancement in lightly-doped metal oxide BiLaFeO by quantum capacitance model. **2020**, 10, 5153 5
- 751 Tailoring the photovoltaic effect in (1 1 1) oriented BiFeO/LaFeO superlattices. **2020**, 32, 135301
- 750 Study of structural, optical and enhanced multiferroic properties of Ni doped BFO thin films synthesized by sol-gel method. **2020**, 831, 154857 16
- 749 Polyguanamine Derivative-Based Supramolecular Assemblies with Multiple Hydrogen Bonding and Their Metal-Scavenging Abilities. **2020**, 36, 3770-3781 3
- 748 1D metal-oxalates H2DABCO[M(C2O4)2]·nH2O (M(II): Co, Mg, Zn): phase transitions and magnetic, dielectric, and phonon properties. **2020**, 8, 6254-6263 4
- 747 Enhanced piezoelectric properties of (1-x)BiFe(ZnHf)O-xBaTiO ceramics near the morphotropic phase boundary. **2020**, 49, 5573-5580 4
- 746 Room temperature ferromagnetism driven by Ca-doped BiFeO3 multiferroic functional material. **2020**, 31, 5599-5607 1
- 745 A first-principles study on the magnetoelectric coupling induced by Fe in a two-dimensional BaTiO(001) ultrathin film. **2020**, 22, 18284-18293 2
- 744 Specific Heat and the Dielectric Properties of Bi0.8Ho0.2FeO3 Multiferroic. **2020**, 62, 1039-1042
- 743 Significantly suppressed leakage current and reduced band gap of BiFeO3 through BaZr Co-Substitution: Structural, optical, electrical and magnetic study. **2020**, 254, 123362 7
- 742 Integration-Friendly, Chemically Stoichiometric BiFeO Films with a Piezoelectric Performance Challenging that of PZT. **2020**, 12, 33899-33907 14
- 741 Effect of calcination temperature on magnetic, structural, thermal and optical properties of BFO-T nanoparticles. **2020**, 2, 1 1
- 740 Mild hydrothermal synthesis of BiFeO3 films on BiFeO3 seed-layer-coated indium tin oxide substrates and their piezo-related applications. **2020**, 31, 13376-13381
- 739 Photoferroelectric Thin Films for Flexible Systems by a Three-in-One Solution-Based Approach. **2020**, 30, 2001897 10
- 738 Hexagonal rare-earth manganites and ferrites: a review of improper ferroelectricity, magnetoelectric coupling, and unusual domain walls. **2020**, 22, 14415-14432 15
- 737 Enhanced dielectric and magnetic properties in Mn-doped bismuth ferrite multiferroic nanoceramics. **2020**, 126, 1 4

736	Development of BiFeO ₃ /MnFe ₂ O ₄ ferrite nanocomposites with enhanced magnetic and electrical properties. 2020 , 2, 2968-2976	8
735	Structural investigation of ferroelectric BiFeO ₃ BaTiO ₃ solid solutions near the rhombohedral-pseudocubic phase boundary. 2020 , 116, 252902	2
734	B-site-doped BiFeO ₃ -based piezoceramics with enhanced ferro/piezoelectric properties and good temperature stability. 2020 , 103, 6245-6254	14
733	Super-hydrophobic Fe ₃ O ₄ @SiO ₂ @MPS nanoparticles for oil remediation: The influence of pH and concentration on clustering phenomenon and oil sorption. 2020 , 315, 113709	5
732	Overview of Phase-Change Materials Based Photonic Devices. 2020 , 8, 121211-121245	12
731	Defect dynamics mediated unusual field-cycling behavior in bismuth ferrite-based ceramics. 2020 , 187, 418-423	6
730	Impact of texturing on the phase transitions in sol-gel-processed Bi(Sm)FeO ₃ thin films on LaNiO ₃ -buffered silicon. 2020 , 103, 6554-6564	3
729	Effect of Mn-doping on the low temperature magnetic phase transitions of BiFeO ₃ . 2020 , 825, 154148	6
728	Quenching Assisted Reverse Micellar Synthesis and Electrical Properties of High Surface Area BiFeO ₃ Nanoparticles. 2020 , 20, 3823-3831	6
727	Laser Fragmentation Synthesis of Colloidal Bismuth Ferrite Particles. 2020 , 10,	20
726	Effects of milling time on structural, electrical and ferroelectric features of mechanothermally synthesized multi-doped bismuth ferrite. 2020 , 126, 1	8
725	Effects of Bi ₂ O ₃ B ₂ O ₃ -ZnO glass additive on structure, ferroelectric and dielectric properties of BiFeO ₃ ceramics. 2020 , 555, 173-182	1
724	Study on Ca Segregation toward an Epitaxial Interface between Bismuth Ferrite and Strontium Titanate. 2020 , 12, 12264-12274	3
723	Field-induced magnetic incommensurability in multiferroic Ni ₃ TeO ₆ . 2020 , 101,	7
722	Probing charge carrier transport regimes in BiFeO ₃ nanoparticles by Raman spectroscopy. 2020 , 181, 6-9	2
721	Strengthened relaxor behavior in (1-x)Pb(Fe _{0.5} Nb _{0.5})O ₃ -BiFeO ₃ . 2020 , 8, 3452-3462	6
720	Effect of Mn substitution on the crystal and magnetic structure of Bi _{1-x} CaxFeO _{3-x/2} multiferroics. 2020 , 266, 127470	3
719	Phonon-induced near-field resonances in multiferroic BiFeO ₃ thin films at infrared and THz wavelengths. 2020 , 116, 071103	11

718	Band gap tuning and optical properties of BiFeO ₃ nanoparticles. 2020 , 28, 168-171	4
717	Lead palladium titanate: A room temperature nanoscale multiferroic thin film. 2020 , 10, 2991	8
716	Electrical and thermal properties of Pr _{0.6} Sr _{0.4} Ag _x MnO ₃ (x = 0.05 and 0.1) manganite. 2020 , 55, 6761-6770	5
715	Phase evolution, magnetic study and evidence of spin-two phonon coupling in Ca modified Bi _{0.80} La _{0.20} FeO ₃ ceramics. 2020 , 827, 154223	5
714	Enhanced multiferroicity in Mn- and Cu-modified 0.7BiFeO ₃ 0.3(Ba _{0.85} Ca _{0.15})TiO ₃ ceramics. 2020 , 127, 064102	
713	Improved ferroelectric response of pulsed laser deposited BiFeO ₃ -PbTiO ₃ thin films around morphotropic phase boundary with interfacial PbTiO ₃ buffer layer. 2020 , 127, 064101	8
712	Structural, Optical, and Multiferroic Properties of Yttrium (Y ³⁺)-Substituted BiFeO ₃ Nanostructures. 2020 , 33, 2017-2029	4
711	Bendable Bi(Fe _{0.95} Mn _{0.05})O ₃ ferroelectric film directly on aluminum substrate. 2020 , 827, 154381	2
710	Structural and multiferroic properties of BiFeO ₃ /MgLa _{0.025} Fe _{1.975} O ₄ nanocomposite synthesized by sol-gel auto combustion route. 2020 , 31, 2777-2788	4
709	Enhanced ferromagnetic and electric properties of multiferroic BiFeO ₃ by doping with Ca. 2020 , 824, 153944	18
708	Flexible lead-free BFO-based dielectric capacitor with large energy density, superior thermal stability, and reliable bending endurance. 2020 , 6, 200-208	22
707	Influence of isothermal structural transition on the magnetic properties of Cr doped Bi _{0.86} Nd _{0.14} FeO ₃ multiferroics. 2020 , 823, 153887	4
706	Influence of Ba and Mo co-doping on the structural, electrical, magnetic and optical properties of BiFeO ₃ ceramics. 2020 , 7, 016312	8
705	Dielectric and Frequency Dependent Transport Properties of Gadolinium Doped Bismuth Ferrite. 2020 , 21, 217-226	6
704	The versatile biomedical applications of bismuth-based nanoparticles and composites: therapeutic, diagnostic, biosensing, and regenerative properties. 2020 , 49, 1253-1321	133
703	Structure, ferroelectric and magnetic characteristics of SmFeO ₃ and BaTiO ₃ co-modified BiFeO ₃ ceramics. 2020 , 31, 3479-3491	4
702	Investigation of the Structural, Magnetic, Dielectric, and Optical Properties of Mn and Co-Doped BiFeO ₃ (Bi _{1-x} CoxFe _{0.8} Mn _{0.2} O ₃) Nanoparticles. 2020 , 56, 1-9	0
701	Universality and origin of ultrashort intrinsic negative dielectric permittivity. 2020 , 101,	3

700	Investigation of room temperature multiferroic properties in sol-gel derived gadolinium, cobalt doped BiFeO ₃ nanoceramics. 2020 , 127, 054101	7
699	Enhanced magnetoelectric coefficient and interfacial compatibility by constructing a three-phase CFO@BT@PDA/P(VDF-TrFE) core-shell nanocomposite. 2020 , 131, 105805	25
698	Structural, morphological, magnetic and spectral studies of Bi ³⁺ substituted YFeO ₃ Nano-powders: Obtained by sol-gel synthesis. 2020 , 44, 195-202	2
697	Observation of relaxor-ferroelectric behavior in gallium ferrite thin films. 2020 , 523, 146459	3
696	Applications of Phase Change Materials in Electrical Regime From Conventional Storage Memory to Novel Neuromorphic Computing. 2020 , 8, 76471-76499	5
695	Tailoring effect of large polaron hopping in the conduction mechanism of Ca-modified BaTiO ₃ system. 2020 , 31, 9212-9223	3
694	Interfacial Strain Gradients Control Nanoscale Domain Morphology in Epitaxial BiFeO ₃ Multiferroic Films. 2020 , 30, 2000343	11
693	Structure, Performance, and Application of BiFeO Nanomaterials. 2020 , 12, 81	41
692	Surface magnetic interactions between Bi _{0.85} La _{0.15} FeO ₃ and BaFe ₁₂ O ₁₉ nanomaterials in (1-x)Bi _{0.85} La _{0.15} FeO ₃ -(x)BaFe ₁₂ O ₁₉ nanocomposites. 2020 , 508, 166862	5
691	Tailoring the morphology and size of perovskite BiFeO ₃ nanostructures for enhanced magnetic and electrical properties. 2020 , 192, 108694	21
690	Study of the magnetic, electrical and magneto-dielectric properties and dielectric relaxation in 0.8BiFeO ₃ -0.2Ba _{0.75} Sr _{0.25} TiO ₃ solid solution. 2020 , 103, 106193	3
689	Observation of Stabilized Monoclinic Phase as a Bridge at the Morphotropic Phase Boundary between Tetragonal Perovskite PbVO ₃ and Rhombohedral BiFeO ₃ . 2020 , 32, 3615-3620	3
688	Antiferromagnetic textures in BiFeO controlled by strain and electric field. 2020 , 11, 1704	20
687	Impact of defects on the electrical properties of BiFeO ₃ thin films. 2020 , 556, 70-78	
686	Ultrafast light-driven simultaneous excitation of coherent terahertz magnons and phonons in multiferroic BiFeO ₃ . 2020 , 101,	3
685	Strong Magnetoelectric Effects of 2D Composites Made of AlN Films Grown by Plasma-Enhanced Atomic Layer Deposition on Magnetostrictive Foils for Energy Harvesting Applications. 2020 ,	1
684	Enhanced UV-Vis Photodegradation of Nanocomposite Reduced Graphene Oxide/Ferrite Nanofiber Films Prepared by Laser-Assisted Evaporation. 2020 , 10, 271	1
683	Piezoelectric BiFeO Thin Films: Optimization of MOCVD Process on Si. 2020 , 10,	2

682	Unraveling optimized parameters for phase pure rhombohedral perovskite bismuth ferrite without leaching. 2020 , 126, 1	4
681	Ferrites: emerging light absorbers for solar water splitting. 2020 , 8, 9447-9482	26
680	A structural phase boundary due to oxygen octahedral tilt-tilt transition in Bi _{0.5} Na _{0.5} TiO ₃ -based piezoelectric ceramics. 2020 , 127, 164101	3
679	Peculiarities of the Crystal Structure Evolution of BiFeO-BaTiO Ceramics across Structural Phase Transitions. 2020 , 10,	26
678	Structural modification and evaluation of dielectric and ferromagnetic properties of Ce-modified BiFeO ₃ BaTiO ₃ ceramics. 2020 , 46, 15840-15850	6
677	A review of the structure, magnetic and electrical properties of bismuth ferrite (Bi ₂ Fe ₄ O ₉). 2020 , 46, 18453-18463	11
676	Room temperature magnetic biasing in Bi _{0.85} La _{0.15} FeO ₃ and BaTiO ₃ composite. 2020 , 126, 1	1
675	Defect engineered enhancement of ferromagnetic properties in samarium doped Bi ₄ Ti ₃ O ₁₂ □ BiFeO ₃ ceramics. 2020 , 556, 62-69	2
674	A green method to prepare magnetically recyclable Bi/Bi ₂₅ FeO ₄₀ -C nanocomposites for photocatalytic hydrogen generation. 2020 , 521, 146342	6
673	Magnetic and electric properties of single crystal MnI. 2020 , 32, 335803	1
672	Enhanced electrical conductivity and multiferroic property of cobalt-doped bismuth ferrite nanoparticles. 2020 , 31, 8727-8736	6
671	Electric field dependence of ferroelectric stability in BiFeO ₃ thin films co-doped with Er and Mn. 2020 , 46, 18690-18697	7
670	Self-assembled line network in BiFeO ₃ thin films. 2020 , 509, 166898	0
669	Optical properties, energy band gap and the charge carriers' effective masses of the R ₃ c BiFeO ₃ magnetoelectric compound. 2020 , 144, 109484	7
668	Influence of B-site doping on structural, optical and dielectric properties of bismuth ferrite. 2020 , 33, 1293-1297	
667	Exchange bias effect in bulk multiferroic BiFe _{0.5} Sc _{0.5} O ₃ . 2020 , 10, 045102	4
666	Structural characterization, dielectric, magnetic and optical properties of double perovskite Bi ₂ FeMnO ₆ ceramics. 2020 , 508, 166891	5
665	Origin of Ferroelectricity and Multiferroicity in Binary Oxide Thin Films. 2021 , 68, 273-278	2

- 664 Compositional Tuning of the Aurivillius Phase Material BiTiFeNbO (0 & 10.4) Grown by Chemical Solution Deposition and its Influence on the Structural, Magnetic, and Optical Properties of the Material. **2021**, 68, 303-313 2
- 663 Ferromagnetic and ferroelectric two-dimensional materials for memory application. **2021**, 14, 1802-1813 9
- 662 Synthesis and characterization of samarium substituted bismuth ferrites nanoparticles. **2021**, 34, 813-816 0
- 661 Optical properties of $\text{BiFe}_{0.95}\text{Mn}_{0.05}\text{O}_3$ nanoparticles & $\text{BiFe}_{0.95}\text{Mn}_{0.05}\text{O}_3/\text{SiO}_2$ nanocomposite. **2021**, 35, 170-174
- 660 Synthesizing $\text{Bi}_{1-x}\text{Co}_x\text{Fe}_{1-y}\text{Zn}_y\text{O}_3$ Nanoparticles and Investigating Their Structural, Optical and Photocatalytic Properties. **2021**, 34, 469-478
- 659 First principle study of band gap nature, spontaneous polarization, hyperfine field and electric field gradient of desirable multiferroic bismuth ferrite (BiFeO_3). **2021**, 148, 109737 7
- 658 Structural, Raman analysis and exchange bias effects in Mn doped multiferroic $\text{Bi}_{0.80}\text{La}_{0.10}\text{Ca}_{0.10}\text{Fe}_{1-x}\text{Mn}_x\text{O}_3$ ceramics. **2021**, 47, 6834-6841 3
- 657 Structural and magnetic behavior of CTAB assisted BiFeO_3 by self-combustion route. **2021**, 43, 2725-2729
- 656 Lead-Free Piezoelectric Ceramics. **2021**, 358-368 0
- 655 Structural, dielectric, ferroelectric and optical properties of Er doped BiFeO_3 nanoparticles. **2021**, 853, 156979 8
- 654 Optoelectronic and thermoelectric properties of double perovskite Rb_2PtX_6 (X = Cl, Br) for energy harvesting: First-principles investigations. **2021**, 148, 109665 17
- 653 Magnetodielectric coupling tuning through domain wall charge accumulation in co-doped BiFeO_3 with Sr^{2+} and Mn^{3+} . **2021**, 857, 157549 3
- 652 Sintering time dependent structural and magnetic phase transformations in Pr doped BiFeO_3 multiferroics. **2021**, 519, 167412 5
- 651 Synergistic effect of N-rGO supported Gd doped bismuth ferrite heterojunction on enhanced photocatalytic degradation of rhodamine B. **2021**, 123, 105538 9
- 650 Identification and comparison of peculiarities in physical properties of multiferroic morphotropic phase boundary sintered BiFeO_3 - xPbTiO_3 nano-ceramics. **2021**, 150, 109868 0
- 649 The influence of Nd substitution on microstructural, magnetic, and microwave absorption properties of BiFeO_3 nanopowders. **2021**, 859, 157757 11
- 648 Structural, ferroelectric, and optical properties of Bi^{3+} doped YFeO_3 : A first-principles study. **2021**, 121, e26551 1
- 647 Correlative chemical and structural nanocharacterization of a pseudo-binary $0.75\text{Bi}(\text{Fe}_{0.97}\text{Ti}_{0.03})\text{O}_3$ - 0.25BaTiO_3 ceramic. **2021**, 104, 2388-2397 1

- 646 Ferrimagnetic and relaxor ferroelectric properties of $R_2\text{MnMn}(\text{MnTi}_3)\text{O}_{12}$ perovskites with $R = \text{Nd}$, Eu , and Gd . **2021**, 9, 947-956 3
- 645 Evolution of spatial spin-modulated structure with La doping in $\text{Bi}_{1-y}\text{La}_y\text{FeO}_3$ multiferroics. **2021**, 517, 167341 2
- 644 Prediction of Strong Converse Magnetoelectric Effect in Nb-Doped BaTiO_3 -Based Polar Metals. **2021**, 258, 2000520
- 643 Impact of (Zr, Cu) Ion Substitution on the Optical, Dielectric, and Impedance Behavior of BiFeO_3 . **2021**, 51, 40-46 5
- 642 Enhanced magnetoelectric coupling in dysprosium-doped BiFeO_3 on the formation of nanocomposite with $\text{SrFe}_{12}\text{O}_{19}$. **2021**, 859, 157821 3
- 641 Electrical properties of Li and Nb modified BiFeO_3 ceramics with reduced leakage current. **2021**, 47, 4217-4225 5
- 640 Correlating Role of Substrate and Modified Physical Properties of $(\text{Bi}_{0.5}\text{La}_{0.5}\text{FeO}_3)_{1-x}(\text{Ba}_{0.7}\text{Sr}_{0.3}\text{TiO}_3)_x$ ($x = 0, 0.5$) Thin Films. **2021**, 34, 425-433 0
- 639 Giant Domain Wall Conductivity in Self-Assembled BiFeO_3 Nanocrystals. **2021**, 31, 2005876 12
- 638 Influence of Al-Cu doping on the efficiency of BiFeO_3 based perovskite solar cell (PSC). **2021**, 35, 62-65 1
- 637 Chemical Solution Route for High-Quality Multiferroic BiFeO_3 Thin Films. **2021**, 17, e1903663 15
- 636 Recent progress in bismuth ferrite-based thin films as a promising photovoltaic material. **2021**, 46, 83-108 12
- 635 An overview on ferroelectric photovoltaic materials. **2021**, 175-199
- 634 Observation of normal and reverse magnetocaloric effect in Ho and Sc co-substituted BiFeO_3 . **2021**, 32, 4372-4379
- 633 Structural characterization of polycrystalline thin films by X-ray diffraction techniques. **2021**, 32, 1341-1368 8
- 632 FTIR: Important tool to investigate the chemical bond formation in the polycrystalline $x\text{BaTiO}_3 \square (1-x)\text{BiFeO}_3$. **2021**, 47, 616-620 1
- 631 Structural and impedance spectroscopy in $\text{BiFeO}_3\text{BiCoO}_3\text{BaTiO}_3$ ternary system. **2021**, 47, 1696-1699 0
- 630 Magnetoelectrics and Multiferroics. **2021**, 1-29
- 629 Behavior of microwave absorption of BiFeO_3 nanoparticles fabricated by sol-gel method. **2021**,

628	Perspective on emerging views on microscopic origin of relaxor behavior. 2021 , 36, 1015-1036	3
627	Introduction. 2021 , 1-23	
626	Environmental effect on structural, magnetic, and dielectric properties of BFO nanostructure and its solar cell applications. 2021 , 32, 3313-3323	2
625	Polarization Rotation at Morphotropic Phase Boundary in New Lead-Free NaBiVTiO Piezoceramics. 2021 , 13, 5208-5215	5
624	Lead-Free BiFeO-BaTiO Ceramics with High Curie Temperature: Fine Compositional Tuning across the Phase Boundary for High Piezoelectric Charge and Strain Coefficients. 2021 , 13, 4192-4202	26
623	Comparative density functional studies of pristine and doped bismuth ferrite polymorphs by GGA+U and meta-GGA SCAN+U. 2021 , 23, 8571-8584	4
622	Perovskite BiFeO ₃ Nanostructure Photocatalysts for Degradation of Organic Pollutants. 2021 , 141-162	
621	Transport properties of nanoscopic solids as probed by spectroscopic techniques. 2021 , 9-37	
620	Performances variations of BiFeO ₃ -based ceramics induced by additives with diverse phase structures. 2021 , 23, 1596-1603	2
619	Forming-free resistive switching in ferroelectric Bi _{0.97} Y _{0.03} Fe _{0.95} Sc _{0.05} O ₃ film for RRAM application. 2021 , 96, 045808	0
618	Enhanced electrical properties by optimizing sintering temperature and dwell time in BiFe _{0.96} Zn _{0.02} Ti _{0.02} O ₃ ceramics. 2021 , 572, 180-191	
617	Effects of defect on thermal stability and photoluminescence in quenched Ho-doped 0.94Na _{0.5} Bi _{0.5} Ti _{0.3} 0.06BaTiO ₃ lead-free ceramics. 2021 , 36, 1125-1133	2
616	Soft-mode spectroscopy of ferroelectrics and multiferroics: A review. 2021 , 9, 020704	8
615	Elastic properties assessment in the multiferroic BiFeO ₃ by pump and probe method. 2021 , 118, 062902	0
614	Experimental investigation on multiferroic properties of Ti-doped BiFeO ₃ bulk and nanoparticles. 2021 , 1091, 012006	
613	Surface engineered Tb and Co co-doped BiFeO ₃ nanoparticles for enhanced photocatalytic and magnetic properties. 2021 , 32, 7956-7972	2
612	Effect of rare earth orthoferrite GdFeO ₃ on the band gap modulation and magnetic switching in Bi _{0.5} Na _{0.5} TiO ₃ ceramics. 2021 , 94, 77-92	
611	Role of Hydroxide Precipitation Conditions in the Formation of Nanocrystalline BiFeO ₃ . 2021 , 66, 163-169	5

610	Electronic and Magnetic Properties of Chemical Solution Deposited BiFeO ₃ Thin Film: a Soft X-ray Magnetic Circular Dichroism Study. 2021 , 34, 1119-1124	5
609	Magnetoelectric and multiferroic properties of spinels. 2021 , 129, 060901	9
608	Surface and bulk ferroelectric phase transition in super-tetragonal BiFeO ₃ thin films. 2021 , 5,	3
607	Effects of solvents and Al doping on structure and physical properties of BiFeO ₃ thin films. 2021 , 98, 45-53	2
606	Non-collinear magnetism & multiferroicity: the perovskite case. 2020 ,	1
605	Theory and phase-field simulations of electrical control of spin cycloids in a multiferroic. 2021 , 103,	
604	Domain-wall photovoltaic effect in Fe-doped BaTiO ₃ single crystals. 2021 , 129, 084101	2
603	Finite-element simulation of photoinduced strain dynamics in silicon thin plates. 2021 , 8, 024103	2
602	High-Performance Lead-Free Piezoelectrics. 2021 , 19-31	
601	Spectacular photocatalytic activity of mechanosynthesized heterostructured Bi-Fe-O nanocomposites in wastewater treatment containing colored and colorless pollutants. 2021 , 326, 115317	3
600	Rietveld Study of the Changes of Phase Composition, Crystal Structure, and Morphology of BiFeO ₃ by Partial Substitution of Bismuth with Rare-Earth Ions. 2021 , 11, 278	1
599	Insight into dynamic magnetic properties of YMnO ₃ /FM bilayer in a time-dependent magnetic field. 2021 , 136, 1	14
598	Empirical approach to measuring interface energies in mixed-phase bismuth ferrite. 2021 , 5,	
597	The multi-ferroelectricity in neodymium ferrite with perovskite structure. 2021 , 56, 10488-10493	0
596	Ab initio determination of crystal stability of di-p-tolyl disulfide. 2021 , 11, 7076	2
595	Chemical Solution Deposition of La-Substituted BiFe _{0.5} Sc _{0.5} O ₃ Perovskite Thin Films on Different Substrates. 2021 , 11, 307	0
594	Electrocaloric effects in multiferroics. 2021 , 103,	0
593	Comparison of Ferroelectric Photovoltaic Performance in BFO/BTO Multilayer Thin Film Structure Fabricated Using CSD & PLD Techniques. 2021 , 50, 1835-1844	1

592	Photostrictive Effect: Characterization Techniques, Materials, and Applications. 2021 , 31, 2010706	6
591	Studies on the multiferroic properties and impedance analysis of (La, Cu) BiFeO ₃ prepared by sol-gel method. 2021 , 573, 104-116	5
590	Direct Sunlight Catalytic Decomposition of Organic Pollutants via Sm- and Ce-Doped BiFeO ₃ Nanopowder Synthesized by a Rapid Combustion Technique. 1	2
589	Electron density distribution and magnetic ordering of polycrystalline Bi _{0.6} Sr _{0.4} FeO ₃ ceramics. 2021 , 573, 224-235	1
588	Ferroelectricity and ferromagnetism in Fe-doped barium titanate ceramics. 2021 , 573, 63-75	4
587	A correlation of lattice distortion with the magnetic properties of calcium doped bismuth ferrite thin films. 2021 , 54, 205002	1
586	Advances in the modification and device integration of multiferroic bismuth ferrite. 2021 , 573, 87-102	0
585	Flexible Epsilon Iron Oxide Thin Films. 2021 , 13, 17006-17012	4
584	Electrochemically manipulating BiFeO ₃ particles via Bi ³⁺ ion extraction. 2021 , 104, 3354-3364	0
583	BiFeO ₃ System. 2021 , 157-196	
582	Enhanced multiferroic characteristics in hexagonal ScMn _{1-x} Fe _x O ₃ ceramics. 2021 , 129, 134101	
581	Multiferroic BiFeO ₃ dithizone functionalized as optical sensor for detection and determination of some heavy metals in environmental samples. 2021 , 44, 1	1
580	Multiscale Domain Structures and Ferroic Properties of Dy-Modified BiFeO ₃ -PbTiO ₃ Single Crystals. 2021 , 21, 3082-3092	2
579	Nanostructured Multiferroics. 2021 , 63-94	
578	Enhanced dielectric, ferroelectric and magnetic properties of Ba ₄ Sm ₂ Fe ₂ Nb ₈ O ₃₀ RT multiferroics prepared by microwave sintering. 2021 , 47, 21024-21024	2
577	Structural, dielectric, magnetic and optical properties of double perovskite oxide SmNiMnO ₆ nanoparticles synthesized by a sol-gel process. 2021 , 32,	1
576	Role of charge states and dopant site in governing electronic properties of Cr doped BiFeO ₃ . 2021 , 263, 124438	1
575	Size-dependent structural parameters, optical, and magnetic properties of facile synthesized pure-phase BiFeO ₃ . 2021 , 32, 13323-13335	4

574	Magnetic properties across the YMnO ₃ -BiFeO ₃ system designed for phase-change magnetoelectric response. 2021 , 266, 115055	1
573	Photoferroelectric perovskite solar cells: Principles, advances and insights. 2021 , 37, 101062	16
572	Preparations, Characterization, and Applications of Multiferroic Nanocomposites. 2021 , 233-247	
571	Structure evidence of Pna21 phase and field-induced transition of Pna21/R3c in Bi _{1-x} Sm _x Fe _{0.99} Ti _{0.01} O ₃ ceramics. 2021 , 118, 142904	1
570	Magnetoelectric Multiferroicity and Magnetic Anisotropy in Guanidinium Copper(II) Formate Crystal. 2021 , 14,	0
569	Room-temperature multiferrocity and magnetodielectric properties of ternary BiFeO ₃ Bi _{0.5} Na _{0.5} TiO ₃ /BaTiO ₃ ceramics across the rhombohedral/orthorhombic phase boundary. 2021 , 32, 11524	1
568	Production of green electricity from strained BaTiO ₃ and TiO ₂ ceramics based hydroelectric cells. 2021 , 262, 124277	5
567	Studies of structural, electrical and ferroelectric characteristics of gadolinium and yttrium modified bismuth ferrite. 2021 , 263, 124359	3
566	Role of Bi chemical pressure on electrical properties of BiFeO ₃ /BaTiO ₃ based ceramics. 2021 , 114, 106562	5
565	Magnetoelectric materials and devices. 2021 , 9, 041114	26
564	Synthesis of Bismuth Ferrite and its Application for Oscillator Material up to 25 GHz Range. 1028, 9-14	
563	Structural, magnetic, and electrical properties of RFeO ₃ (R = Dy, Ho, Yb & Lu) compounds. 2021 , 32, 14286	0
562	Synthesis and Characterization of LFO/BFO Multiferroic Nanocomposites. 2021 , 193-202	
561	Single-Phase Multiferroics. 2021 , 23-50	
560	Correlation Between Grain Size, Transport, and Multiferroic Properties of Ba-doped BiFeO ₃ Nanoparticles. 2021 , 163-192	
559	Nanostructured Multiferroics: Current Trends and Future Prospects. 2021 , 1-22	
558	Super short-range magnetic orderings in a multiferroic relaxor ceramic 0.41Bi(Ni _{1/2} Zr _{1/2})O ₃ 0.59PbTiO ₃ . 2021 , 56, 11838-11846	1
557	Structural, dielectric and magnetic properties of xNi _{0.50} Zn _{0.40} Mn _{0.10} Fe ₂ O ₄ + (1-x)Bi _{0.90} La _{0.10} Fe _{0.93} Eu _{0.07} O ₃ multiferroic composites. 2021 , 8, 046103	1

- 556 Phase formation and spectroscopy analysis of doped bismuth ferrite nanoparticles. **2021**, 49, 3453-3453
- 555 Multiferroic Study of Pure BiFeO₃ Synthesized Using Various Complexing Agents by Sol-Gel Method. **2021**, 51-62
- 554 Effect of Na/Co co-substituted on structural, magnetic, optical and photocatalytic properties of BiFeO₃ nanoparticles. **2021**, 263, 124402 0
- 553 Strain engineering of epitaxial oxide heterostructures beyond substrate limitations. **2021**, 4, 1323-1334 12
- 552 Investigation on Multiferroic Properties and Conduction Mechanism in Cobalt Doped Bi_{0.9}Nd_{0.1}FeO₃ Solid Solutions. **2021**, 80, 142-149 1
- 551 Ferro-photocatalytic Enhancement of Photoelectrochemical Water Splitting Using the WO₃/BiFeO₃ Heterojunction. **2021**, 35, 9623-9634 6
- 550 Role of Fe Doping on Local Structure and Electrical and Magnetic Properties of PbTiO₃. **2021**, 125, 12342-12354
- 549 Improved ferroelectric properties and softening effect in BLTF ceramics. **2021**, 47, 25163-25163 1
- 548 Effects of crystallization kinetics on the dielectric and electrical properties of BiFeO₃ films. 0
- 547 A first principle study: Effect of tin substitution on magnetic properties of bismuth ferrite nanoparticles prepared by sol-gel synthesis method. **2021**, 127, 108483 6
- 546 Electric field poling effect on the photosensitivity of samarium-doped bismuth ferrite ceramics. **2021**, 47, 12574-12582 5
- 545 Enhanced visible-light photocatalytic activity and recyclability of magnetic core-shell Fe₃O₄@SiO₂@BiFeO₃@epiolite microspheres for organic pollutants degradation. **2021**, 335, 116566 10
- 544 Review of Magnetoelectric Sensors. **2021**, 10, 109 7
- 543 Enhanced Electromechanical Response and Thermal Stability of 0.93(Na_{1/2}Bi_{1/2})TiO₃-0.07BaTiO₃ Through Aerosol Deposition of Base Metal Electrodes. **2021**, 8, 2100309 1
- 542 Structural phase instability, mixed-phase, and energy band gap change in BiFeO₃ under lattice strain effect from first-principles investigation. **2021**, 47, 12592-12599 3
- 541 Coexisting morphotropic phase boundary and giant strain gradient in BiFeO₃ films. **2021**, 129, 184101 0
- 540 Structure and dielectric properties of Bi_{1-x}La_xFeO₃ nanostructured ceramics. **2021**, 576, 1-7 0
- 539 Ions substitution effect on the magnetic phase transition temperature of 0.5BiFeO₃-0.5Pb_{1-x}Sr_xTiO₃ multiferroic solid solutions. **2021**, 576, 19-28

538	Lattice effects on the multiferroic characteristics of (La, Ho) co-substituted BiFeO ₃ . 2021 , 863, 158719	3
537	Effect of heat-treatment mechanism on structural and electromechanical properties of eco-friendly (Bi, Ba)(Fe, Ti)O ₃ piezoceramics. 2021 , 56, 13198	7
536	Electric field control of magnetism: multiferroics and magnetoelectrics. 2021 , 44, 251-289	4
535	Grain structure and dielectric characteristics of (1-x-y)BiFeO ₃ -xPbFe _{0.5} Nb _{0.5} O ₃ -yPbTiO ₃ ceramics. 2021 , 576, 111-118	1
534	On the exceptional temperature stability of ferroelectric Al _{1-x} Sc _x N thin films. 2021 , 118, 232905	9
533	The effects of sintering temperature on structural, electrical, and magnetic properties of MgFe _{1.92} Bi _{0.08} O ₄ . 2021 , 46, 151-161	
532	Structural, dielectric, magnetic and magneto-dielectric properties of (1-x)BiFeO ₃ (x)CaTiO ₃ composites. 2021 , 32, 18012-18027	0
531	Enhanced ferroelectric properties of (Zn, Ti) equivalent co-doped BiFeO ₃ films prepared via the sol-gel method. 2021 , 47, 16776-16785	4
530	Low-Temperature Growth of AlN Films on Magnetostrictive Foils for High-Magnetoelectric-Response Thin-Film Composites. 2021 , 13, 30874-30884	3
529	Crafting the multiferroic BiFeO ₃ -CoFe ₂ O ₄ nanocomposite for next-generation devices: A review. 2021 , 36, 1579-1596	8
528	Structural evolution and magnetic properties of Bi _{0.86} Nd _{0.14} Fe _{1-x} Ti _x O ₃ ceramics. 2021 , 270, 124857	0
527	Magnetodielectric study of BiFeO ₃ synthesized by assisted high-energy ball milling. 2021 , 153, 109998	2
526	Structure, dielectric, and multiferroic properties of Bi _{0.85} Nd _{0.15} Fe _{0.98} Zr _{0.02} O ₃ in Ba and Ti co-doping. 2021 , 32, 18439-18449	0
525	Stress-mediated solution deposition method to stabilize ferroelectric BiFe _{1-x} Cr _x O ₃ perovskite thin films with narrow bandgaps. 2021 , 41, 3404-3415	3
524	Trigonal Planar Iron(II) and Cobalt(II) Complexes Containing [RS(NBu)] (R = NBu, = 2; CHPh, = 1) as Acute Bite-Angle Chelating Ligands: Soft P Donor Proves Beneficial to Magnetic Co Species. 2021 , 60, 9580-9588	2
523	Multiferroic and Nanomechanical Properties of Bi _{1-x} Gd _x FeO ₃ Polycrystalline Films (x = 0.00-0.15). 2021 , 11, 900	1
522	Synthesis of doped and undoped Bi _{1-x} M _x FeO ₃ porous networks (M = La, Gd, Nd; x = 0, 0.03, 0.05, 0.10) with enhanced visible-light photocatalytic activity. 2021 , 416, 113334	2
521	Recent progress on 2D ferroelectric and multiferroic materials, challenges, and opportunity. 2021 , 4, 847-863	8

520	An antisite defect mechanism for room temperature ferroelectricity in orthoferrites. 2021 , 12, 4298	8
519	Effect of La/Cr co-doping on dielectric dispersion of phase pure BiFeO ₃ nanoparticles for high frequency applications. 2021 , 13, 1534-1545	1
518	Growth and characterization of Dy _{1-x} Y _x MnO ₃ single crystals by optical floating zone technique: A combined X-ray diffraction and DC magnetization study. 2021 , 565, 126152	0
517	Structural, dielectric, impedance and ferroelectric properties of lead-free Bi(Fe _{0.85} Dy _{0.15})O ₃ ceramic. 2021 , 32, 21337-21349	0
516	Non-d ₀ ferroelectricity from semicovalent superexchange in bismuth ferrite. 2021 , 104,	1
515	New lead-free double perovskites X ₂ Gel ₆ (X' = K, Rb, Cs) for solar cells, and renewable energy as an alternate of hybrid perovskites. 2021 , 45, 19645	3
514	Chemical ordering and magnetic phase transitions in multiferroic BiFeO ₃ -AFe _{1/2} Sb _{1/2} O ₃ (A-Pb, Sr) solid solutions fabricated by a high-pressure synthesis. 2160011	
513	Effect of Y ions incorporation on structural, morphological and magnetic properties of Bi _{1-x} Dy _x FeO ₃ for ferromagnetic applications. 2021 , 44, 1	1
512	(001)-oriented BiFeO ₃ films integrated on Si with enhanced electrical performances. 2021 , 104, 6373	0
511	Electric field control of magnetism. 2021 , 477, 20200942	7
510	Effects of Sm-doping on microstructure, magnetic and microwave absorption properties of BiFeO ₃ . 2021 , 39, 835-843	15
509	La doped BiFeO ₃ ceramics synthesized under extreme conditions: Enhanced magnetic and dielectric properties. 2021 , 47, 20407-20412	4
508	Estimating the true piezoelectric properties of BiFeO ₃ from measurements on BiFeO ₃ -PVDF terpolymer composites. 2021 , 868, 159186	5
507	Effect of polarization rotation on the optical and photovoltaic properties of BiFeO ₃ thin films. 2021 , 33,	1
506	Exploring the one-step synthesis of composite BiFeO ₃ based coatings. 2021 , 47, 18969-18976	0
505	Influence of Gd doping and thickness variation on structural, morphological and optical properties of nanocrystalline bismuth ferrite thin films via sol-gel technology. 2021 , 32, 20612-20624	0
504	TB2J: A python package for computing magnetic interaction parameters. 2021 , 264, 107938	10
503	Local Structure and Magnetic Hyperfine Interactions of ⁵⁷ Fe Probe Nuclei in TlCr _{0.95} Fe _{0.05} O ₃ . 2021 , 133, 49-58	

- 502 Oxide and Organic-Inorganic Halide Perovskites with Plasmonics for Optoelectronic and Energy Applications: A Contributive Review. **2021**, 11, 1057 4
- 501 Progress In Lead Free- Relaxor Ferroelectrics For Energy Storage Applications.. **2021**, 1973, 012117 1
- 500 Monitoring Electrical Biasing of Pb(ZrTi)O Ferroelectric Thin Films In Situ by DPC-STEM Imaging. **2021**, 14, 1
- 499 Spontaneous and Induced Ferroelectricity in the BiFe_{1-x}Sc_xO₃ Perovskite Ceramics. **2021**, 218, 2100173 1
- 498 Lattice symmetry breaking transition and critical size limit for ferroic orders in nanophase BiFeO₃. **2021**, 104, 1
- 497 Lanthanum and Manganese Co-Doping Effects on Structural, Morphological, and Magnetic Properties of Sol-Gel Derived BiFeO₃. **2021**, 14, 2
- 496 Magnetic and electric field dependent anisotropic magnetoelectric multiferroicity in SmMn₃Cr₄O₁₂. **2021**, 104, 3
- 495 Insights on carbapenem-resistant *Pseudomonas aeruginosa*. **2021**, 65, 105-112 6
- 494 . **2021**, 57, 1-57 8
- 493 Emergent properties at oxide interfaces controlled by ferroelectric polarization. **2021**, 7, 1
- 492 Effect of La³⁺ Substitution on Structural, Magnetic, and Multiferroic Properties of Bismuth Ferrite (Bi_{1-x}La_xFeO₃) Nanoceramics. **2022**, 105-113 1
- 491 Crystal structure, physicochemical, and sensory properties of solid solutions Bi_{1-x}La_xFe_{1-x}CoxO₃ (x = 0, 0.05, 0.1). **2021**, 32, 22579-22587 1
- 490 Li-ionic control of magnetism through spin capacitance and conversion. **2021**, 9
- 489 On the magnetic and magnetoelectric coupling properties of lead-free (1 - x) Bi_{0.9}La_{0.1}FeO₃/xLa_{0.7}Sr_{0.3}MnO₃ (x = 0, 0.1, 0.2) composites at room temperature. 1 0
- 488 Photoconductivity and Photovoltaic Studies on Polycrystalline Bi_{1-x}Fe_{1-x}O₃ (M²⁺ = K⁺ and Cs⁺; M³⁺ = Ti⁴⁺; x = y = 0 and 0.1) Thin Films. **2021**, 733, 138804 1
- 487 Electric-field-controlled magnetism due to field-induced transition of Pn_a21/R3c in Bi_{1-x}GdxFeO₃ ceramics. **2021**, 7, 967-975 1
- 486 Tailoring the multiferroic properties of BiFeO₃ by low energy ions implantation. 1 0
- 485 Thin film processing of multiferroic BiFeO₃: From sophistication to simplicity. A review. **2021**, 0

484	Chemical pressure exerted by rare earth substitution in BiFeO ₃ : Effect on crystal symmetry, band structure and magnetism. 2021 , 876, 160178	5
483	Enhancement in electrical and magnetic properties of (Li _{0.5} Ga _{0.5}) ₂₊ and (Li _{0.5} Er _{0.5}) ₂₊ -Modified BiFeO ₃ -BaTiO ₃ ceramics. 2021 , 47, 24020-24030	0
482	Negatively Charged In-Plane and Out-Of-Plane Domain Walls with Oxygen-Vacancy Agglomerations in a Ca-Doped Bismuth-Ferrite Thin Film. 2021 , 3, 4498-4508	1
481	Stabilization of correlated ferroelectric and ferromagnetic domain structures in BiFe _{0.9} Co _{0.1} O ₃ films. 2021 , 119, 132901	1
480	Optical transient grating pumped X-ray diffraction microscopy for studying mesoscale structural dynamics. 2021 , 11, 19322	1
479	Structural and Electrical Behavior of (0.70)BiFe _{1-x} CoxO ₃ (0.30)PbTiO ₃ Solid Solutions Prepared by Simple Sol-Gel Route. 2021 , 10, 093006	0
478	Investigations on Optical and Magnetodielectric Properties of Lead-Free Multiferroic Bi _{0.9} La _{0.1} FeO ₃ and its Composite (0.9) Bi _{0.9} La _{0.1} FeO ₃ /(0.1) La _{0.7} Sr _{0.3} MnO ₃ at Room Temperature. 2021 , 34, 2999	0
477	Enhanced piezoelectric and ferroelectric properties of tetragonal BiFeO ₃ BaTiO ₃ ceramics via tailoring sintering temperature and dwell time. 2021 , 32, 24496-24506	0
476	Actuation mechanisms in mixed-phase K _{0.5} Bi _{0.5} TiO ₃ -BiFeO ₃ -PbTiO ₃ ceramics. 2021 , 41, 6414-6423	1
475	Formaldehyde sensing with a parts-per-billion limit of detection by dielectric properties and crystal symmetry optimization in BiFeO ₃ -based p-type solid solution. 2021 , 344, 130314	3
474	Construction of multi-domain coexistence enhanced piezoelectric properties of Bi _{0.5} Na _{0.5} TiO ₃ -based thin films. 2021 , 41, 6456-6464	3
473	Tuning of electric and magnetic properties of BiFeO ₃ -SrTiO ₃ solid solution ceramics by site-specific doping of Mn. 2021 , 877, 160239	6
472	The origin of the large magnetoelectric coupling in the ceramic Ba _{0.1} Bi _{0.9} (Ti _{0.9} Zr _{0.1}) _{0.1} Fe _{0.9} O ₃ .	
471	Influence on properties of Bi _{0.9} Sm _{0.1} FeO ₃ multiferroic system with Mg substitution at Fe-site. 2021 , 302, 122432	2
470	Adsorption enhanced photocatalytic degradation of Rhodamine B using GdxBi _{1-x} FeO ₃ @SBA-15 (x= 0, 0.05, 0.10, 0.15) nanocomposites under visible light irradiation. 2021 , 47, 29139-29148	1
469	Design, structural evolution, optical, electrical and dielectric properties of perovskite ceramics Ba _{1-x} BixTi _{1-x} FexO ₃ (0 ≤ x ≤ 0.8). 2021 , 273, 125096	2
468	Evidence on the quantum critical point in EuTiO ₃ BiTiO ₃ solid solution. 2021 , 620, 413225	0
467	A molecular dynamics study of domain switching in BiFeO ₃ nanofilm under DC electric field. 2021 , 199, 110718	0

- 466 Structural, magnetic, magneto-dielectric and magneto-electric properties of (1-x) Ba_{0.85}Ca_{0.15}Ti_{0.90}Zr_{0.10}O₃ [(x) CoFe₂O₄ lead-free multiferroic composites sintered at higher temperature. **2021**, 538, 168243 3
- 465 Origin of magnetic, magnetoelectric effect and the influence of reentrant ferroelectric phase on the structural and multiferroic properties of Dy³⁺-Fe³⁺ co-substituted BaTiO₃ ceramics. **2021**, 538, 168260 0
- 464 Sensitivity enhancement by employing BiFeO₃ and graphene hybrid structure in surface plasmon resonance biosensors. **2021**, 121, 111618 1
- 463 Low temperature deposition of BiFeO₃ films on Ti foils for piezoelectric applications. **2021**, 204, 114152 1
- 462 Additives effect on the multiferroic behaviour of BiFeO₃/PbTiO₃. **2021**, 47, 29815-29823 3
- 461 Investigation of multifunctional characteristics in SmFeO₃-BaTiO₃ perovskite system for devices. **2021**, 135, 106071 0
- 460 Magnetoelectric features in the magnetic hysteresis of modified multiferroic BiFeO₃: Release of latent magnetization induced by cationic modification. **2021**, 537, 168198
- 459 Enhanced electric resistivity and dielectric energy storage by vacancy defect complex. **2021**, 42, 836-844 5
- 458 On the effects of dislocations on the magnetism of BiFeO₃ nanoparticles. **2021**, 887, 161421 1
- 457 Prominent ferroelectric properties in Mn-doped BiFeO₃ spin-coated thin films. **2021**, 886, 161168 4
- 456 Prediction of magnetoelectric properties of defect BiFeO₃ thin films using Monte Carlo simulations. **2021**, 539, 168402 3
- 455 Unveiling the spin-phonon coupling in nanocrystalline BiFeO₃ by resonant two-phonon Raman active modes. **2021**, 274, 115444
- 454 Model-based quantification of inter-/intra-grain electrical parameters, hopping polydispersity, and local energy barrier profile of BiFeMnO₃ synthesized by different methods. **2022**, 160, 110334
- 453 Crystal structure refinement and magnetic properties of Sm³⁺ doped BiFeO₃ nanoparticles. **2022**, 624, 413374 0
- 452 Structural Evolution-Enabled BiFeO₃ modulated by strontium doping with enhanced magnetic and photoelectric performance. **2022**, 571, 151130 0
- 451 Sm³⁺-BiFeO₃ nano catalyst: A synergetic effect of Sm³⁺ on enhanced multiferroic properties and photocatalysis. **2022**, 891, 161896 0
- 450 Electronic and optical properties of multifunctional R₃c AFeO₃ (A = Sc or In) compounds: Insights into their potential for photovoltaic applications. **2022**, 160, 110346 0
- 449 Effect of core size on the magnetoelectric properties of Cu_{0.8}Co_{0.2}Fe₂O₄@Ba_{0.8}Sr_{0.2}TiO₃ ceramics. **2022**, 160, 110314 3

448	Magnetic and electrical properties by Ca ²⁺ doping in SmCrO ₃ orthochromites. 2022 , 890, 161823	1
447	Ferromagnetic, ferroelectric, and magnetoelectric properties in individual nanotube-based magnetoelectric films of CoFe ₂ O ₄ /BaTiO ₃ using electrically resistive core-shell magnetostrictive nanoparticles. 2022 , 891, 161861	1
446	Reasons for the High Electrical Conductivity of Bismuth Ferrite and Ways to Minimize It. 2021 , 11, 1025	0
445	Multiferroic properties and impedance spectrum of Ho ³⁺ and Ti ⁴⁺ co-doped BiFeO ₃ ceramics. 2021 , 570, 57-66	
444	A review of in situ transmission electron microscopy study on the switching mechanism and packaging reliability in non-volatile memory. 2021 , 42, 013102	3
443	On structural and morphological characterizations of Ho-BFO multiferroics. 2021 ,	1
442	Retaining graphene structure in the synthesis of its composite with BiFeO ₃ . 2021 , 43, 216-219	0
441	Effect of synthesis method in magnetic properties of Bismuth iron oxide: A prevoskite type multiferroic materials. 2021 , 47, 1000-1005	1
440	Quasiparticle band structures, spontaneous polarization, and spin-splitting in noncentrosymmetric few-layer and bulk EGeSe. 2021 , 9, 9683-9691	1
439	High oxide-ion conductivity in acceptor-doped Bi-based perovskites at modest doping levels. 2021 , 23, 11327-11333	2
438	Formation and physical properties of the self-assembled BFO-CFO vertically aligned nanocomposite on a CFO-buffered two-dimensional flexible mica substrate.. 2021 , 11, 15539-15545	6
437	Giant Ferroelectric Polarization in Ultrathin Ferroelectrics via Boundary-Condition Engineering. <i>Advanced Materials</i> , 2017 , 29, 1701475	24 35
436	Syntheses and Properties of Some Bi-Containing Compounds with Noncentrosymmetric Structure. 2013 , 321-341	1
435	Electrochemical Supercapacitors of Bismuth Ferrites. 2020 , 69-84	1
434	Ferrites Obtained by Sol-Gel Method. 2016 , 1-41	3
433	Ferrites Obtained by Sol-Gel Method. 2018 , 1-41	6
432	Ferrites Obtained by Sol-Gel Method. 2018 , 695-735	25
431	Magnetic Properties in Multiferroic Bi _{1-x} Fe _{1+x} O ₃ (x 0.5) of Nanoparticles. 2013 , 117-124	1

430	Hybrid Ferromagnetic/Ferroelectric Materials. 2016 , 365-398	1
429	Improved ferroelectric properties of BiFeO ₃ -based piezoelectric ceramics through morphotropic phase boundary construction. 2020 , 46, 15991-15997	5
428	Investigation of magnetic, dielectric and optical properties of BiFe _{0.5} Mn _{0.5} O ₃ multiferroic ceramic. 2020 , 753, 137569	3
427	Controlling the ferroelectric and resistive switching properties of a BiFeO thin film prepared using sub-5 nm dimension nanoparticles. 2017 , 19, 26085-26097	18
426	Observation of strong magnetoelectric coupling and ferromagnetism at room temperature in Fe substituted ferroelectric BaZr _{0.05} Ti _{0.95} O ₃ thin films. 2017 , 121, 034101	5
425	Ferroelectric domain structure of Bi ₂ FeCrO ₆ multiferroic thin films. 2020 , 128, 234103	0
424	Fashioning the architectures of the self-assembled multiferroic nanocomposite thin film. 2020 ,	1
423	Effect of Mn substitution on structural and dielectric properties of bismuth ferrite. 2017 , 519, 187-193	8
422	Progress in designing novel single-phase room temperature multiferroics. 2020 , 569, 227-239	1
421	Influence of compositional variation on structural, electrical and magnetic characteristics of (Ba _{1-x} Gd _x)(Ti _{1-x} Fe _x)O ₃ (0.2 ≤ x ≤ 0.5). 2018 , 5, 016101	13
420	Multiferroic bismuth ferrite: Perturbed angular correlation studies on its ferroic Bp phase transition. 2020 , 102,	6
419	Successive field-induced transitions in BiFeO ₃ around room temperature. 2017 , 1,	11
418	Polymorphism in Bi-based perovskite oxides: A first-principles study. 2018 , 2,	7
417	Size-dependent bistability in multiferroic nanoparticles. 2019 , 3,	4
416	Influence of flexoelectricity on the spin cycloid in (110)-oriented BiFeO ₃ films. 2019 , 3,	6
415	Oxygen vacancy order-disorder transition at high temperature in Bi-Sr-Fe-based perovskite-type oxides. 2019 , 3,	6
414	Magnetic field induced antiferromagnetic cone structure in multiferroic BiFeO ₃ . 2020 , 4,	2
413	Giant pressure-enhancement of multiferroicity in CuBr ₂ . 2020 , 2,	1

412	Incommensurate structures of the [CHNH][Co(COOH)] compound. 2019 , 6, 105-115	5
411	Giant piezoelectricity of Sm-doped Pb(MgNb)O-PbTiO single crystals. 2019 , 364, 264-268	242
410	BiFeO ₃ Crystal Structure at Low Temperatures. 2010 , 117, 296-301	70
409	Magnetic Properties of the Bi _{0.65} La _{0.35} Fe _{0.5} Sc _{0.5} O ₃ Perovskite. 2017 , 131, 1069-1071	1
408	Orthorhombic Phase of La _{0.5} Bi _{0.5} NiO ₃ Studied by First Principles. 2018 , 133, 408-410	1
407	Spin dynamics, antiferrodistortion and magnetoelectric interaction in multiferroics. The case of BiFeO ₃ . 2020 ,	1
406	Electronic Structure and Magnetic Properties of FeTe, BiFeO ₃ , SrFe ₁₂ O ₁₉ and SrCoTiFe ₁₀ O ₁₉ Compounds. 2016 , 61, 523-530	3
405	Ferroelectricity of Ca ₉ Fe(PO ₄) ₇ and Ca ₉ Mn(PO ₄) ₇ ceramics with polar whitlockite-type crystal structure. 2020 , 41, 559-564	1
404	Strain Engineering of Epitaxial Oxide Heterostructures Beyond Substrate Limitations.	1
403	A CHEMICAL ROUTE TO THE SYNTHESIS OF Bi _{1-x} Mg _x FeO ₃ (x=0.1 and x=0.07) NANOPARTICLE WITH ENHANCED ELECTRICAL PROPERTIES AS MULTIFERROIC MATERIAL. 2018 , 5, 103-112	1
402	Straintronics: a new trend in micro- and nanoelectronics and material science. 2018 , 188, 1288-1330	7
401	Preparation of La-doped BiFeO ₃ Thin Film and Its Photovoltaic Properties. 2013 , 28, 436-440	5
400	Nanocasting synthesis of BiFeO nanoparticles with enhanced visible-light photocatalytic activity. 2020 , 11, 1822-1833	3
399	First-principles calculation of the electronic and optical properties of BiRhO ₃ compound. 2017 , 4, 894-904	3
398	Multiferroic Property and Crystal Structural Transition of BiFeO ₃ -SrTiO ₃ Ceramics. 2011 , 48, 307-311	15
397	Recent Progress in Ferroelectric Diodes: Explorations in Switchable Diode Effect. 2013 , 5, 81	1
396	Exploring multiferroic materials based on artificial superlattice LaFeO ₃ -YMnO ₃ and natural superlattice n-LaFeO ₃ -Bi ₄ Ti ₃ O ₁₂ thin films. 2015 , 64, 097502	1
395	Recent progress of multiferroic magnetoelectric devices. 2018 , 67, 157507	4

- 394 Enhanced Piezoelectric Constant of $(1-x)\text{BiFeO}_3\text{BiCoO}_3$ Thin Films Grown on LaAlO_3 Substrate. **2011**, 50, 031505 7
- 393 Microstructure of $\text{BaTiO}_3\text{Bi}(\text{Mg}_{1/2}\text{Ti}_{1/2})\text{O}_3\text{BiFeO}_3$ Piezoelectric Ceramics. **2012**, 51, 09LD04 30
- 392 Study on the Structural, Electrical, and Magnetic Properties of Pure and $(\text{Pr}^{3+}, \text{Co}^{2+})$ -Doped BiFeO_3 Powders and Thin Films. **2012**, 51, 11PG06 1
- 391 Modifying BiFeO_3 (BFO) for multifunctional applications - A review. **2021**, 0 0
- 390 Enhanced dielectric stability and coercivity of band gap tuned BaAl Co-doped bismuth ferrite: An experimental and DFT+U investigation. **2021**, 48, 3404-3404 0
- 389 Surface structure and quenching effects in $\text{BiFeO}_3\text{-BaTiO}_3$ ceramics. **2022**, 105, 1265 3
- 388 Achieving Large Switchable Polarization and Enhanced Piezoelectric Response in $\text{BiFeO}_3\text{-PbTiO}_3$ Solid Solution Ceramics. 2100883 1
- 387 Multiple property enhancement in bismuth ferrite-based ferroelectrics by balancing nanodomain and relaxor state. **2022**, 105, 1241 0
- 386 Tunable Magnetic Properties in $\text{SrRuO}_3/\text{BiFeO}_3$ Heterostructures via Electric Field. 0
- 385 Solution processing of morphotropic phase boundary $\text{BiFeO}_3\text{-PbTiO}_3$ thin films with reduced conductivity for high room temperature switchable polarization. **2022**, 105, 888 0
- 384 Nonlinear ion mobility at high electric field strengths in the perovskites SrTiO_3 and $\text{CH}_3\text{NH}_3\text{PbI}_3$. **2021**, 5, 1
- 383 Crystalline texture analyses of sputtered BiFeO_3 thick films on Si with a large polarization. **2021**, 0 0
- 382 Thin Films/Properties and Applications. 0
- 381 Improved electric insulation ability and ferromagnetic property in Nb_2O_5 doped BiFeO_3 -based multiferroic ceramics. 1 0
- 380 High Curie temperature $\text{BiFeO}_3\text{-BaTiO}_3$ lead-free piezoelectric ceramics: Ga^{3+} doping and enhanced insulation properties. **2021**, 130, 144104 3
- 379 DFTTK: Density Functional Theory ToolKit for high-throughput lattice dynamics calculations. **2021**, 75, 102355 4
- 378 Epitaxial ferroelectric interfacial devices. **2021**, 8, 041308 3
- 377 Effect of Mn^{4+} doping on the microstructure and electrical property of BiFeO_3 ceramic. **2012**, 61, 142301

376 Complex Oxide Materials. 1179-1212

375 Structural and Multiferroic Properties of Chemical-Solution-Deposited (Bi_{0.95}La_{0.05})(Fe_{0.97}Cr_{0.03})O₃/NiFe₂O₄ Double-Layered Thin Film. **2012**, 51, 09MD06

1

374 BiFeO₃-based Lead-free Piezoelectric Ceramics. **2012**, 25, 692-701

373 Enhanced Sintering Behavior and Electrical Properties of Single Phase BiFeO₃ Prepared by Attrition Milling and Conventional Sintering. **2012**, 49, 485-492

1

372 Integration of Multiferroic BiFeO₃ Thin Films into Modern Microelectronics. 403-441

371 Ferroelectric BiFeO₃-coated TiO₂ Electrodes for Enhanced Photovoltaic Properties of Dye-sensitized Solar Cells. **2013**, 26, 198-203

370 Hybrid Ferromagnetic/Ferroelectric Materials. **2015**, 1-29

369 Lead-Free Ferroelectric Thin Films. **2016**, 1-28

368 Structural, dielectric and magnetic properties of sol-gel synthesized Bi_{1-x}LaxFeO₃ nanoparticles (x=0.3). **2016**,

367 Review on Enhancement of BiFeO₃ Photocatalytic Property. **2017**, 07, 224-231

366 Role of grain and grain boundary on the electrical and thermal conductivity of Bi_{0.9}Y_{0.1}Fe_{0.9}Mn_{0.1}O₃ ceramics. **2017**,

365 Ferrites Obtained by Sol-Gel Method. **2018**, 1-40

364 Renovation of Interest in the Magnetoelectric Effect in Nanoferroics. **2018**, 63, 1006

3

363 Study of Bismuth Ferrite-Silver Ferrite Nanocomposite About Structure, Characterization, Magnetic Properties and Band Gap Evaluation. **2019**, 581-589

362 Powder and Thin Film Synthesis. **2019**, 75-92

361 First-principles screening of ABO₃ oxides with two magnetic sublattices. **2019**, 3,

360 Crystalline Phases and Ferroelectric Properties of Sputtered BiFeO₃ Thin Films Cooled in Pure O₂ and Mixed Ar/O₂ Atmospheres. 1

o

359 Low-Temperature Surface Phase Transitions in Multiferroic BiFeO₃ Nanocrystals Probed via Electron Paramagnetic Resonance.

o

- 358 Photodeposition of CoO nanoparticles on BiFeO nanodisk for efficiently piezocatalytic degradation of rhodamine B by utilizing ultrasonic vibration energy. **2021**, 80, 105813 8
- 357 Study of magnetic structure of ferrimagnet holmium iron garnet by neutron diffraction at room temperature. **2020**,
- 356 Enhanced electrical conductivity in Zr-Doped (La_{0.7}Ba_{0.3})(Mn_{0.5}Fe_{0.5})O₃ solid solutions. **2020**, 10, 2050032 2
- 355 The Properties of xBiFeO₃(1-x)SrTiO₃ (x = 0.2-1.0; x = 0.1) Solid Solutions: Mössbauer Studies. **2020**, 62, 2340-2349
- 354 Progress and Perspectives on Aurivillius-Type Layered Ferroelectric Oxides in Binary Bi₄Ti₃O₁₂-BiFeO₃ System for Multifunctional Applications. **2021**, 11, 23 4
- 353 Stable piezoelectric response of 0-3 type CaBi₂Nb₂O₉:xwt%BiFeO₃ composites for high-temperature piezoelectric applications. **2021**, 9, 312-322 3
- 352 Multifunctional oxides for topological magnetic textures by design. **2021**, 54, 093001 2
- 351 Optical and electrical properties of impurity-less multiferroic bismuth ferrite nanoparticles. **2022**, 275, 115501 1
- 350 Studies on multiferroic properties of (1-x)BiFeO₃-(x)KNbO₃ composites. **2020**,
- 349 Multiferroic and Ferroelectric Rashba Semiconductors. **2020**, 375-400 0
- 348 Strain Control of Domain Structures in Ferroelectric Thin Films: Applications of Phase-Field Method. **2020**, 1213-1230 0
- 347 Influencia de la ferrita de cobalto en la propiedades magnetoeléctricas de las películas delgadas de ferrita de bismuto depositadas por spin coating. **2020**, 25, 0
- 346 Improved magnetic and electrical characteristics of co doped Bi_{0.80}Ba_{0.10}Nd_{0.10}FeO₃ ceramics. **2020**,
- 345 A pulsed high magnetic field facility for electric polarization measurements. **2020**, 69, 057502 0
- 344 Structural and magnetic properties of transition metal doped BaTiO₃. **2020**, 2
- 343 Crystal Structure and Microstructure Variation of Nonstoichiometric Bi_{1-x}FeO_{3-x} and Ti-doped BiFeO₃ Ceramics under Various Sintering Conditions. **2020**, 30, 61-67
- 342 Toxicity Assessment of Nanoferrites. **2021**, 233-314 1
- 341 Polarization Induced Multiferroic Bismuth Ferrite Nanostructures: Investigation of Dielectric and Magnetic Properties. **2021**,

- 340 Progress in Vacuum Flashover Mechanism: Validity of ETPR Theory. **2021**, 0
- 339 Optoelectronic Functionality of BiFeO₃/SrTiO₃ Interface. 2100665 3
- 338 Trends of complete anion substitution on electronic, ferroelectric, and optoelectronic properties of BiFeX₃ (X = O, S, Se, and Te). **2021**, 11, 115108
- 337 Doping Independent Work Function and Stable Band Gap of Spinel Ferrites with Tunable Plasmonic and Magnetic Properties. **2021**, 21, 9780-9788 3
- 336 Model-based analysis of the ferroelectric response of multiferroic (1-x)BiFeO₃-xPbTiO₃ solid solution thin films around morphotropic phase boundary.. **2021**, 741, 138995
- 335 The effect of thickness-dependent strain relaxation on magnetoelectric behaviors for highly c-axis oriented BiFeO₃ films on Si substrate. **2021**, 545, 168739
- 334 All-optical tunable terahertz modulator based on a BiFeO₃/Si heterostructure. **2020**, 10, 2919 1
- 333 Multiferroic Properties of Rare Earth-Doped BiFeO₃ and Their Spintronic Applications. **2021**, 375-395 0
- 332 Lanthanum and strontium modified bismuth ferrite based perovskites with ultra-narrow band gaps. **2020**, 7, 106303 0
- 331 Effects of defect on thermal stability and photoluminescence in quenched Ho-doped 0.94Na0.5Bi0.5TiO₃-0.06BaTiO₃ lead-free ceramics. **2021**, 36, 1-9
- 330 Pressure induced phase transition of La-substituted BiFeO₃. **2022**, 341, 114595 0
- 329 Influence of cerium substitution on structural and dielectric properties of the modified BiFeO₃-PbTiO₃ ceramics. **2021**, 583, 19-32 3
- 328 Improved energy storage performances of lead-free BiFeO₃-based ceramics via doping Sr0.7La0.2TiO₃. **2021**, 162795 3
- 327 Preparation and photoelectric properties of Bi doped ZnO nanoarrays. **2021**, 162801 0
- 326 Multi-objective Bayesian optimization of ferroelectric materials with interfacial control for memory and energy storage applications. **2021**, 130, 204102 0
- 325 Room-temperature large magnetoelectricity in a transition metal doped ferroelectric perovskite. **2021**, 104, 0
- 324 Structural, electrical, and magnetic study of La-, Eu-, and Er- doped bismuth ferrite nanomaterials obtained by solution combustion synthesis. **2021**, 11, 22746 1
- 323 Structural, morphological and thermal analysis of pure and doped (Ho/Nd)-BFO multiferroics. **2021**, 2070, 012008 0

- 322 Interface engineering to optimize polarization and electric breakdown strength of Ba₂Bi_{3.97}Pr_{0.03}Ti₅O₁₈/BiFeO₃ ferroelectric thin-film for high-performance capacitors. **2021**, 133676 2
- 321 Magnetic Behaviour of Perovskite Compositions Derived from BiFeO₃. **2021**, 7, 151 0
- 320 Disentangling the phase sequence and correlated critical properties in Bi_{0.7}La_{0.3}FeO₃ by structural studies. **2021**, 104,
- 319 Crafting a Next-Generation Device Using Iron Oxide Thin Film: A Review. **2021**, 21, 7326-7352 3
- 318 Multiferroic behavior of the functionalized surface of a flexible substrate by deposition of Bi O and Fe O. **2021**, 4
- 317 Facile synthesis of pure BiFeO₃ and Bi₂Fe₄O₉ nanostructures with enhanced photocatalytic activity. 1 0
- 316 Tuning piezoelectric driven photocatalysis by La-doped magnetic BiFeO₃-based multiferroics for water purification. **2021**, 106792 10
- 315 First-principles Study on Piezoelectricity and Spontaneous Polarization in Bi(Fe,Co)O₃. **2021**, 90,
- 314 Multiferroic Material Bismuth Ferrite (BFO): Effect of Synthesis. **2021**, 143-165
- 313 Study of Structural, Electrical and Magnetic Properties of Nd-Ti Co-Doped BiFeO₃ Nanoparticles. **2021**, 387-393
- 312 Developing sustainable, high-performance perovskites in photocatalysis: design strategies and applications. **2021**, 10
- 311 Magnetoelectrics and Multiferroics. **2021**, 595-623
- 310 Influence of preparation method on phase formation, structural and magnetic properties of BiFeO₃. 1
- 309 Effects of Mn doping on electrical properties of BiFeO₃B_rTiO₃ solid solution. **2022**, 343, 114652 0
- 308 Magnetoelectric coupling in Sm substituted 0.67BiFeO₃- 0.33BaTiO₃ ceramics. **2022**, 901, 163681 0
- 307 Enhanced electrical properties of (Zn, Mn)-modified BiFeO₃BaTiO₃ lead-free ceramics prepared via sol-gel method and two-step sintering. **2022**, 899, 163387 3
- 306 Shift of Neel temperature in (BiFeO₃)_{1-x}/(BaTiO₃)_x composites. **2021**, 584, 31-38
- 305 Designing new polar materials. **2022**,

- 304 Design of multifunctional magnetoelectric particulate nanocomposites by combining piezoelectric and ferrite phases. **2022**, 345-357
- 303 Mechanism of improving ferroelectric properties of BiFe_{0.98}M_{0.02}O₃ (M = Zn, Al, Ti) polycrystalline films. **2022**, 101, 420
- 302 Control of ferroelectric and ferromagnetic domains in BiFe_{0.9}Co_{0.1}O₃ thin films by utilizing trailing fields. **2022**, 15, 023002 0
- 301 Plug and Play Electrodeposition Cell: A Case Study of Bismuth Ferrite Thin Films for Photoelectrochemical Water Splitting. **2022**, 11, 013006
- 300 Reduced leakage current and excellent thermal stability in lead-free BiFeO₃BaTiO₃-based piezoelectric ceramics. **2022**, 33, 3949 1
- 299 Efficient Charge Storage Capability of BiFeO₃-Based Bi-Phase Nanocomposites. **2022**, 11, 023001 0
- 298 Enhanced ferroelectric and piezoelectric properties of BiFeO₃BaTiO₃ lead-free ceramics by simultaneous optimization of Bi compensation and sintering conditions. **2022**, 0
- 297 Symmetry Analysis of Magnetoelectric Effects in Perovskite-Based Multiferroics.. **2022**, 15, 0
- 296 Composition and Structure Optimized BiFeO₃-SrTiO₃ Lead-Free Ceramics with Ultrahigh Energy Storage Performance.. **2022**, e2106515 16
- 295 Lanthanum-Induced Morphotropic Phase Boundary in BiFeO₃BaTiO₃-Based Lead-Free Piezoelectric Ceramics. 2100747 0
- 294 Synergistic magnetic proximity and ferroelectric field effect on a 2H-VS₂ monolayer by ferromagnetic termination of a BiFeO₃(0001) surface. **2022**, 10, 1498-1510 2
- 293 Phase-Field Simulations of Tunable Polar Topologies in Lead-Free Ferroelectric/Paraelectric Multilayers with Ultrahigh Energy Storage Performance.. *Advanced Materials*, **2022**, e2108772 24 6
- 292 Temperature and Frequency Dependence of Negative Capacitance, Dielectric and Electric Properties in La_{0.57}Nd_{0.1}Sr_{0.13}Ag_{0.2}MnO₃ Ceramic. **2022**, 206, 250-268 0
- 291 Materials for a Sustainable Microelectronics Future: Electric Field Control of Magnetism with Multiferroics.. **2022**, 1-23 0
- 290 A novel bentonite-cobalt doped bismuth ferrite nanoparticles with boosted visible light induced photodegradation of methyl orange: synthesis, characterization and analysis of physiochemical changes. 1-16 4
- 289 Enhanced Multiferroic Properties in Er and Mn Co-Doped BiFeO₃ Nanoparticles. 1 0
- 288 Strain and orientation engineering in ABOperovskite oxide thin films.. **2022**, 3
- 287 Complementary Insights from Neutron and Resonant X-Ray Reflectometry for the Study of Perovskite Transition Metal Oxide Heterostructures. 2100253 1

- 286 Studies of structural, dielectric and electrical characteristics of nickel-modified barium titanate for device applications. **2022**, 33, 1657-1669 3
- 285 DFT study of X-site ion substitution doping of Cs₂PtX₆ on its structural and electronic properties. 2
- 284 Rare earth-based ceramic nanomaterials: Changanites, ferrites, cobaltites, and nickelates. **2022**, 205-230
- 283 Self-Poled Heteroepitaxial Bi_(1-x)Dy_xFeO₃ Films with Promising Pyroelectric Properties. 2101539 1
- 282 Ferroic phase transition molecular crystals. 4
- 281 Unveiling the Electrochemical Mechanism of High-Capacity Negative Electrode Model-System BiFeO₃ in Sodium-Ion Batteries: An In Operando XAS Investigation.. **2022**, 1
- 280 Electrical studies of Pb_{0.6}Bi_{0.4}Fe_{0.7}Nb_{0.3}O₃ multiferroic. **2022**, 0
- 279 Comments on the paper Effect of holmium (Ho) partial substitution in structure and ferroelectric properties of bismuth ferrites (BFO) by S.G. Nair et al.. **2022**, 903, 163875
- 278 Enhanced UV photosensing properties by field-induced polarization in ZnO-modified (Bi_{0.93}Gd_{0.07})FeO₃ ceramics. **2022**, 902, 163779 2
- 277 Synthesis and Optimization of BiFeO₃ and La-Doped BiFeO₃ Prepared by the Solid State Reaction Method. **2022**, 593-598
- 276 Magnetic dipolar correlations in sillenite-structure bismuth ferrite: Magnetic and Mössbauer effect studies. **2022**, 164, 110632 0
- 275 Compositional dependence of structural, magnetic and spin-phonon coupling properties in Fe_{2-x}Ga_xO₃ (x = 0.6-1.2) system with orthorhombic symmetry. **2022**, 905, 164164 0
- 274 Influence of Electric Poling on Pb_{0.9}Bi_{0.1}Fe_{0.55}Nb_{0.45}O₃ Multiferroic. 1
- 273 Large-Scale Epitaxial Growth of Ultralong Stripe BiFeO₃ Films and Anisotropic Optical Properties.. **2022**, 1
- 272 Magnetically controlled insertion of cobalt ferrite nanoparticles into a porous anodic aluminum oxide (AAO) membrane. 1
- 271 Analysis of size-dependent variation in nonlinear absorption coefficient of multiferroic bismuth ferrite nanoparticles synthesized at different sintering temperature. 0
- 270 Unique multiferroics with tunable ferroelastic transition in antiferromagnet Mn₂V₂O₇. **2022**, 23, 100623 0
- 269 Modeling of Ferroelectric Oxide Perovskites: From First to Second Principles. **2022**, 13, 2

268 Tuning the Magnetisation in $0.7\text{pbfe}0.5\text{nb}0.5\text{o}3 - 0.3\text{bifeo}3$ Multiferroic by Electric Poling.

267 Electrical Properties of the Polycrystalline $\text{BiFe}0.95\text{Co}0.05\text{O}3$ Films. **2021**, 63, 897-903

1

266 Dy-Doped $\text{BiFeO}3$ thin films: piezoelectric and bandgap tuning.

1

265 Multiferroic bismuth ferrite nanomagnets as potential candidates for spintronics at room temperature. **2022**, 55, 42-45

0

264 Hot hole transfer from Ag nanoparticles to multiferroic $\text{YMn}2\text{O}5$ nanowires enables superior photocatalytic activity. **2022**, 10, 4128-4139

0

263 Phase engineered gallium ferrite: a promising narrow bandgap, room-temperature ferroelectric.

1

262 New multiferroic BiFeO with large polarization.. **2022**,

0

261 The comparison of optical and microstructure properties of $\text{BiFeO}3$, $\text{Bi}0.9\text{Pr}0.1\text{FeO}3$ and $\text{BiFe}0.9\text{Mn}0.1\text{O}3$ films fabricated via chemical solution deposition (CSD). **2022**,

260 Experimental and Theoretical Investigations of Low-Dimensional $\text{BiFeO}3$ System for Photocatalytic Applications. **2022**, 12, 215

1

259 In-plane magnetization and electronic structures in $\text{BiFeO}3/\text{graphene}$ superlattice. **2022**, 120, 084002

0

258 Crossover between Bulk and Interface Photovoltaic Mechanisms in a Ferroelectric Vertical Heterostructure. **2022**, 17,

1

257 Electron density distribution influencing the electrical and magnetic properties of polycrystalline $\text{Bi}0.9\text{Sm}0.1\text{FeO}3$ ceramics. **2022**, 113, 278-286

0

256 Enhanced dielectric, ferroelectric, and ferromagnetic properties of $0.7\text{Bi}1-x\text{M FeO}3-0.3\text{BaTiO}3$ ceramics by Tm-induced structural modification. **2022**,

0

255 Light-enhanced gating effect at the interface of oxide heterostructure. **2022**, 55, 255301

0

254 Strong magnetoelectric coupling at an atomic nonmagnetic electromagnetic probe in bismuth ferrite. **2022**, 105,

1

253 Multiferroic behaviour in Bi-doped solid solution $\text{SmFeO}3\text{-BaTiO}3$ perovskite system. **2022**,

0

252 Enhanced electrical properties of $0.7\text{BiFeO}3-0.3\text{BaTiO}3$ lead-free ceramics obtained by optimizing the calcination temperature and time. 1

0

251 Hybrid improper dipolar density wave in $\text{NaLaCoWO}6$. **2022**, 6,

- 250 Conduction mechanisms in thin (0.6)BiFeO₃-(0.4)PbTiO₃ films. **2022**, 17, 2888-2896 0
- 249 Sm-Eu Co-Doped BiFeO₃ Nanoparticles With Superabsorption and Electrochemical Oxygen Evolution Reaction. 10, 0
- 248 Observation of Anomalous Large Magnetoelectric Coupling in the Hexagonal Z-Type Ferrite Films. 2101294 0
- 247 Exploring far-from-equilibrium ultrafast polarization control in ferroelectric oxides with excited-state neural network quantum molecular dynamics.. **2022**, 8, eabk2625 1
- 246 Domain-wall-induced electromagnons in multiferroics. **2022**, 6, 0
- 245 Symmetry evolution and modulation of multiferroic characteristics in Bi_{1-x}LaxFeO₃ ceramics. **2022**, 120, 132904 0
- 244 Zr and Mo doped YMnO₃: The role of dopants on the structural, microstructural, chemical state, and dielectric properties. **2022**, 0
- 243 Piezoelectric Materials: Properties, Advancements, and Design Strategies for High-Temperature Applications.. **2022**, 12, 2
- 242 Structural and electrical properties of Ca doped BiFeO₃ multiferroic nanomaterials prepared by sol-gel auto-combustion method. **2022**, 100465 1
- 241 A comparative study of the lattice structure, optical band gap, electrical conductivity and polarization at different stages of the heat treatment of chemical routed Al(OH)₃. **2022**, 48, 10677-10687 1
- 240 Impact of electric poling on structure, magnetism and ferroelectricity of 0.7PbFe_{0.5}Nb_{0.5}O₃-0.3BiFeO₃ multiferroic. **2022**, 114766 0
- 239 Effects of Surface Polarity on the Structure and Magnetic Properties of Epitaxial h-YMnO₃ Thin Films Grown on MgO Substrates. 1
- 238 Neutron powder-diffraction study of phase transitions in strontium-doped bismuth ferrite: 1. Variation with chemical composition.. **2022**, 0
- 237 Theoretical study on the multiferroic materials In₂FeX (X=V, Cr, Mn, Co, and Ni) O₆ for high photovoltaics and photocatalysis performance. **2022**, 35, 105368 0
- 236 What ails the photovoltaic performance in single-layered unpoled BFO? The role of oxygen annealing in improving the photovoltaic efficiency. **2022**, 236, 822-831 0
- 235 Chemical solution deposition of single phase BiFeO₃ thin films on transparent substrates. 0
- 234 Microwave-Assisted Solvothermal Route for One-Step Synthesis of Pure Phase Bismuth Ferrite Microflowers with Improved Magnetic and Dielectric Properties.. **2022**, 7, 12910-12921 2
- 233 Ferromagnetic properties of conducting filament nanodots formed on epitaxial BiFeO₃ thin film. **2022**, 18, 2232-2239 0

232	Great ferroelectric properties and narrow bandgaps of BiFeO ₃ thin films by (Mg, Mn) modifying. 2022 , 586, 152751	1
231	Large electric field driven strain and enhanced multiferroic properties of Ce ³⁺ /BiFeO ₃ Nano photo-catalyst. 2022 , 144, 106576	0
230	Controllable electrical, magnetoelectric and optical properties of BiFeO ₃ via domain engineering. 2022 , 127, 100943	4
229	Effect of Nd doping on structural, dielectric, magnetic and ferroelectric properties of 0.8BiFeO ₃ 0.2PbTiO ₃ solid solution. 2022 , 905, 164228	0
228	Auto-combustion synthesis as a method for preparing BiFeO ₃ powders and flexible BiFeO ₃ /PVDF films with improved magnetic properties. Influence of doping ion position, size and valence on electric properties. 2022 , 280, 115686	0
227	Highly (00l)-textured BiFeO ₃ thick films integrated on stainless steel foils with an optimized piezoelectric performance. 2022 , 42, 3454-3462	1
226	A review on the structural and magnetic properties of differently doped bismuth-ferrite multiferroics. 2021 , 27, 178-205	0
225	Crystal Structure, Rietveld Refinement and Improved Dielectric and Magnetic Properties of Ti Doped Bi _{0.90} Pr _{0.10} Fe _{1-x} Ti _x O ₃ Multiferroic Ceramics. 2021 , 221, 100-113	
224	Nanoscale Multiferroic Properties at Room Temperature of Lead Zirconate Titanate Iron Tantalate for Memory Device Applications. 2021 , 221, 53-63	0
223	Anti-polar state in BiFeO ₃ /NdFeO ₃ superlattices. 2021 , 130, 244101	
222	Multiferroic Nanocrystals and Diluted Magnetic Semiconductors as a Base for Designing Magnetic Materials. 2021 , 57, 1340-1366	0
221	Deterministic Dual Control of Phase Competition in Strained BiFeO ₃ : A Multiparametric Structural Lithography Approach. 2022 , 5, 60-66	
220	Photovoltaic-Ferroelectric Materials for the Realization of All-Optical Devices. 2022 , 10, 2102353	3
219	Complex Structural Disorder in a Polar Orthorhombic Perovskite Observed through the Maximum Entropy Method/Rietveld Technique. 2022 , 34, 29-42	
218	Synthesis and Investigation of Structural and Magnetic Properties of Nickel Doped BiFeO ₃ . 2021 , 11, 2737-2745	
217	Hydrogen Production through Catalytic Water Splitting Using Liquid-Phase Plasma over Bismuth Ferrite Catalyst.. 2021 , 22,	0
216	Shape dependent multiferroic behavior in Bi ₂ Fe ₄ O ₉ nanoparticles.. 2022 ,	0
215	Electronic Properties of Fully Strained La Sr MnO Thin Films Grown by Molecular Beam Epitaxy (0.15 0.45).. 2022 , 7, 14571-14578	2

- 214 Solvent Selective Effect Occurs in Iodinated Adamantanone Ferroelectrics.. **2022**, e2201702 1
- 213 Study of structural, electrical and magnetic characterization of (1-x)BiFeO₃-xBaTiO₃ solid solution. **2022**, 587, 63-69
- 212 Ca Solubility in a BiFeO₃-Based System with a Secondary BiO Phase on a Nanoscale.. **2022**, 126, 7696-7703 0
- 211 Influence of sintering temperature on structural, electrical, and magnetoelectric properties of multiferroic Fe-substituted BaTiO₃ ceramics. **2022**, 128, 1
- 210 Enhanced electromagnetic interference (EMI) shielding in BiFeO₃/graphene oxide nanocomposites over X-band frequency region. **2022**, 131, 174101 0
- 209 Synergistic effect of V₂O₅ and Bi₂O₃ on the grain boundary structure of high-frequency NiCuZn ferrite ceramics. 1
- 208 Magnetic Topological Insulators Nano-Crystallites Fe_{1.4}Bi_{0.6}Se_{2.5}Y_{0.5}Pr_x: Preparation, Characterization and Physical Properties.
- 207 High depolarization temperature and superior piezoelectric performance with complex structural evolution in BiFeO₃/PbTiO₃(Sr_{0.7}Bi_{0.2}?0.1)TiO₃ systems. **2022**, 1
- 206 Structural phase transition, phase purity, inter-/intra-grain electrical parameters and local energy barrier profile as a function of aliovalent and isovalent substitution in BiFeO₃. **2022**, 167, 110748
- 205 Ferroelectric and piezoelectric characteristics of epitaxial BiFeO₃ films sputtered on different oxide bottom electrodes. **2022**, 320, 132387
- 204 Magnetic properties of Ni/BiFeO₃ hybrid nanostructures. **2022**, 912, 165133 1
- 203 A study of Cr³⁺-substitution induced defects restructuring in BiFeO₃ by positron annihilation and other supportive methods. **2022**, 142, 115286
- 202 A comparative study of structural and multiferroic properties of Ca, Sr and Ba doped 0.2BiFeO₃-0.8PbTiO₃ solid solutions. **2022**, 111983
- 201 Structural modification and evaluation of dielectric, magnetic and ferroelectric properties of Nd-modified BiFeO₃/PbTiO₃ multiferroic ceramics. **2022**, 589, 161-176 0
- 200 Energy storage performance of polycrystalline Bi_{0.85}Ho_{0.05}Sm_{0.1}FeO₃ ceramics. **2022**, 589, 55-63 1
- 199 Electric conductivity and dielectric relaxation properties of BiFeO₃-YMnO₃ solid solution. **2022**, 589, 103-122 0
- 198 Effect of thickness and frequency of applied field on the switching dynamics of multiferroic bismuth ferrite thin films. **2022**, 6, 2
- 197 Thickness-dependent dielectric and ferroelectric properties of 0.7Bi(Fe_{0.98}Mn_{0.02})O₃-0.3PbTiO₃ thin films on stainless steel substrates.

- 196 Reduction inhibition of Fe³⁺ ions in Mn-doped 0.7BiFeO₃-0.3BaTiO₃ ceramics by direct reaction sintering. **2022**, o
- 195 Investigations of structural and optoelectronic properties of bismuth ferrite nanoparticles synthesized using sol-gel method. **2022**,
- 194 Science and Technology of Complex Correlated Oxides: The Legacy of John Goodenough.
- 193 Study of the role of dysprosium substitution in tuning structural, optical, electrical, dielectric, ferroelectric, and magnetic properties of bismuth ferrite multiferroic. **2022**, 165743 1
- 192 Exploring the correlation between the spin-state configuration and the magnetic order in Co-substituted BiFeO₃. **2022**, 6, o
- 191 Robust ferroelectric-gating-dependent electronic and magnetic properties in a 1T-VSe₂/BiAlO₃(0001) multiferroic heterostructure. **2022**, 26, 100743
- 190 BiFeO₃/Fe₂O₃ electrode for photoelectrochemical water oxidation and photocatalytic dye degradation: A single step synthetic approach. **2022**, 303, 135071 1
- 189 Internal friction in thin-film ferrite bismuth with an amorphous structure. **2022**, 918, 165610 o
- 188 Hidden piezoelectric performances of BiFeO₃-based textured ceramics.
- 187 Bismuth ferrite (BiFeO₃) perovskite-based advanced nanomaterials with state-of-the-art photocatalytic performance in water cleanup. 1
- 186 Modeling and Design for Magnetoelectric Ternary Content Addressable Memory (TCAM). **2022**, 1-1 1
- 185 Giant bulk photovoltaic effect driven by the wall-to-wall charge shift in WS₂ nanotubes. **2022**, 13, 1
- 184 Solution-Based Synthesis Routes for the Preparation of Noncentrosymmetric 0-D Oxide Nanocrystals with Perovskite and Nonperovskite Structures. 2200992
- 183 Enhanced magnetoelectric response of Mn-doped BiFeO₃-based multiferroic ceramics.
- 182 Proximity Effects in 2D VSe₂ Magnets via Interface Coupling with a BiFeO₃(0001) Ferromagnetic Surface. o
- 181 Importance of Hubbard U parameter to explore accurate electronic and optical behaviour of BiFeO₃.
- 180 All-Magnetic Slabs and Multiferroism in (Bi₂□O₂)(MF₄) Aurivillius Oxyfluorides (M = Fe and Ni). o
- 179 Study on electrical transport and relaxation process of ceramic-based nanocomposites of (1□) BiFeO₃-xCoFe₂O₄ (x = 0.0, 0.2, 0.5, 0.8, 1.0). **2022**, 102, 665-678

- 178 XPS Study in BiFeO₃ Surface Modified by Argon Etching. **2022**, 15, 4285 ○
- 177 The rise of 2D materials/ferroelectrics for next generation photonics and optoelectronics devices. **2022**, 10, 060903 3
- 176 Lead-Free BiFeO₃-Based Piezoelectrics: A Review of Controversial Issues and Current Research State. **2022**, 15, 4388 1
- 175 Structural and dielectrical analysis of rare earth doped bismuth ferrite nanoparticle at high frequency. **2022**, ○
- 174 Tutorial: Piezoelectric and magnetoelectric N/MEMS Materials, devices, and applications. **2022**, 131, 241101 1
- 173 Typical superparamagnetism with improved electrical properties of nano modified bismuth ferrite multiferroic composites. **2022**, 99, 100565 ○
- 172 Improved optical, dielectric, impedance, and magnetic properties of (BiFeO₃)_{0.6}(CaTiO₃)_{0.4} for multifunctional utilities. **2022**, 142, 109664 ○
- 171 An exploration for new strategy: Achieving both excellent temperature stability and good electrostrain in BiFeO₃BaTiO₃-based relaxor ferroelectrics by domain engineering. **2022**, 27, 100747
- 170 Influence of Eu³⁺ substitution on structural, magnetic and dielectric properties of Bi_{0.9}La_{0.1}FeO₃. **2022**, 560, 169350
- 169 Flux Crystal Growth of Rubidium-Iron Silicates and Germanates and Their Ion-Exchange Using Alkali Nitrate Salts. ○
- 168 Magnetoelectric ferrite nanocomposites. **2022**, 301-367
- 167 Structural, Magnetic and Transport Properties of Gd and Cu Co-Doped BiFeO₃ Multi ferroics. **2022**, 10, 2026-2039 ○
- 166 Comparative density functional studies of BiMO₃ polymorphs (M = Al, Ga, In) based on LDA, GGA, and meta-GGA functionals. ○
- 165 Influence of Radiation on the Crystal Structure of BiFeO₃. **2022**, 67, 588-597 ○
- 164 Evidence for negative differential resistance and switchable diode effect in multiferroic BiFe_{0.95}Sc_{0.05}O₃-based resistive random access memory under doping engineering. **2022**, 33, 15848-15857
- 163 Structural, magnetic, optical, and photocatalytic properties of Ca²⁺/Li⁺ doped BiFeO₃ nanoparticles. **2022**, 33, 16856-16873
- 162 Enhanced multiferroic properties and magnetoelectric coupling in Nd modified 0.7BiFeO₃0.3PbTiO₃ solid solution. **2022**, 33, 17161-17173
- 161 Enhanced dielectric and magnetic properties of Cr / Co and Mn co-doped single phase multiferroic bismuth ferrite nanoparticles. **2022**, 100649 ○

- ¹⁶⁰ Structural characteristics, impedance spectroscopy, ac-conductivity and dielectric loss studies on RF-magnetron sputtered F doped ZnO (FZO) thin films. **2022**,
- ¹⁵⁹ Ti doping and low-temperature sintering of BiFeO₃ nanoparticles synthesized by the solvothermal method. **2022**, ○
- ¹⁵⁸ Coupling of piezocatalysis and photocatalysis for efficient degradation of methylene blue by Bi_{0.9}Gd_{0.07}La_{0.03}FeO₃ nanotubes. **2022**, 11, 1069-1081 1
- ¹⁵⁷ The Effect of Bi₂O₃ and Fe₂O₃ Impurity Phases in BiFeO₃ Perovskite Materials on Some Electrical Properties in the Low-Frequency Field. **2022**, 15, 4764
- ¹⁵⁶ Ferromagnetic Ordering with High Curie Temperature in a New Pr₂FeNiO₆ Double Perovskite Material.
- ¹⁵⁵ Freestanding complex-oxide membranes. **2022**, 34, 383001 1
- ¹⁵⁴ Lead-free Ca²⁺-doped Bi_{0.80}La_{0.20}FeO₃ multiferroic material for solar cell applications. **2022**,
- ¹⁵³ Physical characterization of BiFeO₃-based thin films with enhanced properties for photovoltaic applications. ○
- ¹⁵² Fantastic Energy Storage Performances and Excellent Stability in BiFeO₃/SrTiO₃-Based Relaxor Ferroelectric Ceramics. 1
- ¹⁵¹ Green Synthesis of Sr²⁺ doped multiferroic BiFeO₃ nanoceramics using Aloe vera biotemplates and their characterizations. **2022**, 166107 ○
- ¹⁵⁰ Effects of Sm and Cr co-doping on structural, magnetic, optical and photocatalytic properties of BiFeO₃ nanoparticles. **2022**, 283, 115859 ○
- ¹⁴⁹ Studies on characterization and enhanced magnetic field sensing performance of Bi_{1-x}K_xMn_{1-y}Co_yO₃ nanopowders as a fiber optic clad modified region. **2022**, 560, 169683
- ¹⁴⁸ Ferroelectric control of band alignments and magnetic properties in the two dimensional multiferroic VSe₂/In₂Se₃.
- ¹⁴⁷ General aspects of the physical behavior of polycrystalline BiFeO₃/VO₂ bilayers grown on sapphire substrates. **2022**, 128, ○
- ¹⁴⁶ Spin glass and magnetoelectric effect in BiFeO₃-Bi_{0.5}K_{0.5}TiO₃-Bi_{0.5}Na_{0.5}TiO₃ single crystals. **2022**, 132, 044101
- ¹⁴⁵ James Floyd Scott. 4 May 1942– April 2020.
- ¹⁴⁴ Synthesis and characterization of Bi_{1-x}La_xFeO₃ multiferroic thin films. **2022**, 2298, 012016
- ¹⁴³ Emergence of low-temperature glassy dynamics in Ru substituted non-magnetic insulator CaHfO₃. **2022**, 34, 415802

142 Complex dielectric behaviours in BiFeO₃/Bi₂Fe₄O₉ ceramics.

141 BiFeO₃/Bi₂Fe₄O₉ S-scheme heterojunction hollow nanospheres for high-efficiency photocatalytic o-chlorophenol degradation. **2022**, 121893 3

140 Growth of heteroepitaxial La and Mn co-substituted BiFeO₃ thin films on Si (100) substrate by pulsed laser deposition. **2022**, 128,

139 Temperature dependence of the local electromagnetic field at the Fe site in multiferroic bismuth ferrite. **2022**, 106, 0

138 Temperature-Driven Transformation of the Crystal and Magnetic Structures of BiFe_{0.7}Mn_{0.3}O₃ Ceramics. **2022**, 12, 2813 0

137 Study of new double perovskite halides Rb₂Ti(Cl/Br)₆ for solar cells and thermoelectric applications. **2022**, 32, 104106 0

136 Multiferroic Self-Assembled BaTiO₃/BaTiO₃ Vertically Aligned Nanocomposites on Mica Substrates toward Flexible Electronics. **2022**, 4, 4077-4084

135 Electric and magnetic properties of Bi_{0.80}Ba_{0.20}FeO₃ doped Ba_{0.85}Ca_{0.15}Ti_{0.90}Zr_{0.10}O₃ ceramics prepared via the solid-state combustion technique.

134 Direct fabrication of single-phase multiferroic BiFe_{0.95}Co_{0.05}O₃ films on polyimide substrates for flexible memory. **2022**, 758, 139424 0

133 A review on recent progressions of Bismuth ferrite modified morphologies as an effective photocatalyst to curb water and air pollution. **2022**, 144, 109834 1

132 Superior high-temperature piezoelectric performances in BF-PT-BT ceramics via electric field constructed phase boundary. **2022**, 239, 118285 0

131 Enhanced ferroelectric, dielectric and magnetodielectric properties of Ba and Y co-doped Bismuth Ferrite nanoparticles. **2022**, 645, 414243

130 Flux crystal growth of rubidium iron silicates and germanates and their ion-exchange using alkali nitrate salts. **2022**, 132, 106995 0


129 Barium titanate/Bismuth ferrite/polyvinylidene fluoride nanocomposites as flexible piezoelectric sensors with excellent thermal stability. **2022**, 346, 113885 0

128 Influence of substitution of different transition metal elements (Mn, Cr, Co) on the properties of Bi_{0.88}Sm_{0.12}FeO₃-based ceramics. **2022**, 563, 169922 0

127 Effectively coupled BiFeO₃-MnFe₂O₄-Cr₂O₃ tri-phase multiferroic composites for efficient energy storage and fast switching. **2022**, 929, 167274 1

126 Influence of Tb substitution on the structural and magnetic properties of BiFeO₃ multiferroic. **2022**, 563, 169947 1

125 The correlation between electric polarization and magnetic properties in [N(C₂H₅)₄]₂CoCl₂Br₂ crystal at low temperatures. **2022**, 646, 414299 0

124	Structural transition and enhanced magnetic, optical and photocatalytic properties of novel Ce/Ni co-doped BiFeO ₃ nanoparticles. 2022 , 152, 107086	1
123	Implementing (K,Na)NbO ₃ -based lead-free ferroelectric films to piezoelectric micromachined ultrasonic transducers. 2022 , 103, 107761	1
122	Magnetoelectric coupling at microwave frequencies observed in bismuth ferrite-based multiferroics at room temperature. 2023 , 137, 100-103	0
121	AC conductivity and phase transition of the BST/BFO ceramic doped with Yb. 2022 , 12, 27154-27161	0
120	 BFO/SBN/MgO(001), "BFO-SBN" 2022 , 19-24	0
119	Recent Progress and Applications of HfO ₂ -Based Ferroelectric Memory. 2023 , 28, 221-229	1
118	Crystal structure of the system of (1-y)(BiFeO ₃) ₃ -y(Ba _{1-x} Sr _x TiO ₃) ₃ solid solution.. 2022 , 66, 397-403	0
117	Formation of ferroelectric multi-domains and electrical conduction in epitaxial BiFeO ₃ nanodots fabricated with AAO nanotemplates. 2022 ,	0
116	Room temperature tunability of ferroelectricity and dielectricity in La and Mn codoped BiFeO ₃ nanoflakes: Implications for electronic devices applications. 2022 ,	0
115	Magnetocapacitance on the transition fields in Ni ²⁺ doped Y-type hexaferrite Ba _{0.6} Sr _{1.4} Co ₂ Fe ₁₁ AlO ₂₂ obtained by high-energy ball milling. 2022 ,	0
114	Structural transformation, dielectric and multiferroic properties of (Gd _{1-x} Ba _x)(Fe _{1-x} Ti _x)O ₃ ceramics by tuning composition. 2022 ,	0
113	Bipolar resistive switching in Mn-doped BiFeO ₃ thin films synthesized via sol-gel-assisted spin coating technique. 2022 , 128,	0
112	Modulating self-biased near-UV photodetection of Gd-doped bismuth ferrite ceramics by introducing zinc oxide as electron transport layer. 2022 ,	0
111	Interface-Driven Multiferroicity in Cubic BaTiO ₃ -SrTiO ₃ Nanocomposites. 2022 , 16, 15413-15424	2
110	Emergence of collinear magnetic structure in Tb-doped BiFeO ₃ . 2022 , 170031	0
109	Enhanced multiferroic properties in Ba and Sm co-doped BiFeO ₃ ceramics.	0
108	Temperature-Dependent Crystal Structure and Physical Properties of BiFeO ₃ Bulk Ceramics. 2022 , 230, 29-39	0
107	Effects of 120 MeV Ag ⁹⁺ swift heavy ion irradiation on the structural, optical and electrical properties of pristine and Ni doped BiFeO ₃ thin films grown by pulsed laser deposition. 2022 , 760, 139487	0

- 106 Hopping Mechanism and Impedance Properties of Mg Doped NBT-KBT Solid Solution near Ambient Temperature. 0
- 105 Investigation on the structural, electrical and thermistor parameters of La-doped BiFeO₃PbZrO₃ for energy storage devices. **2022**, 45, 2
- 104 Annealing temperature effects on BiFeO₃ nanoparticles towards photodegradation of Eosin B dye. **2022**, 57, 18726-18738 0
- 103 Aliovalent Calcium Substitution an Effective way to Enhance the Magnetoelectric Coupling Properties of Multiferroic BiFeO₃. 0
- 102 Piezoelectric properties of mechanochemically processed 0.67BiFeO₃-0.33BaTiO₃ ceramics. **2022**, 0
- 101 Morphotropic Phase Boundary Enhanced Photocatalysis in Sm Doped BiFeO₃. **2022**, 27, 7029 0
- 100 BiFeO₃-based Z scheme photocatalytic systems: Advances, mechanism, and applications. **2022**, 0
- 99 First-principles Landau-like potential for BiFeO₃ and related materials. **2022**, 106, 0
- 98 Rare-earth doped BiFe_{0.95}Mn_{0.05}O₃ nanoparticles for potential hyperthermia applications. 10, 0
- 97 Effective A-site modulation and crystal phase evolution for high ferro/piezoelectric performance in ABO₃ compounds: Yttrium-doped BiFeO₃-BaTiO₃. **2023**, 933, 167709 0
- 96 Investigation of crystal structure and variable range hopping conduction mechanism in Gd doped Na_{0.5}Bi_{0.5}TiO₃ ceramics. **2023**, 1274, 134413 0
- 95 Effect of cobalt substitution on the structural, ferroelectric, and magnetic properties of bismuth ferrite thin films. **2022**, 132, 194102 1
- 94 Ferrite-Based Magnetoelectronics. **2022**, 309-323 0
- 93 Electrical characteristics of multiferroic BiFeO₃ electronic system. **2022**, 0
- 92 Study on quantitative Rietveld analysis of XRD patterns of different sizes of bismuth ferrite. **2022**, 128, 0
- 91 Spontaneous exchange bias and large dielectric constant in Bi_{0.8}Tb_{0.2}Fe_{0.8}Mn_{0.2}O₃ multiferroic. **2022**, 132, 183909 0
- 90 Rietveld refined crystal structure, magnetic, dielectric, and electric properties of Li- substituted Ni_{0.7}Cu_{0.3}Zn ferrite and Sm, Dy co-doped BaTiO₃ multiferroic composites. **2022**, 0
- 89 Co-Substituted BiFeO₃ : Electronic, Ferroelectric, and Thermodynamic Properties from First Principles. 2200673 0

- 88 Mechanisms for point defect-induced functionality in complex perovskite oxides. **2022**, 128, 10
- 87 Norfloxacin mineralization under light exposure using Sb₂SnO₂ ceramic anodes coated with BiFeO₃ photocatalyst. **2023**, 313, 137518 0
- 86 Theory of hard magnetic soft materials to create magnetoelectricity. **2023**, 171, 105136 1
- 85 Bottom electrode dependence of electrical and optical properties in Bi_{0.96}Sm_{0.04}Fe_{0.98}Mn_{0.02}O₃ films. **2023**, 155, 107236 0
- 84 Synthesis, characterization and machine learning assisted optical emission studies of dysprosium doped bismuth ferrites. **2023**, 160, 112108 0
- 83 Structural, electrical, and thermistor behavior of BiFeO₃-PbZrO₃ for energy storage devices. **2023**, 12, 1-8 0
- 82 Operational parameters and major active species responsible for the photodegradation of malachite green dye by ZnO/ZnS core-shell nanocomposite photocatalyst. 0
- 81 Synthesis and properties of ultra-small BiFeO₃ nanoparticles doped with cobalt. **2022**, 0
- 80 Complex dielectric behaviours in BiFeO₃/Bi₂Fe₄O₉ ceramics. **2022**, 128, 0
- 79 Structural, magnetic, optical, and photocatalytic properties of Bi_{1-x}Sm_xFe_{1-y}Cr_yO₃ nanostructure synthesized by hydrothermal method. **2023**, 129, 0
- 78 Low Temperature Magnetic Transition of BiFeO₃ Ceramics Sintered by Electric Field-Assisted Methods: Flash and Spark Plasma Sintering. **2023**, 16, 189 1
- 77 Pressure-Induced Abnormal Electrical Transport Transition from Pure Electronic to Mixed Ionic/Electronic in Multiferroic BiFeO₃ Ceramics. 0
- 76 Strain induced structural phase transition and compositional dependent magnetic phase transition in Ti doped Bi_{0.80}Ba_{0.20}FeO₃ ceramics. **2022**, 8, e12530 0
- 75 Stable self-polarization in lead-free Bi(Fe_{0.93}Mn_{0.05}Ti_{0.02})O₃ thick films. 0
- 74 Synthesis, structural, micro structural, optical, magnetic and dielectric properties of Nd doped multiferroic Bismuth iron oxide. **2022**, 100359 0
- 73 Centrosymmetric Tetragonal Tungsten Bronzes A₄Bi₂Nb₁₀O₃₀ (A = Na, K, Rb) with a Bi 6s Lone Pair. 0
- 72 Optical co-alignment in the electrical and magnetic induction of Dy and Tb-doped BFO-based multiferroic. **2023**, 129, 0
- 71 Dielectric characterization of the BiFe_{0.5}Cr_{0.5}O₃ ceramics. **2022**, 62, 0

- 70 Large increase in photo-induced conductivity of two-dimensional electron gas at SrTiO₃ surface with BiFeO₃ topping layer. **2022**, 121, 241601 ○
- 69 High temperature piezoelectric accelerometer fabricated by 0.75BiFeO₃0.25BaTiO₃ ceramics with operating temperature over 450 °C. **2022**, 121, 232902 ○
- 68 Observation of room-temperature out-of-plane switchable electric polarization in supported 3R-MoS₂ monolayers. ○
- 67 Can the ferroelectric soft mode trigger an antiferromagnetic phase transition?. **2023**, ○
- 66 Effect of BiFeO₃ Doping and Annealing Temperature on the High-Temperature Dielectric Relaxation Properties in BaTiO₃/SrTiO₃ Lead-Free Ceramics. 2200414 ○
- 65 Structure, ferroelectric and magnetic behavior in Mn doped 0.75 BiFeO₃-0.25BaTiO₃ ceramics. **2023**, 127302 ○
- 64 Ferroelectric, ferromagnetic and magneto-capacitance properties of Sm-doped BiFeO₃-BaTiO₃ solid solution. **2023**, 129, ○
- 63 Coupling Oxygen Vacancy Gradient Distribution and Flexoelectric Effect for Enhanced Photovoltaic Performance in Bismuth Ferrite Films. ○
- 62 Enhanced ferroelectric properties in La-doped BiFeO₃ films by the sol-gel method. ○
- 61 Comparative studies by X-ray diffraction, Raman, vibrating sample magnetometer and Mössbauer spectroscopy of pure, Sr doped and Sr, Co co-doped BiFeO₃ ceramic synthesized via tartaric acid-assisted technique. **2023**, ○
- 60 Enhancement in the magneto-dielectric and ferroelectric properties of BaTiO₃/CoFe_{1.9}Yb_{0.1}O₄ core-shell multiferroic nanocomposite.. **2023**, 168841 ○
- 59 Sn-modified BaTiO₃ thin film with enhanced polarization. **2023**, 41, 022701 ○
- 58 Solvent-Free Combustion-Assisted Synthesis of LaFe_{0.5}Cr_{0.5}O₃ Nanostructures for Excellent Photocatalytic Performance toward Water Decontamination: The Effect of Fuel on Structural, Magnetic, and Photocatalytic Properties. **2023**, 8, 555-570 ○
- 57 Multiferroic/Polymer Flexible Structures Obtained by Atomic Layer Deposition. **2023**, 13, 139 ○
- 56 Low Dielectric Permittivity and Losses of BaTi_{0.80}Fe_{0.20}O₃ Ceramic Doped with Zr at Ba Site: Comparative Study with Zr Doped in Ti Site. **2022**, 67, S71-S77 ○
- 55 A brief study on exploration of Ni doped PrFeO₃ perovskite as multifunctional material□ **2023**, 34, ○
- 54 Comparison of the structure-property relationships between sillenite and perovskite phases of Bi_{0.9}Dy_{0.1}FeO₃ nanostructures. ○
- 53 Non-volatile electric field-mediated magnetic anisotropy in CoZr/ PMN-PT structure. 10, ○

- 52 Perovskite-based emerging memories. **2023**, 401-484 o
- 51 Single Unit-Cell Layered Bi₂Fe₄O₉ Nanosheets: Synthesis, Formation Mechanism, and Anisotropic Thermal Expansion. 2207202 o
- 50 Multiferroic perovskite ceramics: Properties and applications. **2023**, 339-381 o
- 49 A new technique to achieve thick Tl₂Ba₂CaCu₂O₈ films for advanced applications. **2023**, o
- 48 Theoretical insight of origin of Rashba-Dresselhaus effect in tetragonal and rhombohedral phases of BiFeO₃. o
- 47 Controlling magnetoelectric coupling effect of CoFe₂O₄/Ba_{0.8}Sr_{0.2}TiO₃ multiferroic fluids by viscosity. o
- 46 Improved chemical defects and electrical properties of Li/Al co-doped BiFeO₃-BaTiO₃ lead-free ceramics. **2023**, 34, o
- 45 Characterization of nanostructured bismuth ferrite (BiFeO₃) prepared by sol-gel method. **2023**, o
- 44 Hydrothermal synthesis of multiferroics ferrite bismuth nanoparticles with lanthanum and barium: structural and magnetic properties investigation. **2023**, 135505 o
- 43 Effect of Cooling Rate on the Crystalline Morphology of Bi₂O₃-Fe₂O₃ Pseudo-Binary System. o
- 42 Correlation between the unit cell parameters and electronic transitions in Bi_{1-x}Eu_xFeO₃ thin films. **2023**, 300, 127541 o
- 41 Self-powered dual-wavelength polarization-sensitive photodetectors based on ZnO/BiFeO₃ heterojunction. **2023**, 623, 157032 o
- 40 Energy storage and magnetoelectric coupling in neodymium (Nd) doped BiFeO₃-PbTiO₃ solid solution. **2023**, 946, 169333 o
- 39 Promotion of photo-induced charge carrier separation in a heterostructure via introducing an enhanced polarization electric field. **2023**, 35, 105624 o
- 38 Composition-, temperature- and pressure-induced transitions between high-pressure stabilized perovskite phases of the (1-x)BiFe_{0.5}Sc_{0.5}O₃ - xLaFe_{0.5}Sc_{0.5}O₃ series. **2023**, 322, 123937 o
- 37 Precipitation Method and Sonication Technique for Advanced Superiority of Nanospherical BiFe₂O₃ and its Multi-Applications. **2023**, 35, 345-351 o
- 36 Investigations on Dielectric, Transport, and Ferroelectric Properties of Ca-Modified Bi_{0.80}La_{0.20}FeO₃ Ceramic Synthesized by Solid State Reaction Route. o
- 35 Gelation Chemistry and Phase Development of Chemical Solution Deposition-Derived Sm-Doped BiFeO₃ Thin Films: The Role of Sm Dopant. **2023**, 5, 1302-1310 o

- 34 A Ferroelectric Domain-Wall Transistor. **2023**, 40, 038501 ○
- 33 Magnetic Ordering and Interplay between the Magnetic and Charge Subsystems in New Franciscite-Analog $\text{Cu}_3\text{Dy}(\text{SeO}_3)_2\text{O}_2\text{Cl}$ as Studied by the Spectroscopy of Kramers Doublets. 2200460 ○
- 32 Effect of Nd^{3+} substitution on structural, morphological, and electrical properties of Bismuth Ferrite ceramics. **2023**, 34, ○
- 31 Crystal Structure, Magnetic and Photocatalytic Properties of Solid Solutions $\text{Bi}_{2-x}\text{La}_x\text{Fe}_4\text{O}_9$ ($x=0.05, 0.1$). **2023**, 8, ○
- 30 Facile Control of Ferroelastic Domain Patterns in Multiferroic Thin Films by a Scanning Tip Bias. **2023**, 15, 11983-11993 ○
- 29 A comparative study on structural, magnetic and optical properties of rare earth ions substituted $\text{Bi}_{1-x}\text{R}_x\text{FeO}_3$ (R: Ce^{3+} , Sm^{3+} and Dy^{3+}) nanoparticles. **2023**, ○
- 28 Investigation on structural, magnetic and optical properties of $\text{Sm}_{1-x}\text{Co}_x$ Co-substituted BiFeO_3 samples. **2023**, ○
- 27 Revisiting the Ferroelectric Photovoltaic Properties of Vertical BiFeO_3 Capacitors: A Comprehensive Study. **2023**, 15, 12070-12077 ○
- 26 Multiferroic perovskite bismuth ferrite nanostructures: A review on synthesis and applications. **2023**, 572, 170569 ○
- 25 Growth of Samarium-Substituted Epitaxial Bismuth Ferrite Films by Chemical Vapor Deposition. **2023**, 23, 2065-2074 ○
- 24 Intersecting multiaxial domain walls in plastic ferroelectric crystal films. **2023**, 7, ○
- 23 Control of multiferroic features in BiFeO_3 nanoparticles by facile synthetic parameters. **2023**, 49, 18552-18564 ○
- 22 Structural and magnetic quantification of rhombohedral \leftrightarrow orthorhombic phase transition in gadolinium substituted bismuth ferrite. **2023**, 572, 170600 ○
- 21 Effect of nano-size on magnetostriction of BiFeO_3 and exceptional magnetoelectric coupling properties of BiFeO_3 /P(VDF-TrFE) polymer composite films for magnetic field sensor application. **2023**, 32, 045017 ○
- 20 High Temperature Dielectric Relaxation Properties of SrTiO_3 - Zn_2SnO_4 Composite Ceramics. **2023**, 232, 63-73 ○
- 19 Fine Control of Multiferroic Features of Nanoscale BiFeO_3 Powders Synthesized by Microwave-Assisted Solid-State Reaction. ○
- 18 Multiferroic properties in Fe-site engineered $\text{PbFe}_{1/2}\text{Nb}_{1/2}\text{O}_3$ with distinct antisymmetric spin interaction. **2023**, 122, 112906 ○
- 17 High-entropy design for dielectric materials: Status, challenges, and beyond. **2023**, 133, 110904 ○

- 16 Multiferroics Made via Chemical Co-Precipitation That Is Synthesized and Characterized as $\text{Bi}(1-x)\text{Cd}x\text{FeO}_3$. **2023**, 11, 134 ○
- 15 Investigation of structural, microstructural and optical properties of barium yttrium titanium ferric oxides prepared using solid-state route for photorefractive material. **2023**, 34, ○
- 14 Multiferroic and nanomechanical properties of $\text{Bi}_{1-x}\text{Y}_x\text{FeO}_3$ polycrystalline films ($x = 0.00.1$). **2023**, 34, ○
- 13 Optimizing Structural, Optical, Dielectric, and Magnetic Properties of $(\text{Bi}_{1-x}\text{La}_x)\text{FeO}_3$ ($0.00 \leq x \leq 0.06$) Sintered Ceramics. **2023**, 8, 13222-13231 ○
- 12 Ferromagnetic vanadium disulfide VS_2 monolayers with high Curie temperature and high spin polarization. **2023**, 25, 10143-10154 ○
- 11 Great multiferroic properties in $\text{BiFeO}_3/\text{BaTiO}_3$ system with composite-like structure. **2023**, 122, 152904 ○
- 10 Structural and Magnetic Properties and Graphene-Induced Photocatalytic Activity of BiFeO_3 Ceramics. ○
- 9 Increasing Electrical Resistivity of P-Type BiFeO_3 Ceramics by Hydrogen Peroxide-Assisted Hydrothermal Synthesis. **2023**, 16, 3130 ○
- 8 Structural, microstructural, dielectric, transport, and optical properties of modified bismuth ferrite. ○
- 7 Piezoelectric ceramic materials for power ultrasonic transducers. **2023**, 65-81 ○
- 6 Novel Insights of Enhanced Magnetization and Magnetoelectric Coupling in the Nanocomposite of BiFeO_3 with Lanthanum Strontium Manganite. ○
- 5 Magnetic Domain Change Induced by In-Plane Electric Polarization Switching in $\text{Bi}(\text{Fe}, \text{Co})\text{O}_3$ Thin Film. ○
- 4 Investigation of the effect of sintering temperatures on the structural and magnetic properties of $(\text{Bi}_{0.90}\text{Sm}_{0.10}\text{Fe}_{0.93}\text{Cr}_{0.07}\text{O}_3)$ ferrite. **2023**, 127790 ○
- 3 Experimental and DFT investigation of structural and optical properties of lanthanum substituted bismuth ferrites. **2023**, 661, 414927 ○
- 2 Temperature Dependence of the Hyperfine Magnetic Field at Fe Sites in Ba-Doped BiFeO_3 Thin Films Studied by Emission Mössbauer Spectroscopy. **2023**, 13, 724 ○
- 1 A generalized synthesis method for freestanding multiferroic two-dimensional layered supercell oxide films via a sacrificial buffer layer. ○